การตรวจสอบการเปลี่ยนแปลงอัตราการไหวสะเทือนและขั้นตอนวิธีบริเวณ-เวลา-ความยาวรอยเลื่อนตามแนวชายแดนประเทศไทย-ลาว-พม่า

นายประโยชน์ ปวงจักร์ทา

วิทยานิพนธ์นี้เป็นส่วนหนึ่งของการศึกษาตามหลักสูตรปริญญาวิทยาศาสตรมหาบัณฑิต
สาขาวิชาโลกศาสตร์ ภาควิชาธรณีวิทยา
คณะวิทยาศาสตร์ จุฬาลงกรณ์มหาวิทยาลัย
ปีการศึกษา 2557

SEISMICITY RATE CHANGE AND REGION-TIME-LENGTH ALGORITHM INVESTIGATIONS ALONG THAILAND-LAOS-MYANMAR BORDERS

Mr. Prayot Puangjaktha

A Thesis Submitted in Partial Fulfillment of the Requirements

for the Degree of Master of Science Program in Earth Sciences

Department of Geology

Faculty of Science

Chulalongkorn University

Academic Year 2014

Thesis Title	SEISMICITY RATE CHANGE AND REGION-TIME-LENGTH ALGORITHM INVESTIGATIONS ALONG THAILAND-LAOS-MYANMAR BORDERS
By	Mr. Prayot Puangjaktha
Field of Study	Earth Sciences
Thesis Advisor	Assistant Professor Santi Pailoplee, Ph.D.

Accepted by the Faculty of Science, Chulalongkorn University in Partial Fulfillment of the Requirements for the Master's Degree

.....Dean of the Faculty of Science

(Professor Supot Hannongbua, Dr.rer.nat.)

THESIS COMMITTEE

.....Chairman

(Assistant Professor Sombat Yumuang, Ph.D.)

.....Thesis Advisor

(Assistant Professor Santi Pailoplee, Ph.D.)

.....Examiner

(Kruawun Jankaew, Ph.D.)

.....External Examiner

(Paiboon Nuannin, Ph.D.)

ประโยชน์ ปวงจักร์ทา : การตรวจสอบการเปลี่ยนแปลงอัตราการไหวสะเทือนและขั้นตอนวิธีบริเวณ-เวลา-ความยาวรอยเลื่อนตามแนวชายแดนประเทศไทย-ลาว-พม่า (SEISMICITY RATE CHANGE AND REGION-TIME-LENGTH ALGORITHM INVESTIGATIONS ALONG THAILAND-LAOS-MYANMAR BORDERS) อ.ที่ปรึกษาวิทยานิพนธ์หลัก: ผศ. สันติ ภัยหลบลี้, 134 หน้า.

เพื่อที่จะวิเคราะห์พฤติกกรมการเกิดแผ่นดินไหวขนาดใหญ่ ($M_w \geq 6$) ที่จะเกิดขึ้นในพื้นที่ศึกษา ข้อมูลแผ่นดินไหวในบริเวณชายแดนไทย-ลาว-พม่าได้ถูกนำมาทดสอบโดยวิธีการทางสถิติ อ้างอิงจากงานวิจัยที่ประสบความสำเร็จในอดีต วิธีการทดสอบการเปลี่ยนแปลงอัตราการไหวสะเทือนและขั้นตอนวิธีบริเวณ-เวลา-ความยาวรอยเลื่อนจึงถูกนำมาใช้ในการศึกษานี้ แผ่นดินไหวขนาดใหญ่จำนวน 8 เหตุการณ์ที่เกิดขึ้นในพื้นที่ศึกษา ถูกนำมาเป็นกรณีศึกษาในการทดสอบย้อนหลัง กรณีวิธีการเปลี่ยนแปลงอัตราการการเกิดแผ่นดินไหว เมื่อกำหนดตัวแปรอิสระ T = 1.2 ปี และ N = 50 เหตุการณ์ สำหรับค่า Z ในขณะเดียวกันเมื่อกำหนดตัวแปรเฉพาะสำหรับ *RTL* r_0 = 120 กิโลเมตร และ t_0 = 2 ปี พบภาวะเงียบสงบก่อนเกิดแผ่นดินไหว 5 จากทั้งหมด 8 เหตุการณ์ นอกจากนี้ผลจากการทดสอบกับข้อมูลแผ่นดินไหวสังเคราะห์ พบว่าค่าความผิดปกติที่ตรวจวัดได้จากการศึกษานี้นั้น ไม่ได้เกิดจากความบังเอิญหรือการสุ่มของข้อมูล ดังนั้นจึงสรุปได้ว่าการศึกษาทั้งสองวิธีในพื้นที่บริเวณชายแดนไทย-ลาว-พม่า มีประสิทธิภาพเพียงพอที่สามารถตรวจจับการเปลี่ยนแปลงก่อนการเกิดแผ่นดินไหวขนาดใหญ่ได้

ซึ่งจากตัวแปรอิสระและตัวแปรเฉพาะที่เหมาะสมกับพื้นที่ศึกษา ผู้วิจัยได้ได้ประเมินร่วมกับข้อมูลแผ่นดินไหวที่ตรวจวัดได้ล่าสุด ผลการประเมินพบว่าทั้งวิธีการทดสอบการเปลี่ยนแปลงอัตราการไหวสะเทือนและขั้นตอนวิธีบริเวณ-เวลา-ความยาวรอยเลื่อนแสดงผลสอดคล้องกับงานวิจัยในอดีต ซึ่งบ่งชี้ว่าบริเวณทางตอนเหนือของประเทศไทยติดกับประเทศพม่านั้นเป็นพื้นที่ที่แสดงภาวะเงียบสงบแผ่นดินไหว และมีโอกาสที่จะเป็นแหล่งกำเนิดแผ่นดินไหวใหญ่ในอนาคต

ภาควิชา ธรณีวิทยา ลายมือชื่อนิสิต .....

สาขาวิชา โลกศาสตร์ ลายมือชื่อ อ.ที่ปรึกษาหลัก .....

ปีการศึกษา 2557

5572034023 : MAJOR EARTH SCIENCES

KEYWORDS: SEISMIC HAZARD ASSESSMENT / Z-VALUE INVESTIGATION/ RTL ALGORITHM/ THAILAND

PRAYOT PUANGJAKTHA: SEISMICITY RATE CHANGE AND REGION-TIME-LENGTH ALGORITHM INVESTIGATIONS ALONG THAILAND-LAOS-MYANMAR BORDERS. ADVISOR: ASST. PROF. SANTI PAILOPLEE, Ph.D., 134 pp.

In order to investigate the prospective areas of the upcoming strong earthquakes, i.e., $M_w \geq 6$, the seismicity data have been posed in the vicinity of Thailand-Laos-Myanmar borders were investigated statistically. Based on the successful investigation of previous work, two statistic techniques were applied in this study, i.e., seismicity rate change (*Z* value) and Region-Time-Length (*RTL*) algorithm. According to the completeness of the earthquake data, the available 8 case studies of strong earthquakes were investigated retrospectively. Regarding to the *Z* value, the condition of time window = 1.2 years, the number of earthquakes = 50 events, and fixed node radius = 250 km showed the locations of *Z* anomalies conformed to 5 of 8 earthquakes. Meanwhile, using characteristic parameters r_0 = 120 km, t_0 = 2 years, the *RTL* anomalies quite related to 5 of 8 earthquakes. Therefore, it is concluded that both *Z* and *RTL* methods applied in this study are fairly effective to evaluate the earthquake precursor. In order to evaluate the prospective area for the upcoming earthquake, both *Z* and *RTL* were analyzed with the complement by the suitable characteristic parameters mentioned above and the most up-to-date completeness seismicity data. The results reveal that the small area in the vicinity of Thailand-Myanmar border are quiescence seismically conforming to that proposed by the previous investigation of *b* value of the frequency-magnitude distribution. Therefore, it is concluded that according to both *Z*, *RTL*, and *b* value methods that the prospective areas proposed in this study might be posed by the upcoming earthquake.

Department:	Geology	Student's Signature	.....
Field of Study:	Earth Sciences	Advisor's Signature	.....
Academic Year:	2014		

ACKNOWLEDGEMENTS

I would like to sincerely and gratefully thank my advisor, Assistance Professor Dr. Santi Pailoplee, Department of Geology, Faculty of Science, Chulalongkorn University for his tolerant guidance, assistance, understanding and everything he has provided throughout this thesis. Moreover, I am indebted to him and his wife, Mrs. Teerarat Pailoplee, for helping the scholarship throughout my time as his student; without their generosity, I might complete this work difficulty.

I would also like to thank Associate Professor Dr. Montri Chuwong, Department of Geology, Faculty of Science, Chulalongkorn University for his valuable advices. I learned so much from his experiences. Moreover, without his suggestions, I might not have the important opportunities.

I also want to thank Professor Dr. Josaphat Tetuko Sri Sumantyo, Center for Environmental Remote Sensing, Chiba University for his kindness and encouragement. His suggestion provided me to gain a wider breadth of attitude and vision. In addition, I am grateful for all TWINKLE members (all International student exchange and all staffs of Twinkle program 2013, Chiba University) and Jasso scholarships for making me have a lot of important experiences throughout living in Japan.

Furthermore, I must express my gratitude to my parents, Mr. Jumrus Puangjaktha and Mrs. Sumalee Puangjaktha, for their motivation and everything support throughout my life; without them I might not have any inspirations.

Moreover, I would like to sincerely thank everyone who has contributed to my student life and this thesis. Even though bad or good actions, all things are the experiences that they can teach me to be better.

Finally, I hope this thesis would be educated and be useful to all readers. However, if there is anything missing or incomplete from this thesis, I would like to apologize to any readers. I always welcome your feedback.

CONTENTS

Page

Page

Page

LIST OF TABLES

LIST OF FIGURES

CHAPTER I

INTRODUCTION

1.1 Background

Among the various natural disasters, earthquake is one of the most devastating disasters. Based on United State Geological Survey (USGS, 2014), it is estimated that there are 500,000 detectable earthquakes strike the earth's surface each year. Around 100 of them can damage to the economy and made the massive loss of life, especially earthquakes along the subduction zone. Severe earthquakes all over the world are generally caused by plate tectonic activities, for example, the latest well known earthquake is the great earthquake magnitude (M_w) 9.0 occurred at 02:46:23 pm local time (05:46:23 UTC) on March 11, 2011 off the coast of Tohoku, Japan, caused from thrust faulting on the subduction zone plate boundary between the Pacific and North America plates, produced devastating tsunami waves larger than any recorded in this area during the past 1,000 years hit Japan's coast. As of August 8, 2012, the World Bank casualties reported 17,500 dead and 2,848 missing and 6,109 injured. The tsunami collapsed 130,000 buildings and severely damage 260,000 more, estimated economic damage $210 billion US dollars that it is resulting the costliest natural disaster in the history of the world (Federica and Mikio, 2014). Furthermore, the Great Hanshin earthquake (Kobe earthquake) magnitude (M_w) 6.8 occurred at 03:46 pm local time (20:46 UTC) on January 17, 1995, in the southern part of Hyogo Prefecture, Japan, realized the strike-slip fault system can make the severe devastation as well. The Great Hanshin earthquake belonged to an earthquake called "inland shallow earthquake". The inland shallow earthquakes usually occur along active faults. Even the lower magnitudes, they can lead to very catastrophic if they occur near city areas and if they hypocenters are located less than 20 km below the surface. The Great Hanshin earthquake caused over 6,000 deaths and approximately $100 billion in damage, 2.5% of Japan's GDP at the time. Hence, these events reminded us that the earthquake can be harmful to everywhere and every life.

Therefore, several methods were developed for reduce loss of life and diminish property damage during an impending earthquake. According to previous research works, seismologist divided the earthquake forecasting techniques in the long-term (10 years – 30 years) (Sykes, 1996), intermediate-term (months - 10 years) (Sykes, 1996), or even short-term (days-month) (Shebalin et al., 2006) (Table 1.1.).

Table 1.1. Different kinds of the earthquake forecasting (modified after Shebalin et al. (2006) and Pailoplee (2009c).

Method	Examples
A. Long-term (years)	
A1. Paleo-seismological study	McCalpin (1996); Pailoplee et al. (2009a)
A2. Historical study	McCue (2004); Stirling and Petersen (2006)
A3. Seismic hazard analysis	Kramer (1996); Pailoplee et al. (2009b)
A4. Global positioning system	Yagi et al. (2001); Fu and Sun (2006)
B. Intermediate-term (months-year)	
B1. b-value anomaly	Nuannin et al. (2005)
B2. Fractal dimension	Maryanto and Mulyana (2008)
B3. Artificial neural network	Bodri (2001); Alves (2006)
B4. Coulomb stress failure	Du and Sykes (2001); Bufe (2006)
C. Short-term (days-month)	
C1. Animal perception	Kirschvink (2000)
C2. Cloud Precursor	Menshikov et al. (2012)
C3. Ground water fluctuation	Oki and Hiraga (1988)
C4. Radon fluctuation	Zmazek et al. (2000)

Most techniques designed for approximation the time, location, or size of earthquakes that may occur in the future. Among these techniques, seismicity rate change (*Z*-value investigation) (Wyss and Habermann, 1988) and Region-Time-Length

algorithm (Sobolev and Tyupkin, 1997) are the success intermediate-term earthquake forecasting for using investigate the anomalous of seismic activities before hazardous earthquakes, i.e., Murru et al. (1999) used *Z* value to evaluate seismicity rate change before the 1983 Nihonkai-Chubu Earthquake (M = 7.7), the result shown seismic quiescence anomaly started 3.5 years before the main shock, Huang and Sobolev (2002) applied *RTL* algorithm to evaluate precursory seismicity changes before the 2000 Nemuro Peninsula earthquake (M = 6.8), the result shown seismic quiescence started 5 years before the occurrence earthquake, etc. Therefore, using both methods for investigating prior to earthquake may strengthen the understanding and provide useful information for determining earthquake activities and hazards that might be pose in the future.

At present, it is recognized that the Northern and Western Thailand is one of the seismotectonically active region. According to Polachan et al. (1991), Thailand is located on the Eurasian plate whose boundary is noticeable by an active east-dipping subduction zone enlarging from north India (Himalaya Frontal Thrust), passing to west Myanmar and west of Andaman - Nicobar Islands, and swinging eastward to southward along the Sumatra-Java trench The collision between Eurasian plate and Indo-Australian plate is the cause of the high seismic activity along the Sumatra-Andaman Subduction Zone. In addition, according to plate collision mentioned above, a number of inland seismogenic faults are dominated particularly for the Eurasian intraplate where Thailand, Laos, Myanmar including Southern China are located. Thus, various sizes of earthquakes generate continuously in the vicinity of mentioned region, especially the Thailand-Laos-Myanmar borders (Pailoplee et al., 2013). For example, the latest mentioned earthquake in Thailand is the 2014 Mae Lao earthquake magnitude (M_w) 6.0 occurred at 18:08:43 local time (11:08:43 UTC) on May 5, 2014, the epicenter was located in of Mae Lao District, southwest of Chiang Rai, Thailand (Figure 1.1). It is harmful directly to Northern Thailand people and killed one person and damage more than 1,400 buildings in Chiang Rai province. However, not only local earthquakes can affect to Thailand, but also earthquakes from the other seismic zones mentioned in the neighborhood countries are also dangerous. As the effective radius of seismic waves corresponding to their

magnitude, the severe earthquakes with high magnitude around Thailand can lead the ground shaking effect to the building in this country. This earthquake generating tsunami driven from epicenter to 14 countries along the Indian Ocean region, caused over 230,000 deaths or missing and up to 5 million people lost homes, estimated economic damage $10 billion US dollars. While the M_w-9.0 Sumatra-Andaman earthquake occurred, there are many areas in Thailand reported the felt. The effective radius of the main shock spanned more than 2,500 km around the epicenter (Figure 1.2).

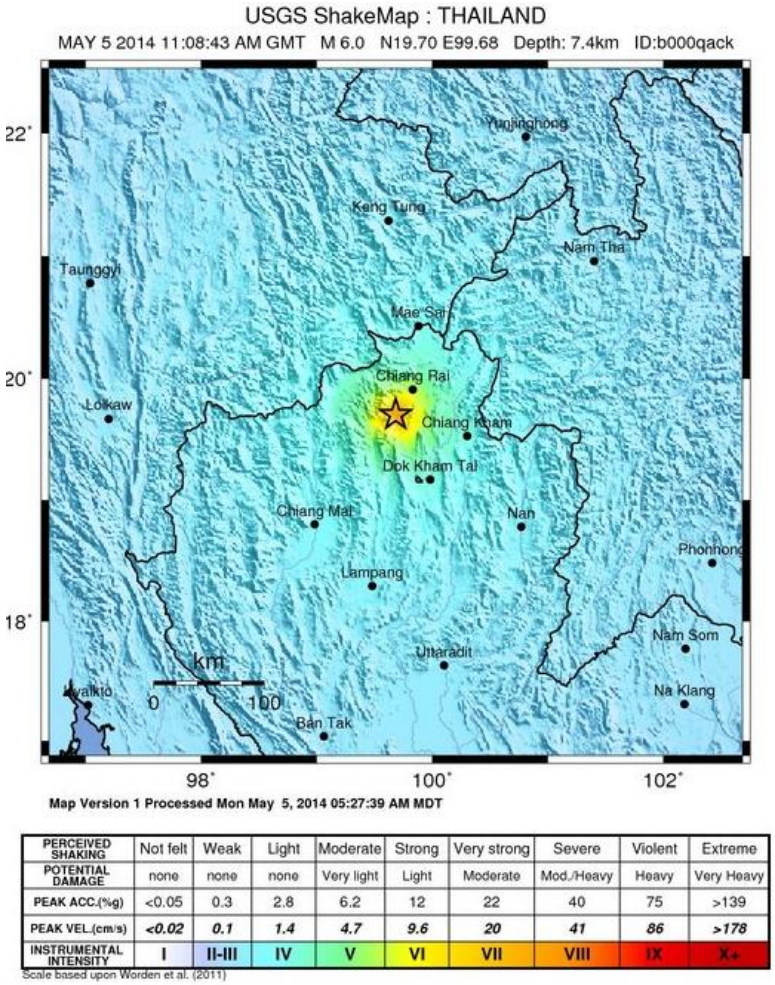

Figure 1.1. Map showing location of the M_w-6.2 (recalculated by GCMT) Mae Lao Earthquake on May 5, 2014 epicenter (orange star) and the area over which it was felt (yellow shaded area). Colored shades depict the maximum observed European Macro-seismic Scale intensity (USGS, 2014).

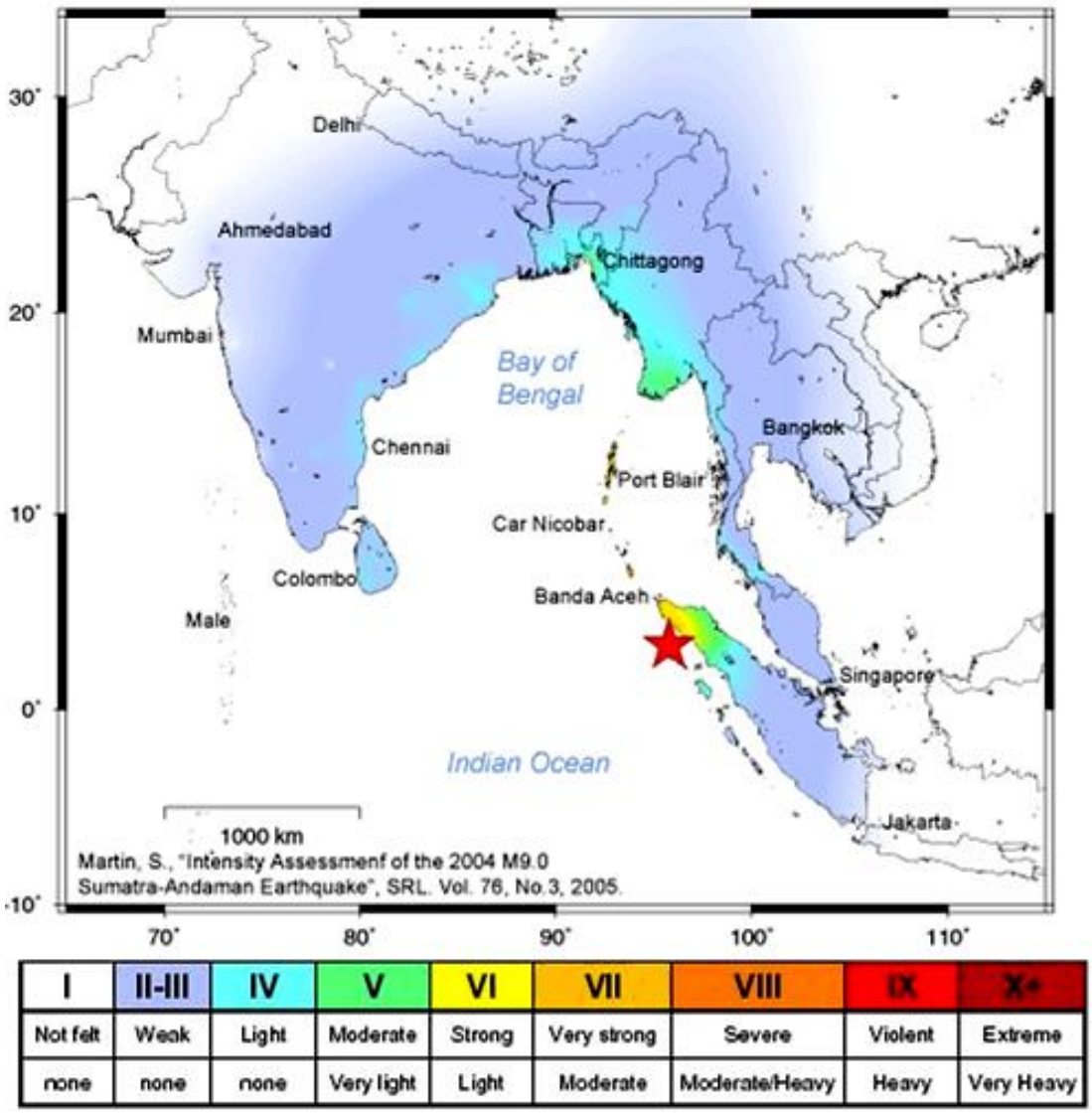

Figure 1.2. Map of mainland Southeast Asia showing location of the M_w-9.0 Sumatra-Andaman earthquake on December 24, 2004 (red star) and the area over which it was felt. Colored shades depict the maximum observed European Macro-seismic Scale intensity (Martin, 2005).

Regarding to the seismic hazard, Thailand can suffering by earthquakes, the example areas damaged by the M_w-9.0 Sumatra-Andaman earthquake and tsunami on December 24, 2004 and the M_w-6.0 Mae Lao earthquake on May 5, 2014 as shown in Figure 1.3.

Figure 1.3. a) A severely damaged Buddha statue in the Udomwaree temple, Chiang Rai, Thailand, after the occurrence of the M_w-6.2 Mae Lao Earthquake on May 5, 2014 (Chiangrai Times, 2014). b) The a large crack (over 50 meters stretch) on the highway No. 118 around kilometer marker 141, between Mae Lao and Mae Sruay districts, Thailand (Perawongmetha, 2014). c and d) Khao Lak beach before and after the M_w-9.0 Sumatra-Andaman earthquake on December 24, 2004, respectively (Jarl, 2005).

Hence, it can mention that Thailand is surrounded by high activity seismic sources, for example in Pailoplee and Choowong (2014), the great strike-slip Sagaing fault of Central Myanmar (Bertrand and Rangin, 2003), a complex shear zone near the Laos-southwestern China border (Socquet and Pubellier, 2005), the Andaman basin (Cattin et al., 2009) and etc., (Figure. 1.4).

According to the reasons introduced above, this thesis focuses mainly on applying *Z* value and *RTL* algorithm investigation for understanding the activities of an

earthquake and evaluating the hazard areas, which related to an impending earthquake in Thailand.

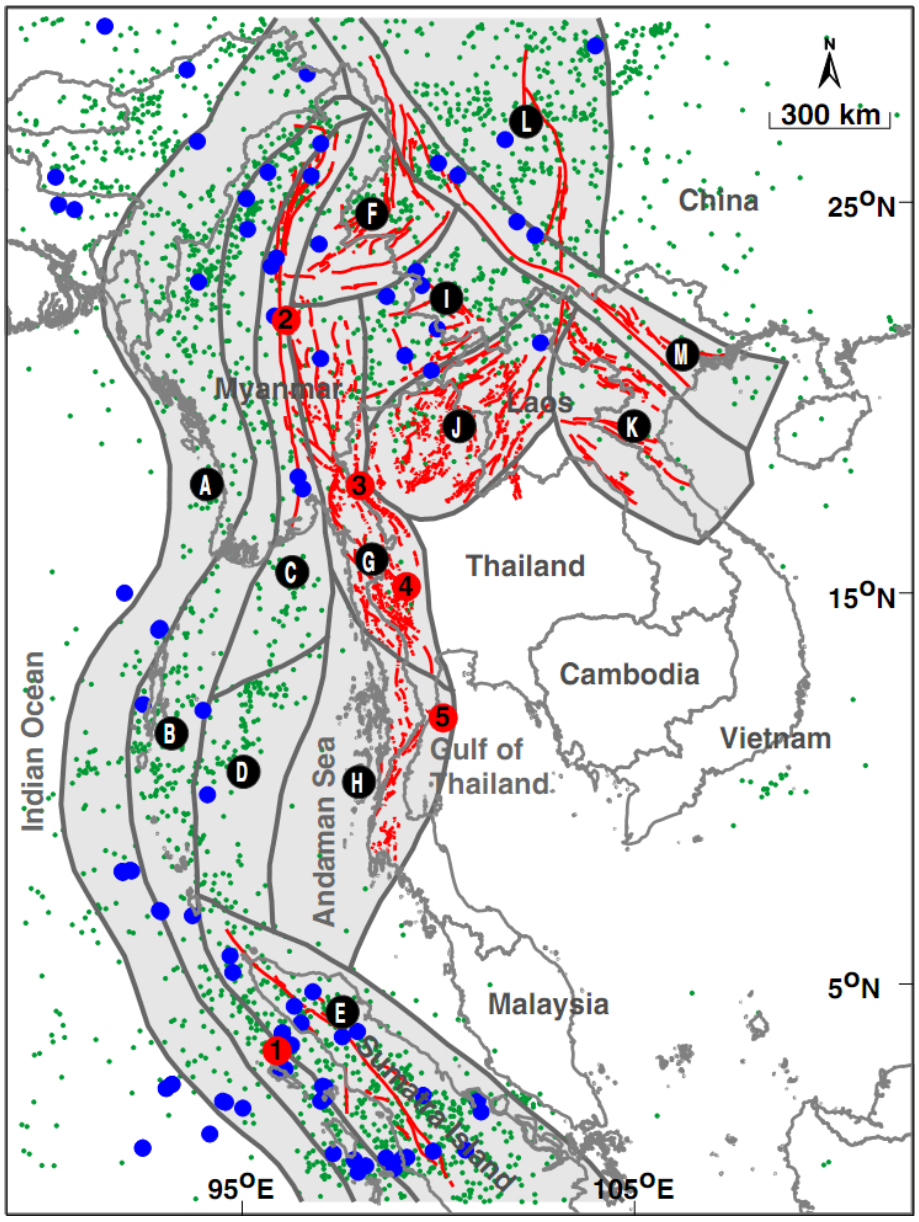

Figure 1. 4. Map of mainland Southeast Asia and the 13 designated seismic zones (A to M). Red lines indicate the fault lines compiled by Pailoplee et al. (2009a). Grey polygons represent the geometry of the individual seismic source zones proposed by Pailoplee and Choowong (2014).

1.2 Study Area

This research work focuses mainly on applying *Z* value and *RTL* algorithm along the Thailand-Laos-Myanmar borders region (16.76° – 22.30°N and 97.48° – 103.16°E) because this area is one of the earthquake hazard area that contains major cities, famous tourist attractions, hydropower dams, ancient architectures, and etc. Furthermore, as the Central of Thailand located on soft clay zone, the seismic wave of earthquake along Thailand-Laos-Myanmar borders can be amplified and affect to the buildings in the Central of Thailand, especially Bangkok. These building surrounded by risk active faults. Moreover, there are 8 strong earthquakes occurred in this area (Table 1.2 and Figure 1.5) since 1982. Therefore, this is the reason why these areas are considered. However, for completeness empirical calculation (Das et al., 2006) by both methods, this study investigate over radius 300 km around the study area. Therefore, the boundary area where the earthquake source spreads out to the latitude 13.77°N - 25.35°N and longitude 94.48°E - 106.07°E (Figure 1.6).

Table 1. 2. List of earthquake with moment magnitude (M_w) ≥ 6.0 posed in the Thailand Laos-Myanmar borders during 1982-2014.

No.	Longitude	Latitude	Date	Time	Depth (km)	Magnitude (M_w)
1	102.58	21.36	24/6/1983	09:07	49.0	6.9
2	99.62	21.79	23/4/1984	22:30	17.0	6.3
3	99.06	20.32	28/9/1989	21:52	15.0	6.2
4	99.22	21.89	11/7/1995	21:46	15.0	6.8
5	101.90	18.77	7/6/2000	21.48	33.0	6.5
6	100.89	20.52	16/5/2007	08:56	12.6	6.3
7	100.00	21.49	23/6/2007	08:17	16.1	6.1
8	100.02	20.62	24/3/2011	13:55	13.2	6.8
9	99.68	19.72	5/5/2014	11:08	12.0	6.2

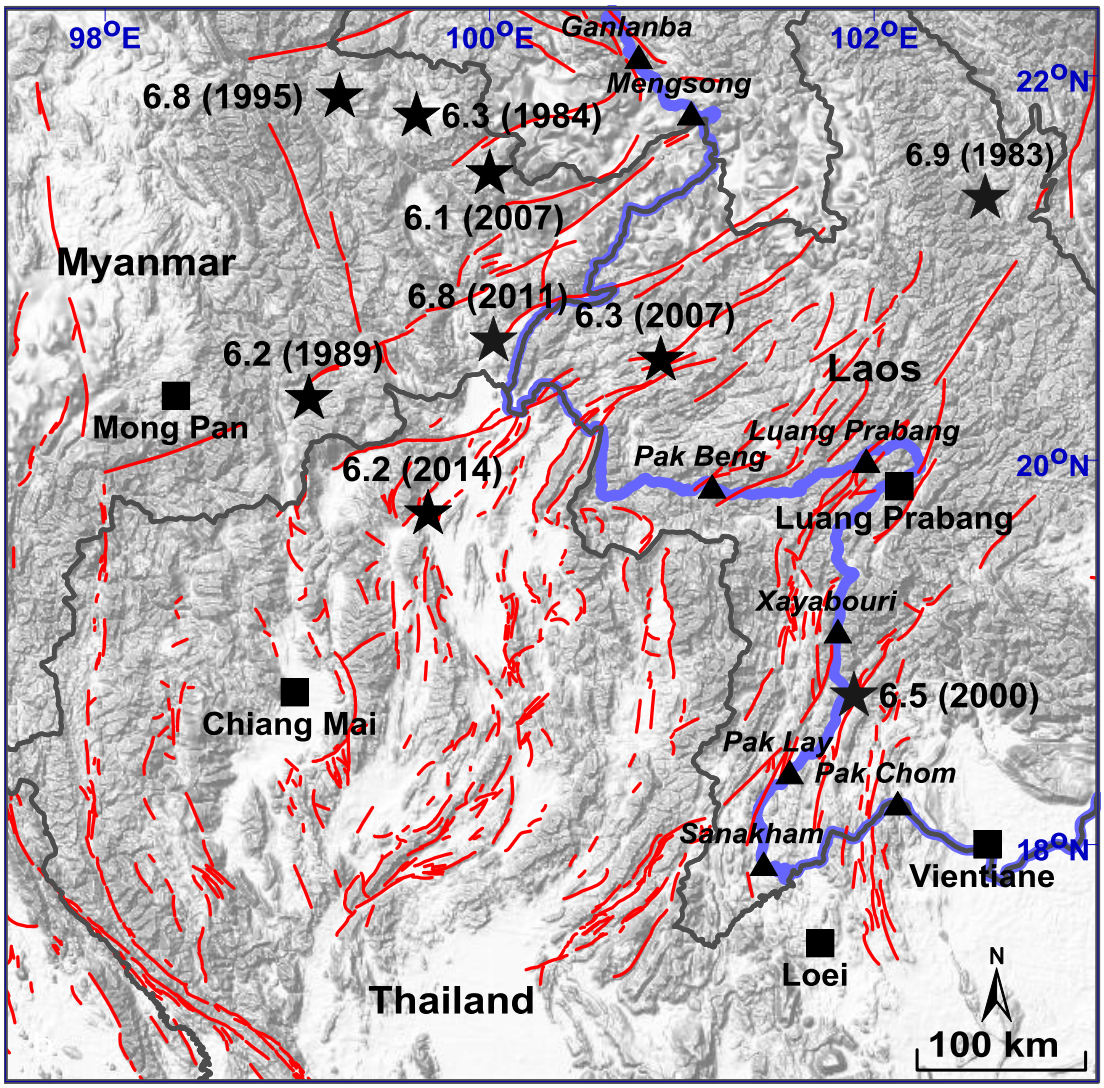

Figure 1.5. Map of study area showing the earthquake with $M_w \geq 6.0$ (black stars) distribution along Thailand-Laos-Myanmar borders during the period 1989 and 2014. The fault lines, hydro-power dams and major cities were shown by thin red lines, black triangles and black squares, respectively.

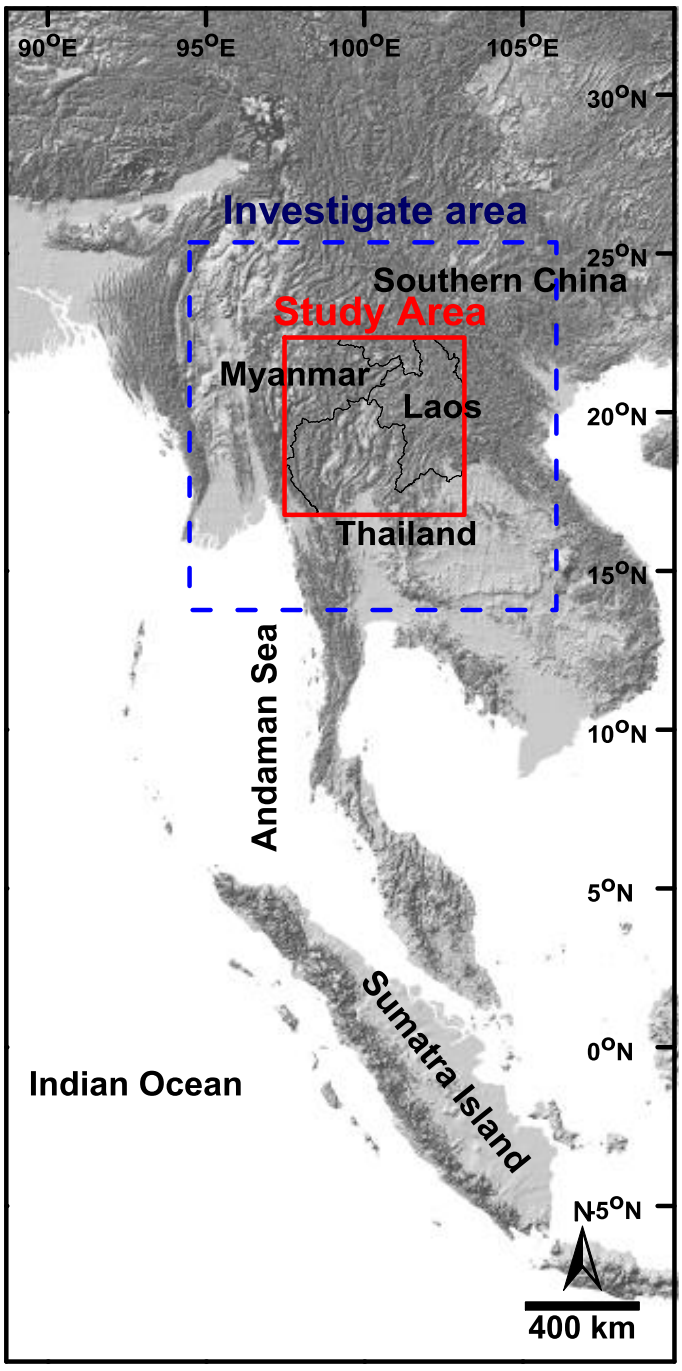

Figure 1.6. Map of mainland Southeast Asia showing the area which the earthquake sources were investigated (13.77° – 25.35°N and 94.48° – 106.07°E, outer box with blue dash line) and the study area for illustrating seismic quiescence patterns (16.76° – 22.30°N and 97.48° – 103.16°E, inner box with red line).

1.3 Objectives

The purposes of this study are;

1. To investigate the precursory seismicity preceding large earthquake in Thailand-Laos-Myanmar border by using Seismicity Rate Change (Z-value investigation),
2. To investigate the precursory seismicity preceding large earthquake in Thailand-Laos-Myanmar border by using Region-Time-Length (*RTL*) algorithm, and
3. To compare the results obtained from two techniques mentioned above and contribute the hazard map showing the locations of prospective areas that the hazardous earthquake generated in the future.

CHAPTER II

THEORY AND METHODOLOGY

Earthquakes worldwide are known to be related to tectonic activities both regional and local scales. However, the mechanism of earthquakes is not clearly understood and still controversy. While this question has yet to be decided, seismologists try to develop several earthquake forecasting methods by deducing on the basis of geotectonics, field investigation, and past historical earthquakes (Charusiri et al., 2007). Recently, the development of process to analyze the earthquake hazard (e.g., earthquake network, earthquake recording instrument, earthquake analyzing software and so on) were developed rapidly. Then, there are many researches about seismology were reported in the last decade. Among these researches, the statistical seismicity analysis is one of the popular concepts using to evaluate and understand earthquake behavior in long-term, intermediate-term, or short-term. Therefore, seismologists have created a number of new methods for seismicity based earthquake forecasting. Most techniques designed for approximation the time, location, or size of earthquakes that may occur in the future.

According to the past historical earthquake studies, earthquake forecasting techniques can classify in the duration of long-term, short-term and intermediate-term. However, after seismicity system improved in the last decade, the intermediate-term earthquake forecasting was more popular than the others. Then, there are many techniques created for forecasting an earthquake in the intermediate-term, divided into 2 models as physical process and smoothed process, i.e., Accelerating Moment Release (*AMR*) (Ben-Zion and Lyakhovsky, 2002), Pattern Informatics (*PI*) index (Holliday et al., 2006), Variation in *b*-value (Cao et al., 1996), Region-Time-Length (*RTL*) algorithm (Sobolev and Tyupkin, 1997; 1999) The Load–Unload Response Ration (*LURR*) (Yin et al., 1995), and so on (Table 2.1.) (Tiampo and Shcherbakov, 2012). Among those methods, there are many researches confirmed that Seismicity Rate Change (*Z* value) (Bachmann, 2001; Chouliaras, 2009b; Katsumata, 2011a; Katsumata and Sakai, 2013; Maeda and

Wiemer, 1999; Murru et al., 1999; Öztürk, 2013; Wiemer and Wyss, 1994; Wu et al., 2008; Wu and Chiao, 2006; Wyss et al., 1999) and Region-Time-Length (*RTL*) algorithm (Chen and Wu, 2006; Gambino et al., 2014; Gentili, 2010; Huang, 2004; 2005; Huang et al., 2001; Jiang et al., 2004; Nagao et al., 2011; Rong and Li, 2007; Sobolev and Tyupkin, 1997; 1999) can investigate an earthquake precursor (Tables 2.2 and 2.3). For understanding the concept of both techniques, the details about Seismicity Rate Change and *RTL* algorithm are defined in topics 2.1 and 2.2.

Table 2.1. List of the seismicity-based earthquake forecasting techniques: Ten years of progress, modified after Tiampo and Shcherbakov (2012).

Method	Examples
A. Physical process models	
A1. Accelerating moment release (*AMR*)	Ben-Zion and Lyakhovsky (2002)
A2. Characteristic earthquakes	Schwartz et al. (1981)
A3. Variation in *b*-value	Imoto et al. (1990); Cao et al. (1996)
A4. The M8 family of algorithms	Keilis-Borok and Kossobokov (1990)
A5. Region-Time-Length (*RTL*) algorithm	Sobolev and Tyupkin (1997)
A6. The Load-Unload Response Ration (*LURR*)	Yin et al. (1995)
A7. Pattern Informatics (*PI*) index	Holliday et al. (2006)
B. Smoothed seismicity models	
B1. *EEPAS*	Evison and Rhoades (1997)
B2. Time-independent smoothed seismicity	Werner et al. (2010)
B3. *ETAS* methodologies	Ogata (1988)
B4. Relative Intensity (*RI*) method	Holliday et al. (2005)
B5. TripleS	Zechar and Jordan (2010)
B6. Non-Poissonian earthquake clustering	Ebel et al. (2007)
B7. Seismic earthquake potential models	Ward (2007)

Table 2.2. The example list of worldwide previous studies for investigating on the phenomenon of precursory seismic quiescence before crustal main shocks using Seismicity Rate Change (*Z* value). *Q*-Detection indicated the estimated duration between the beginning of seismic quiescence and the occurrence time of main shock.

Earthquake Location	Year	Magnitude (M_W)	*Q*-Detection (year)	References
Southern California (USA)	1992	7.5	4.00	Wiemer and Wyss (1994)
Nihonkai-Chubu (Japan)	1983	7.7	> 3.50	Murru et al. (1999)
Chiba-toho-oki (Japan)	1987	6.7	1.5 ± 0.5	Maeda and Wiemer (1999)
Off-Sanriku (Japan)	1989	7.1	2.5 ± 1.0	Wyss et al. (1999)
Kefalonia Island (Greece)	1983	6.2	6.00	Chouliaras and Stavrakakis (2001)
Chi-Chi (Taiwan)	1999	7.6	0.75	Wu and Chiao (2006)
Cheng Kung (Taiwan)	2003	6.8	1.10	Wu et al. (2008)
Peloponesus (Greece)	2008	6.4	7.00	Chouliaras (2009a)
Bingöl (Turkey)	2009	6.4	5.73	Öztürk and Bayrak (2009)
Coast of Tohoku (Japan)	2011	9.0	23.40	Katsumata (2011b)
Elazığ region (Turkey)	2010	6.0	5.00	Öztürk and Bayrak (2012)
Ibaraki-oki (Japan)	2008	7.0	2.40	Katsumata and Sakai (2013)

Table 2.3. The example list of worldwide previous and ongoing studies for investigating on the phenomenon of precursory seismic quiescence before crustal main shocks using *RTL* algorithm. *Q*-Detection indicated the estimated duration between the beginning of seismic quiescence and the occurrence time of main shock.

Earthquake Location	Year	Magnitude (M_w)	*Q*-Detection (year)	References
Kamchatka region	1992	7.1	1.00-2.50	Sobolev and Tyupkin (1997)
(Russia)	1993	7.4		and Sobolev and Tyupkin
	1993	7.1		(1999)
Reggio Emilia	1996	4.8	4.00	Giovambattista and Tyupkin
(Russia)				(2009)
Kobe (Japan)	1995	7.2	1.20	Huang et al. (2001)
Nemuro Peninsula	2000	6.8	5.00	Huang and Sobolev (2002)
(Japan)				
Izmit (Turkey)	1995	7.4	4.00	Huang (2004)
Totori (Japan)	2000	7.3	1.50	Huang (2005)
Chi-Chi (Taiwan)	1999	7.6	2.00	Chen and Wu (2006)
Umbria-Marche	1997	6	2.40	Mignan and Giovambattista
(Italy)				(2008)
Iwate (Japan)	2008	7.2	1.00	Nagao et al. (2011)
Aeolian	2010	4.8	1.25	Gambino et al. (2014)
Archipelago (Italy)				

Remark: Even though *Z*-value investigation and *RTL* algorithm can use for investigating seismic quiescence and seismic activation before the main shock of earthquake, there are few studies about seismic activation at present. Therefore, this study focus to investigate seismic quiescence stage mainly.

2.1 Seismicity Rate Change (Z value)

A gridding technique (*ZMAP*, Wiemer and Wyss (1994)) is designed to investigate or monitor the spatiotemporal changes in seismicity quantitatively prior to large earthquakes, using statistical factors based on the hypothesis that the significant reduction of seismicity from the background rate (seismic quiescence) restricted to a main shock (possibly its vicinity) in the intermediate-term (months to years). For simplification shortly, the illustrations explain about seismic quiescence are Figure 2.1 and Figure 2.2.

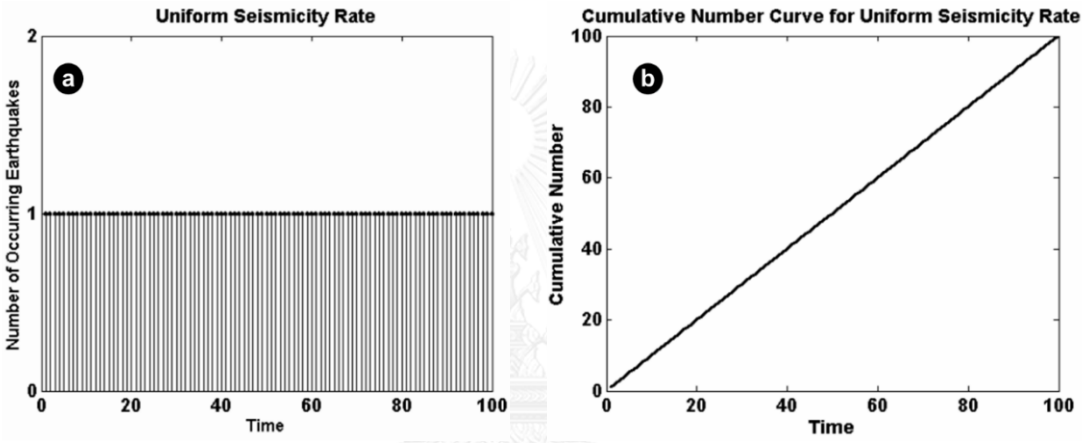

Figure 2.1. Showing a) uniform seismicity rate and b) cumulative number plotted against time (Bachmann, 2001).

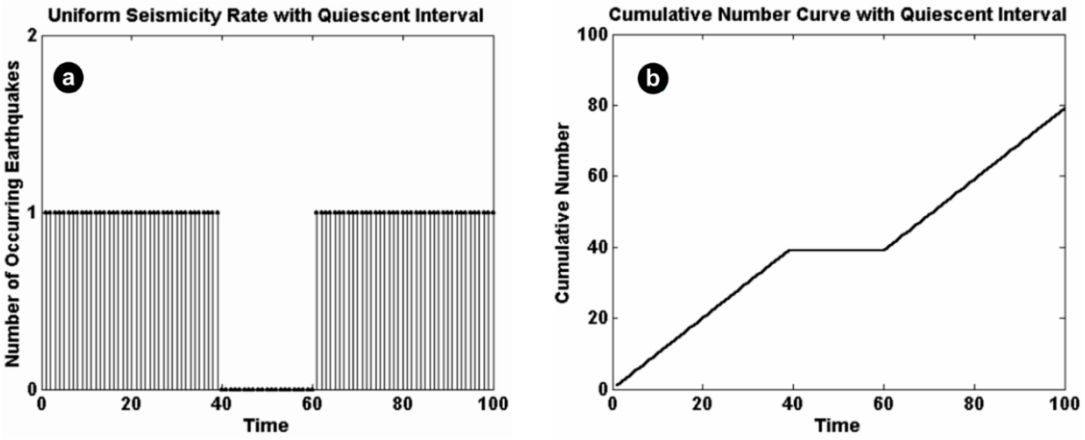

Figure 2.2. Showing a) seismicity rate with quiescence stage and b) cumulative number with quiescence stage plotted versus time (Bachmann, 2001).

During the uniform seismicity rate (Figure 2.1a), the cumulative number curve shows a straight line (Figure 2.1b). However, while the seismicity rate during time 40 and 60 do not occur (Figure 2.2a), the cumulative number curve indicates a flat part during time 40 and 60 (Figure 2.2b). The absence of seismicity rate in Figure 2.2a and the flattening in the cumulative number curve in Figure 2.2b are ways of how seismic quiescence stage can be detected (Bachmann, 2001). For summary this technique briefly, the study area is separated by a suitable grid spacing. In each grid node, a circle is drawn with the node radius (r) spanned until it can select a total number of earthquake events (n), the resolution depending on the value of earthquake events. The grid spacing, radius and total number of earthquakes are variable and inversely related to the local seismicity pattern because r and n is kept constant to allow statistical comparisons. Thus, the cumulative number of earthquakes is plotted versus time period at each grid node, starting at a time t_0 and ending at a time t_e. A time window is then placed, starting at T_S and ending at $T_S + T_W$, where $t_0 \leq T_S \leq T_S + T_W \leq t_e$. For each node radius, the Z value is computed, using the function LTA (Long Term Average) defined by Wiemer and Wyss (1994) (Figure 2.3), and the Z value that we can defined as equations (2.1) – (2.5).

$$Z(x,y,t) = (R_{bg} - R_w)/[(S_{bg}/n_{bg}) + (S_w/n_w)]^{1/2} \quad (2.1)$$

$$R_{bg} = (\sum_{i=t_0}^{T_S-1} r_i + \sum_{i=T_S+T_W}^{t_e} r_i)/[((T_s - 1) - t_0) + (t_e - (T_s + T_w))] \quad (2.2)$$

$$R_{bg} = (\sum_{i=T_S}^{T_S+T_W} r_i)/[(T_s + T_w) - T_s) + 1] \quad (2.3)$$

$$S_{bg} = [\sum_{i=t_0}^{T_S-1} (r_i - R_{bg})^2 + \sum_{i=T_S+T_W}^{t_e} (r_i - R_{bg})^2]/[((T_s - 1) - t_0) + (t_e - (T_s + T_w))] \quad (2.4)$$

$$S_w = [\sum_{i=T_S}^{T_S+T_W} (r_i - R_{bg})^2]/[(T_s + T_w) - T_s) + 1] \quad (2.5)$$

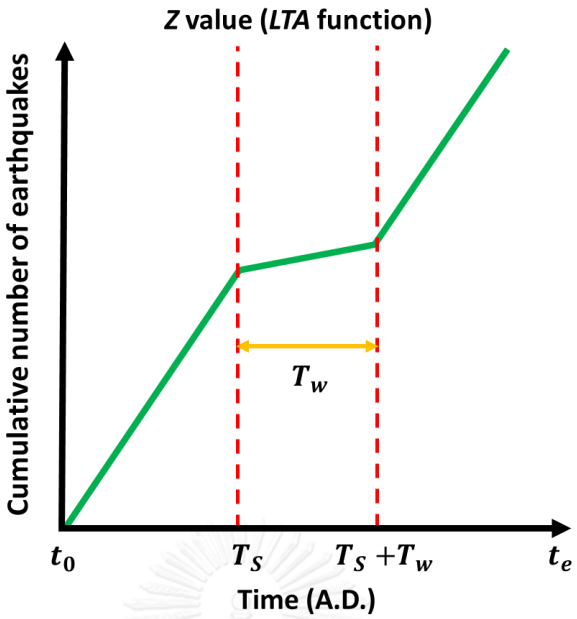

Figure 2.3. Showing temporal diagram clarification of how to calculate Z value. In each grid nodes, the Z value are computed for all times T_s between t_0 and t_e to T_w and is statistically suitable for analyze seismicity rate change in a time window (T_w) in difference with background seismicity. T_w is the length of the time window in year and T_s is the "current time" ($t_0 < T_s < t_e$) (Öztürk, 2013).

Where $Z(x, y, t)$ is the value of Z at the node location (x, y) is the interest time, R_{bg} is the background of seismicity rate in overall period including $T_W (t_0 - t_e)$, R_w is the mean of seismicity rate in the considered time window ($T_s - T_s + T_w$), S_{bg} and S_w are the standard deviations of R_{bg} and R_w, respectively, n_{bg} and n_w are the corresponding numbers of samples. A positive Z value represents that the seismicity rate is lower than the background rate. A decrease of the seismic rate indicates that seismic quiescence occurred in the interest area (Katsumata, 2011a).

An example procedure about the temporal of *ZMAP* computation is as follows; first, the events of earthquakes are collected within a time window called a bin with a period of 14 days (following as previous works). The period of seismicity catalogue is 3,653 days during 1 Jan 2000 and 31 December 2009. Consequently, the number of bins is 3,653/14~261. Assuming that the i^{th} bin includes r_i (i = 1 to 261) events, T_w is set for 5

years from the 120^{th} to the 180^{th} bin. R_{bg} and R_w, are the calculated in equations (2.6) – (2.9).

$$R_{bg} = (\sum_{i=1}^{119} r_i + \sum_{i=181}^{261} r_i)/(199+81) \quad (2.6)$$

$$R_w = (\sum_{i=120}^{180} r_i)/(61) \quad (2.7)$$

$$S_{bg} = [\sum_{i=1}^{119} (r_i - R_{bg})^2 + \sum_{i=181}^{261} (r_i - R_{bg})^2]/(119+81) \quad (2.8)$$

$$S_w = [\sum_{i=120}^{180} (r_i - R_{bg})^2]/61 \quad (2.9)$$

Then, the *Z*-value is calculated from equation (2.1) using R_{bg}, R_w, S_{bg}, S_w, n_{bg} = 200 and n_w = 61. For generating hazard map, a sketch of *ZMAP* calculation is given in Figure 2.4.

Regarding to Figure 2.4, at first, the study area is gridded spacing (blue dashed line) (Figure 2.4a), Secondly, in each grid node (red point), the minimum number of collected earthquake events (*n*, orange points) are determined depending on the density of earthquake events in the study area, the more collecting number of earthquake events, the more collecting radius. Then, the closest earthquake events (black dashed arrow) that there have occurred in set time window (T_w) are collected until it includes a total of epicenters *n* (Figure 2.4b). Next, in each time window, all nodes are calculated using *Z*-value equation by Wiemer and Wyss (1994) (Figure 2.4c). Finally, the *ZMAP* were generated after estimating seismicity rate change in the study area, the positive *Z* indicates seismic quiescence and the negative *Z* indicates seismic activation, the anomaly (red shaded) zone implies the area that its trend to have an impending earthquake (Figure 2.4d).

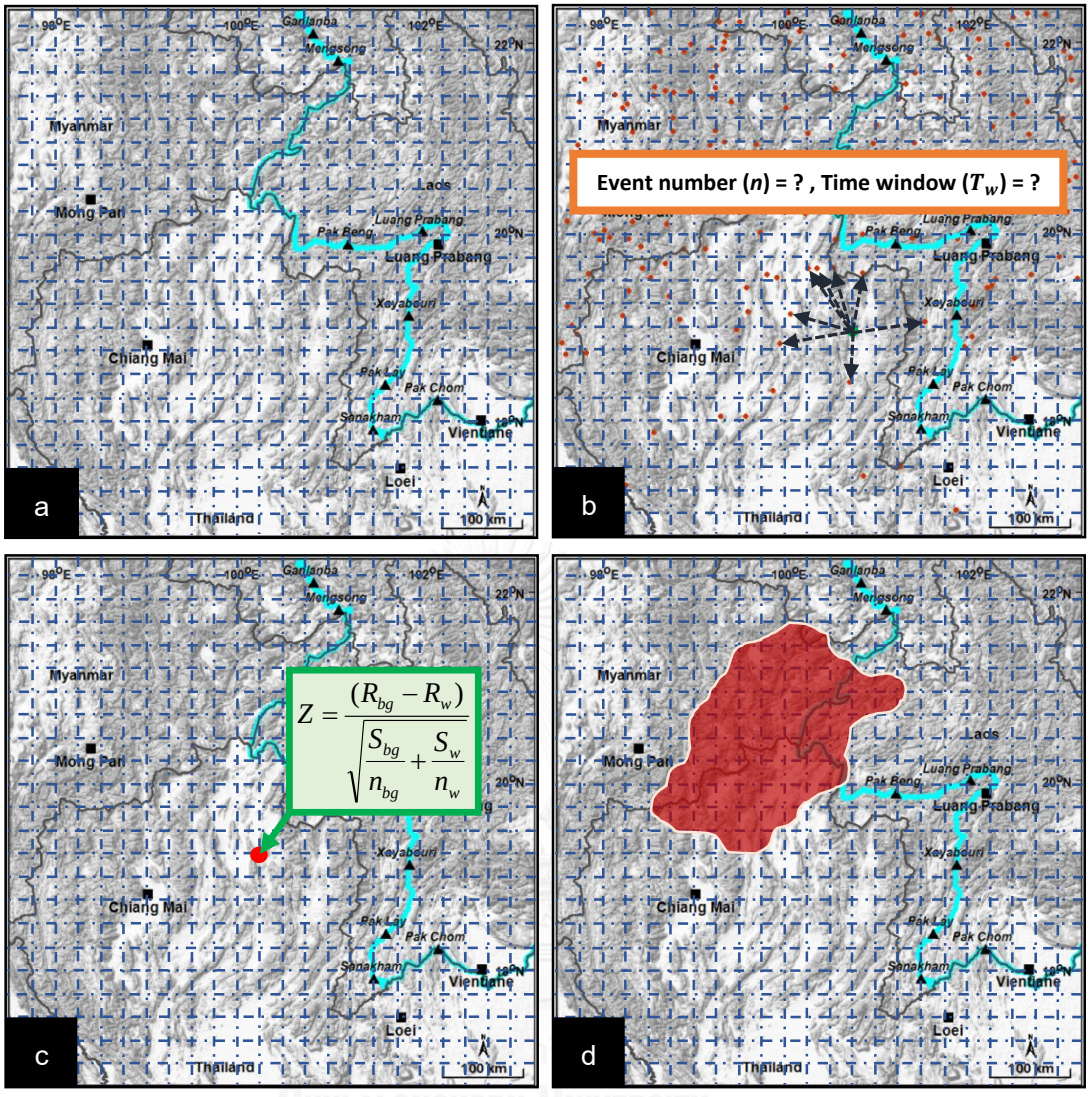

Figure 2.4. The illustrations showing the methodology for spatial investigation of Z values. a) The study area is gridded with the equal spacing (blue dashed line). b) Using Z parameter to determine T_w and n, the closest earthquake events (black dashed arrow) that there have occurred in the set time window (T_w) are collected until it includes a total of epicenters n. c) Calculate the Z value by using Z equation. d) Positive Z value indicates seismic quiescence (red shade).

2.2 Region-Time-Length Algorithm

According to Huang (2004), Region-Time-Length (*RTL*) algorithm is another useful gridding technique developed recently to analyze the precursory seismicity pattern changes, i.e., seismic quiescence and seismic activation stages, before the occurrence of the main shock. This statistic method was initially tested at Kamchatka, Russia. The results found that the major earthquakes with $M \geq 7.0$ in Kamchatka had been preceded by a significant seismic quiescence stage started 1.5 – 3.5 years prior to the main shock of a major earthquake. Moreover, after the end of seismic quiescence stage (lasted 1.0 – 2.5 years before events), seismic quiescence stage changes to be activation stage with a duration varying from 0.5 –1.5 years (Sobolev and Tyupkin, 1997; 1999). This success is the beginning of the present-day *RTL* investigation.

The concept of *RTL* algorithm base on the seismo-acoustic experiments by Sobolev (1995), the results indicated that the acoustic emission may rise as the loading increases. However, the number of relatively weak signals tends to decrease after the loading reaches the maximum, because small cracks are no longer generated due to the partial reduction of stress. During the final stage before the main rupture, acoustic signal activity increases again. In other word, acoustic emission can experience the stages of quiescence and activation prior to the main rupture. After then, Sobolev and Tyupkin (1997) suggested the *RTL* algorithm by using the basic hypothesis based on three dimensionless parameters called *R* (interested region), *T* (time) and *L* (rupture length) that we can define as equations (2.10) – (2.13).

$$R(x,y,z,t) = \left[\sum_{i=1}^{n} \exp\left(-\frac{r_i}{r_0} \right) - R_{bg}(x,y,z,t) \right] \tag{2.10}$$

$$T(x,y,z,t) = \left[\sum_{i=1}^{n} \exp\left(-\frac{t-t_i}{t_0} \right) - T_{bg}(x,y,z,t) \right] \tag{2.11}$$

$$L(x,y,z,t)=\left[\sum_{i=1}^{n}\exp\left(-\frac{l_i}{r_i}\right)-L_{bg}(x,y,z,t)\right] \quad (2.12)$$

$$V_{RTL}(x,y,z,t)=R(x,y,z,t)\bullet T(z,y,z,t)\bullet Z(x,y,z,t) \quad (2.13)$$

Where (*x, y, z, t*) specifies the focused location and time; r_i is the range from the interested location of (*x, y, z*) to the i^{th} earthquake's epicenter; t_i is the incident time of the i^{th} earthquake, r_0 and t_0 are the characteristic distance and characteristic time-span of interested region; l_i is the rupture length of the i^{th} considering earthquake, converted by using the empirical relationship among magnitude and rupture length as defined in equation (2.14), *M* is magnitude of earthquake and *SRL* indicate surface rupture length (Wells and Coppersmith, 1994); $R_{bg}(x, y, z, t)$, $T_{bg}(x, y, z, t)$ and $L_{bg}(x, y, z, t)$ are the background values of $R(x, y, z, t)$, $T(x, y, z, t)$ and $L(x, y, z, t)$, respectively; *n* is the number of events with *RTL* parameters satisfying some criteria, e.g., $M_i \geq M_{min}$ (M_i is the magnitude of the i^{th} earthquake and M_{min} is the cut-off magnitude assuring the completeness of earthquake data), $2r_0 = R_{max} \geq r_i$ and $2t_0 = T_{max} \geq t - t_i$ and $V_{RTL}(x, y, z, t)$ is the *RTL* function.

$$M = 5.08 + 1.16 * \log(SRL) \quad (2.14)$$

Afterward, we bounded the variation range of the numerical values of *RTL* functions in [-1, 1] before plotting the temporal *RTL* curves by using the normalized equation as equation (2.15) (Jiang et al., 2004). The result of normalized *RTL* function can insulate the earthquake behavior in the interested region that $V_{RTL} = 0$ represented normal earthquake activity, $V_{RTL} > 0$ represented seismic activation and $V_{RTL} < 0$ represented seismic quiescence.

$$V_{RTL}(x,y,z,t)=\frac{R(x,y,z,t)}{R(x,y,z,t)_{\max}}\bullet\frac{T(x,y,z,t)}{T(x,y,z,t)_{\max}}\bullet\frac{L(x,y,z,t)}{L(x,y,z,t)_{\max}} \quad (2.15)$$

Eventually, to quantify the seismic quiescence stage, we used $Q(x, y, z, t_1, t_2)$ function or *Q*-parameter developed by Huang (2004) for average the *RTL* values at the position (x, y, z) during the interested time window $[t_1, t_2]$. The $Q(x, y, z, t_1, t_2)$ function is defined as equation (2.16).

$$Q(x,y,z,t_1,t_2) = \left[\sum_{i=1}^{n} V_{RTL}(x,y,z,t_i) \right] \tag{2.16}$$

Where t_i is the focus time in the time window $[t_1, t_2]$ $V_{RTL}(x, y, z, t_i)$ is the normalized *RTL* values calculated as the product of the equation (2.15) applying to the earthquakes in cylindrical volume, n is the minimum number of earthquake data for computing V_{RTL} values. In this study, the *Q*-parameter at each grid node is computed at a bin (time step) of 14 days available in $[t_1, t_2]$. For generating hazard map, a sketch of the *RTL* value calculation is given in Figure 2.5.

According to Figure 2.5, at first, the study area is gridded with the equally spacing (blue dashed line) (Figure 2.5a). Secondly, in each grid node (red point), the characteristic distance r_0 and characteristic time span t_0 are determined depending on the density of earthquake events in the study area. The area of the collecting seismicity data is fixed by $2r_0$ (red dash circle), the distance from selected grid node (x, y) to the position of i^{th} earthquake's epicenter (r_i, black dashed arrow) that have occurred in the maximum of radius (R_{max}, black arrow) and during the time window (T_{max}) are collected altogether (Figure 2.5b). Then, in each time window, all nodes are calculated using the *RTL* algorithm by (Sobolev and Tyupkin, 1997) (Figure 2.5c). Finally, the *RTL* map was generated after normalizing *RTL* values all nodes, positive *RTL* indicates seismic activation and negative *RTL* indicates seismic quiescence, the quiescence anomaly (red shaded) zone implies the area that might be posed by the impending earthquake (Figure 2.5d).

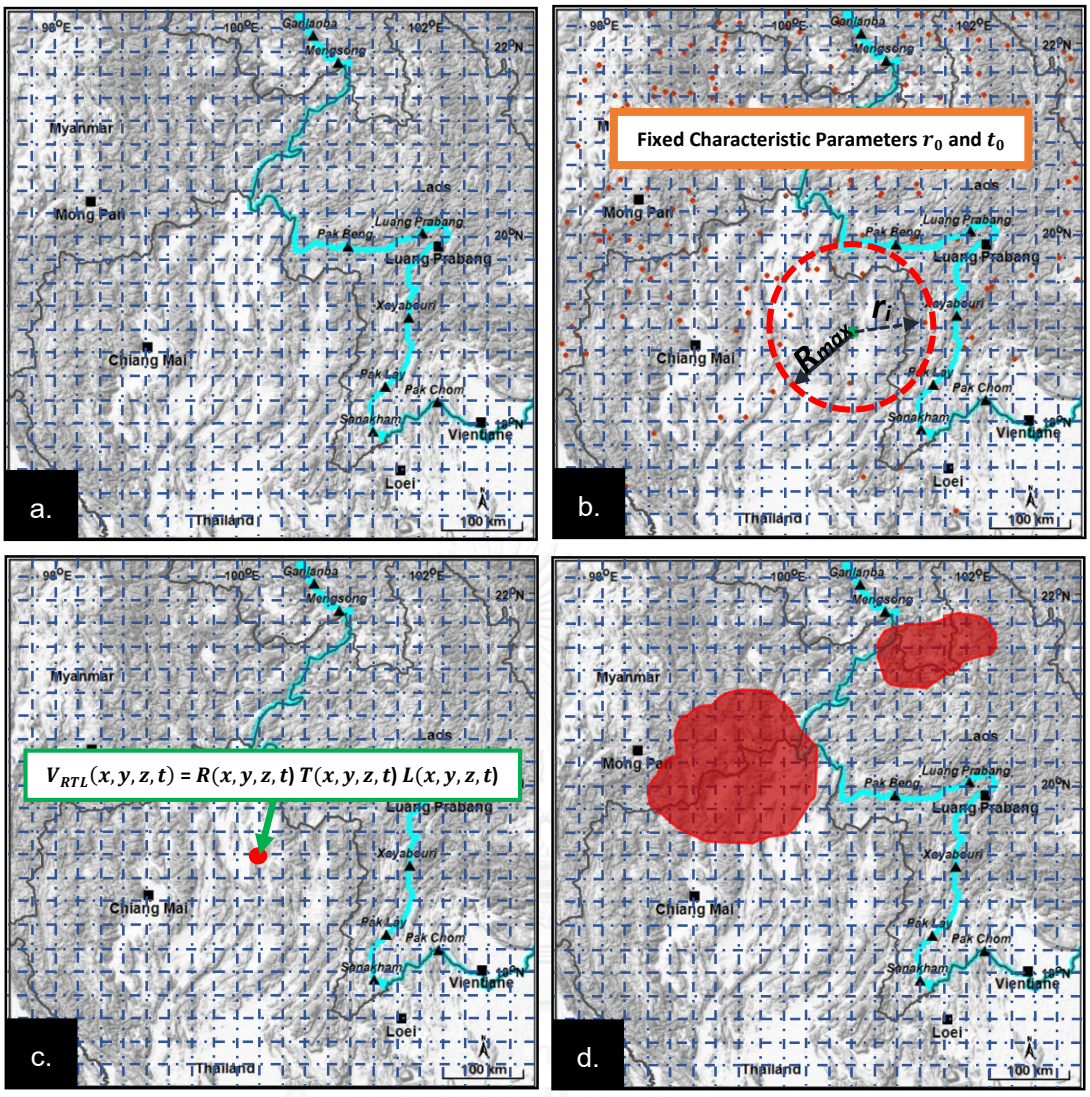

Figure 2.5. The illustrations showing the methodology of spatial investigation of the *RTL* value, a) the study area is gridded with the equally spacing (blue dashed line), b) using *RTL* parameter to determined T_w and $R_{max,}$ then, calculate *RTL* value, c) Normalize *RTL* value by using V_{RTL} equation and d) negative normalized *RTL* value indicates seismic quiescence (red shade).

2.3 Literature Reviews

2.2.1 *Z*-value Investigation

Wu et al. (2008) applied *ZMAP* for investigation the variations in seismicity pattern changes in the Taiwan region prior to the M_w-6.8 Chengkung earthquake, Taiwan, on December 10, 2003 by computing the standard normal deviate of the *Z* values and *b* values from the Gutenberg–Richter relation using the seismicity catalogue from the Central Weather Bureau Seismic Network (CWBSN). The result detected the relation between *Z*-values and *b*-values investigation, the high *Z* value areas corresponding to the region of low *b* value (Figure 2.6). The anomalies of both methods surrounding the Chengkung earthquake source region before the main shock occurred. Wu et al. (2008) mentioned that the relatively low seismicity rate and the decrease in the *b* values may be the precursory phenomena conform with the quiescence in overall seismicity and the activation of moderate-sized events occurred around the epicenter area before the Chengkung earthquake.

Chouliaras (2009b) applied *ZMAP* for identifying seismic quiescence and seismic activation before the M_s-5.7 earthquake on December 13, 2008 (08:27:20 GMT), which the main shock occurred near the city of Lamia in Central Greece. In this investigation, Choliaras calculated *ZMAP* by using the earthquake catalogue from the National Observatory of Athens-Institute of Geodynamics (NOA-IG) for the region 37.00° - 39.00° N and 19.00° - 23.50°E during 1964 and 2008. After varying conditions, the results shows the choice of using number of events (n) = 70, time window (T_w = 4.5 years) and grid spacing = 0.05 ° can detect the seismic quiescence started 8 years cover the epicenter of impending main shock with a duration of almost 2.5 years (Figure 2.7).

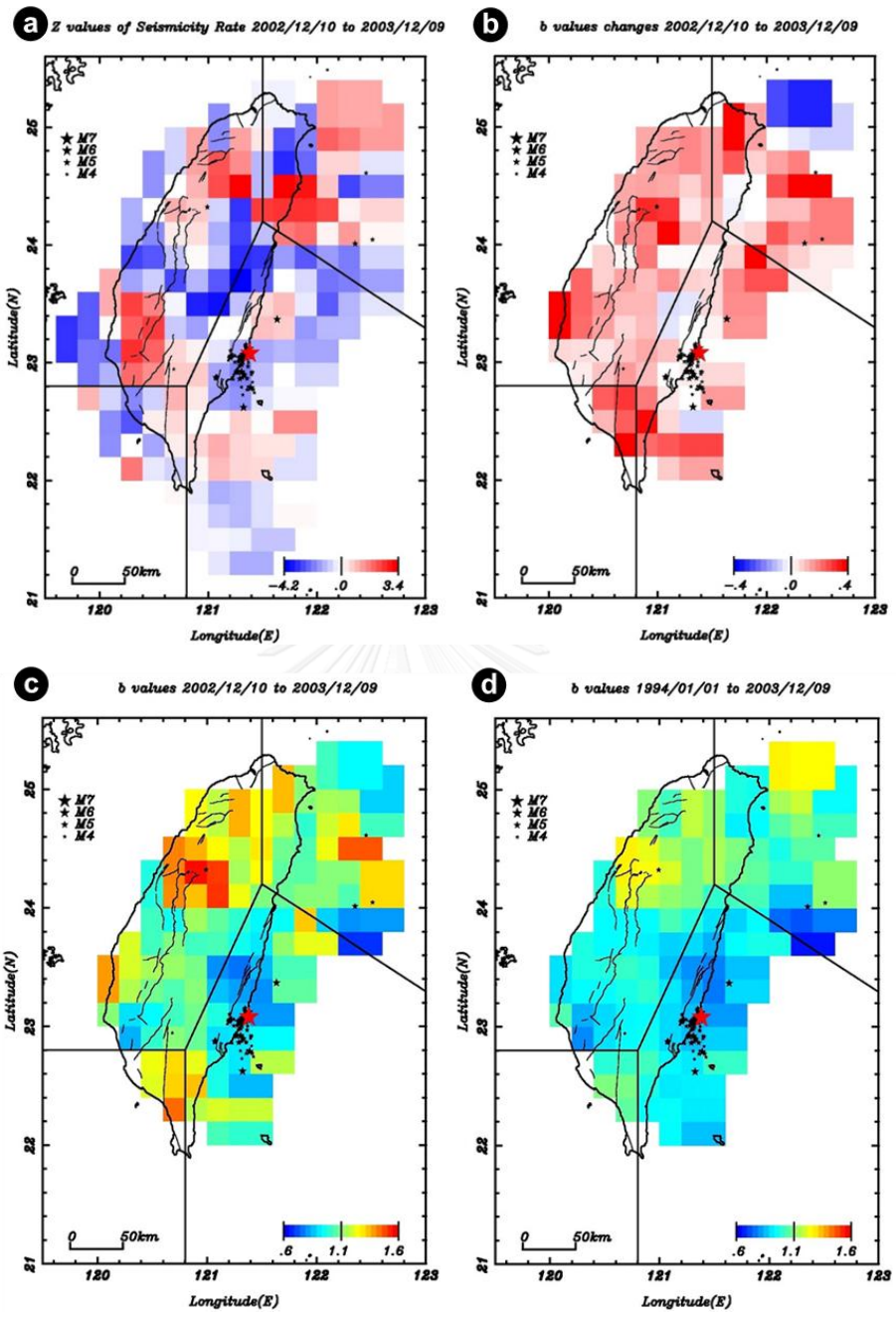

Figure 2.6. Spatial distribution before the 2003 M_W-6.8 Chengkung earthquake calculated by using a) ZMAP during 10 December 2002 – 9 December 2003 and, b and c) b value during December 10, 2002 – December 9, 2003, d) b value during January 1, 1994 and December 9, 2003. Shaded areas indicate the anomalies of both methods and the red star indicates the epicenter of the Chengkung main shock (Wu et al., 2008).

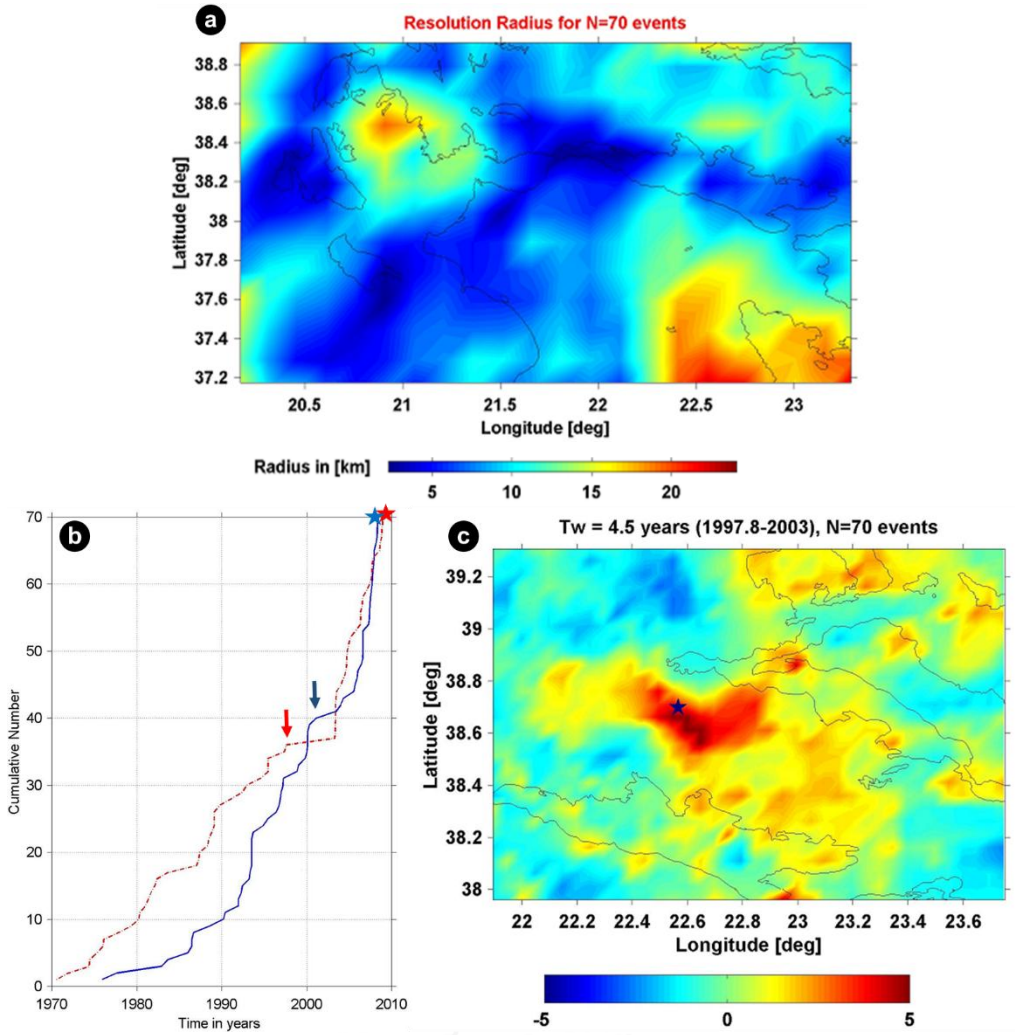

Figure 2.7. a) Map showing the resolution of the radius needed to collect n = 70 earthquake events. b) Cumulative number of earthquakes at the epicenter area of the December 8, 2008 (blue) (Chouliaras, 2009a) and December 13, 2008 (red) main shocks. Red arrow is the quiescence stage started around 1997.8 and blue arrow denotes the quiescence stage started around 2001.03 corresponding to Figure 2.7c. Blue and red stars indicate the occurrence time of the December 8, 2008 and December 13, 2008 main shocks, respectively. c) Spatial distribution of *ZMAP* for investigating region based on the NOA-IG earthquake catalogue during 1997.8 – 2003. By using Z parameters T_w = 4.5 years, n = 70 events and grid spacing = 0.05°. Blue star represent the epicenter of the December 13, 2008 main shock (Chouliaras, 2009b).

Katsumata (2011b) investigated the seismicity rate change before the *M*-9.0 Tohoku earthquake on March 11, 2011 which occurred near the northeast coast of Honshu, Japan. Katsumata used a seismicity catalogue by the Japan Meteorological Agency (JMA), the catalogue includes 5,770 earthquake occurred between 1965 and 2010 shallower than 60 km with $M \geq 4.5$ applied to *ZMAP*. By using a time window (T_W) of 15 years, an event of number (n) = 150 earthquakes, T_S is moved through time, in step of 0.08 years (~28 days), and grid spacing of 0.05°. The results show that the 2011 Tohoku earthquake is detected by a seismic quiescence anomaly started on November 1987 (23.4 years) before the main shock (Figure 2.8). Katsumata found the positive of *Z* value is +4.9 and the anomaly apparent closely to the 2011 Tohoku earthquake epicenter. It is indicated a seismic quiescence before the main shock is common to mega earthquake (M ~ 9.0) in subduction zones.

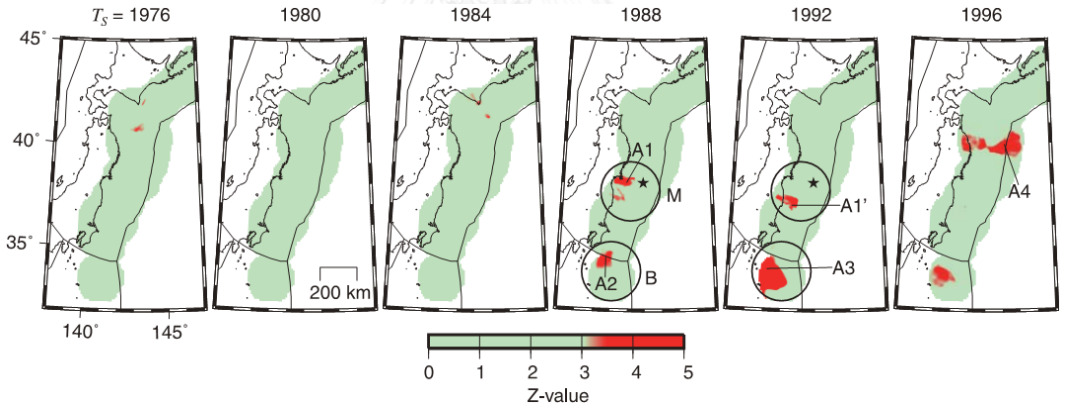

Figure 2.8. Time slices of *Z*-value distribution using the JMA non-declustered catalogue during 1965 - 2010. The conditions for calculating *ZMAP* using a time window T_W = 15 years, the number of events (n) = 150 earthquakes and the number of effective grids are 12815 in each time slices. A red color (positive *Z* value) indicates a decrease in the seismicity rate. Circles labeled by M and B show Miyagi and Boso quiescence region, respectively. A1 and A1′ are nodes in the Miyagi quiescence region. A2 and A3 are nodes in the Boso quiescence region. A4 is a node in the Sanriku-haruka-oki quiescence region (Katsumata, 2011b).

Furthermore, Katsumata (2011a) analyzed the seismicity rate changes before the M_w-8.3 Tokachi-oki earthquake on September 26, 2003, which the epicenter occurred around the southeast offshore of Hokkaido, Japan. Based on 2,000 number of earthquake data with $M \geq 3.3$, recorded by the Institute of Seismology and Volcanology, Hokkaido University during 1993 and 2003, the Z-value investigation by using the number of events (n) = 100 events and the time window (T_w) = 4 years indicated two neighborhood seismic quiescence stages started around the beginning of 1999 (around 5 years before the main rupture) (Figure 2.9).

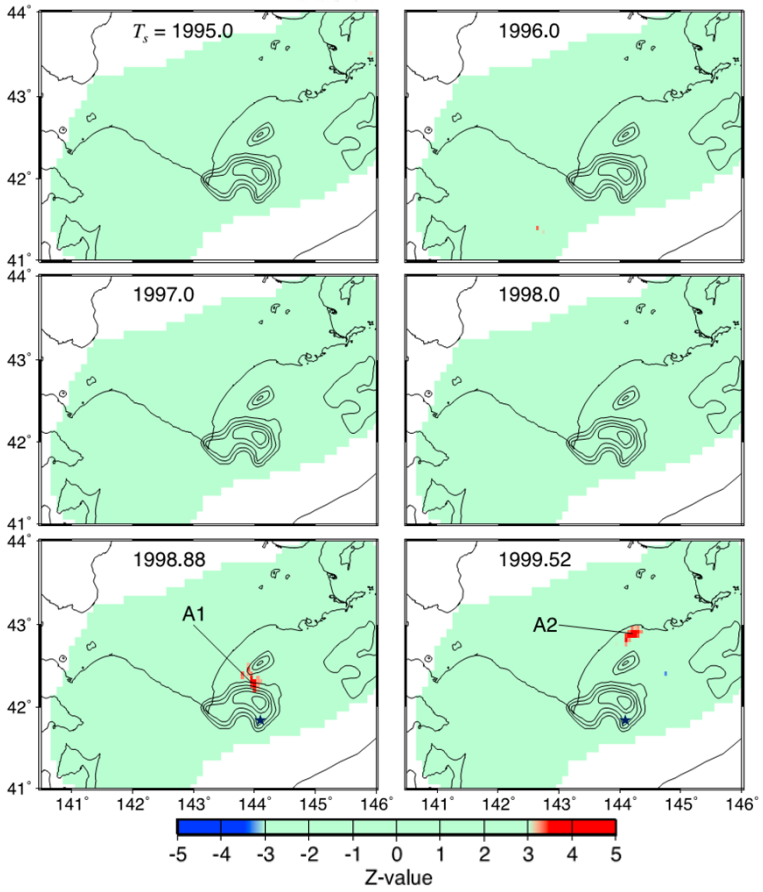

Figure 2.9. Time slices of Z-value distribution before the M_w-8.3 Tokachi-oki earthquake. A red shaded (positive Z value) and blue shaded (negative Z value) represent the decrease and increase in the seismicity rate, respectively. Blue star indicates the M_w-8.3 Tokachi-oki earthquake epicenter (Katsumata, 2011a).

Regarding to the studies of Katsumata (2011a) and Katsumata (2011b), the vicinity area of quiescence anomalies also risk to the upcoming earthquake. Therefore, based on the previous studies introduced above, it can mention that the *Z*-value investigation is one of the interesting methods, which can use for forecasting impending earthquake.

2.2.2 *RTL* Algorithm

Based on applied *RTL* algorithm for investigation the variations in seismicity pattern changes before the *M*-7.2 Kobe earthquake on January 17, 1995, which occurred in the southern of Hyogo Prefecture, Japan. In this event, Huang et al. computed the temporal variations and spatial distribution of the *RTL* parameters based on the seismicity catalogue of JMA during 1977 and 1995 with a completeness magnitude $M_{min} \geq 3.0$. By using characteristic parameters $r_0 = 50$ km and $t_0 = 1$ year, an obvious result of *RTL* parameters at the epicenter of Kobe earthquake implied that a quiescence stage started in 1993 and reached its minimum in May 1994, following by an activation stage that its detected around seven months (Figure 2.10a). The anomaly area around main shock location reached 300 km (Figure 2.10b). However, the anomalies have reasonable correlation prior to the Kobe earthquake. Therefore, Huang et al. mentioned that the seismicity pattern changes of the Kobe earthquake revealed by using *RTL* algorithm, this may provide useful information for seismic hazard estimation.

Mignan and Giovambattista (2008) investigated the spatiotemporal extent of seismic quiescence stage impending to the M_w-6.0 Umbria-Marche earthquake on September 26, 1997, which occurred in the regions of Umbria and Marche, Central Italy. By applying the *RTL* algorithm based on the seismicity catalogue from the Instituto Nazionale di Geofisica (ING) during 1986 and 1998 with a completeness magnitude $M_{min} \geq 2.3$. By using characteristic *RTL* parameters $r_0 = 50$ km, $t_0 = 1$ year. The results of temporal variation indicate seismic quiescence stage start observed clearly in 1996.85

and revealed around 0.5 year before the ending time at 1997.45. The quiescence stage related to the cumulative number of earthquakes (Figure 2.11).

Furthermore, after comparing temporal variation of the *RTL* algorithm at the epicenter of the Umbria-Marche main shock with spatiotemporal evolution and cumulative number of background events. The comparisons give relative results while the quiescence stage occurred (Figure 2.12).

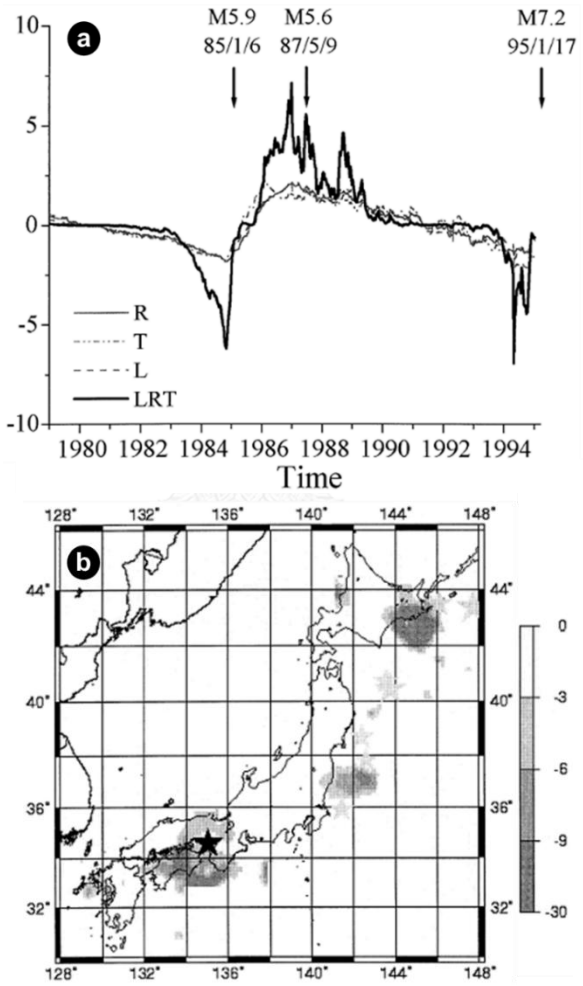

Figure 2.10. The results of a) temporal investigation of *RTL* values at the epicenter of the Kobe earthquake main shock. b) Spatial distribution before the *M*-7.2 Kobe earthquake, January 17, 1995. Map duration during June 1, 1994 and December 31, 1995. Shades areas indicate quiescence anomaly and black star indicates the epicenter of Kobe earthquake (Huang et al., 2001).

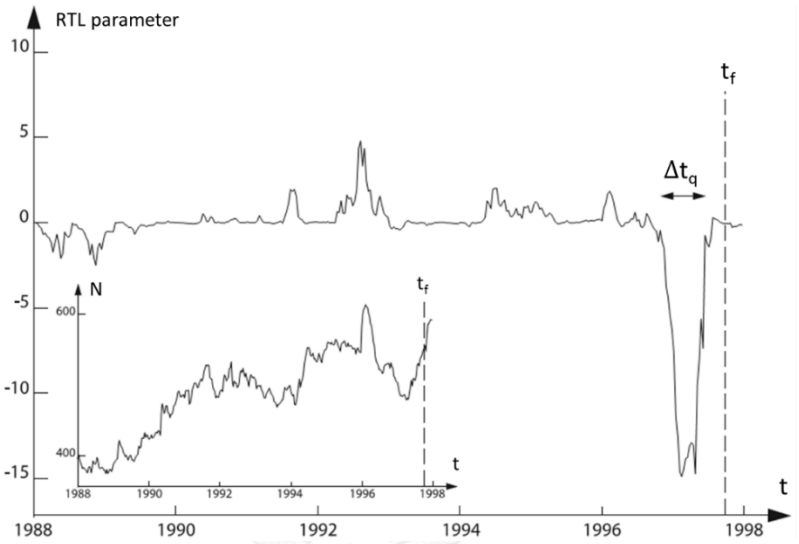

Figure 2.11. The results of temporal variation at the epicenter of the M_w-6.0 Umbria-Marche earthquake on September 26, 1997. Δ_{tq} indicate the period of quiescence stage occurred during 1996.85 and 1997.45 (0.5 years). t_f indicate the occurrence time of the Umbria-Marche main shock, calculation reproduced from Giovambattista and Tyupkin (2000).

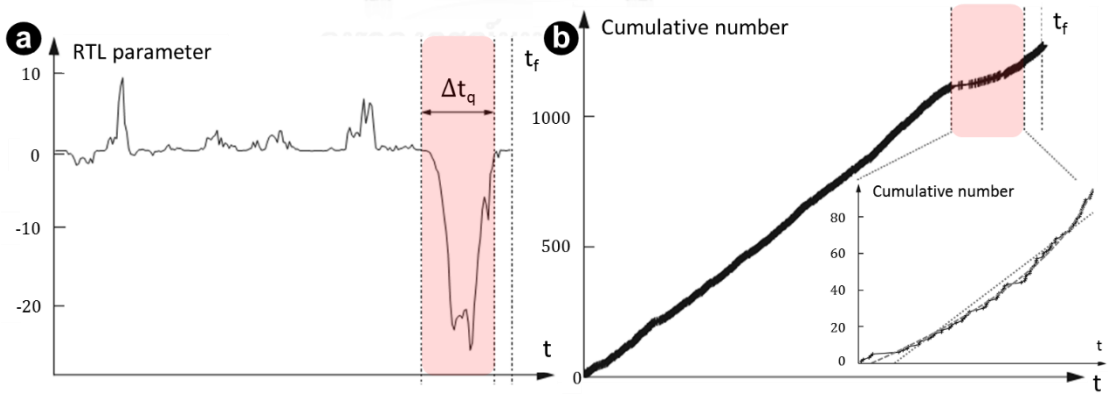

Figure 2.12. The comparison of a) the temporal variation of *RTL* algorithm at the M_w-6.0 Umbria-Marche epicenter, Δ_{tq} indicate the period of quiescence stage and b) the cumulative number of background earthquakes along the space time interval. Red shade indicate quiescence stage during 1996.85 and 1997.45 (Mignan and Giovambattista, 2008).

Moreover, the retrospective investigation indicates the anomalous areas corresponding to the M_w-6.0 Umbria-Marche epicenter (Figure 2.13a), the cumulative number of background events during quiescence stage showed in Figure 2.13b. The results introduced above is a step forward in the understanding of seismicity precursory prior to large earthquakes.

Gambino et al. (2014) used *RTL* algorithm for studying the seismicity pattern changes corresponding to the *M*-4.8 Archipalego earthquake on August 16, 2010 (12.54 GMT), which occurred in Aeolian Archipelago, Italy. After vary *RTL* parameters, the temporal investigation of many conditions found seismic quiescence started around 15 months before the *M*-4.8 Archipalego earthquake and the quiescence stage revealed 6-7 months (Figure 2.14a and Figure 2.14b). Then seismic quiescence stage ending 8-9 months before main shock, the similar time shift during the end of the quiescence stage and the occurrence time of the earthquake was found by Sobolev and Tyupkin (1999), Huang and Sobolev (2002), Gentili (2010), and etc. However, the spatial distribution of *RTL* values still showed the epicenter of *M*-4.8 Archipalego earthquake occurred in the negative *RTL* values area (Figure 2.14c). Hence, Gambino et al. recommended the *RTL* algorithm can use for investigating precursory seismicity of moderate earthquakes as well.

According to the previous studies introduced above, it can mention that not only *Z*-value investigation, but also the *RTL* algorithm is one of the potential methods, which can use for investigating the seismicity precursor prior to the strong earthquake.

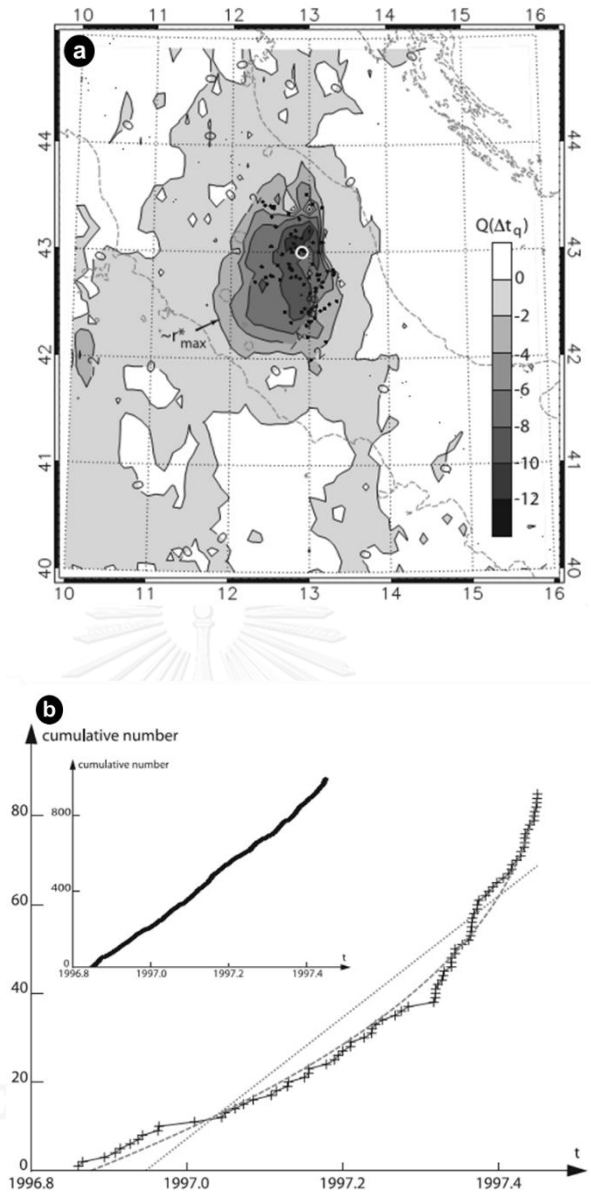

Figure 2.13. a) Spatial distribution of *RTL* values between 1996.85 and 1997.45 by using characteristic *RTL* parameters r_0 = 50 km and t_0 = 1 year. Shaded areas indicate the anomalous area of seismic quiescence. White circle indicates the location of the M_w-6.0 Umbria-Marche main shock on September 26, 1997. b) Cumulative number of earthquakes in Umbria-Marche region during seismic quiescence stage, power-law fit and linear fit indicate the dashed curve and pointed line, respectively (Mignan and Giovambattista, 2008).

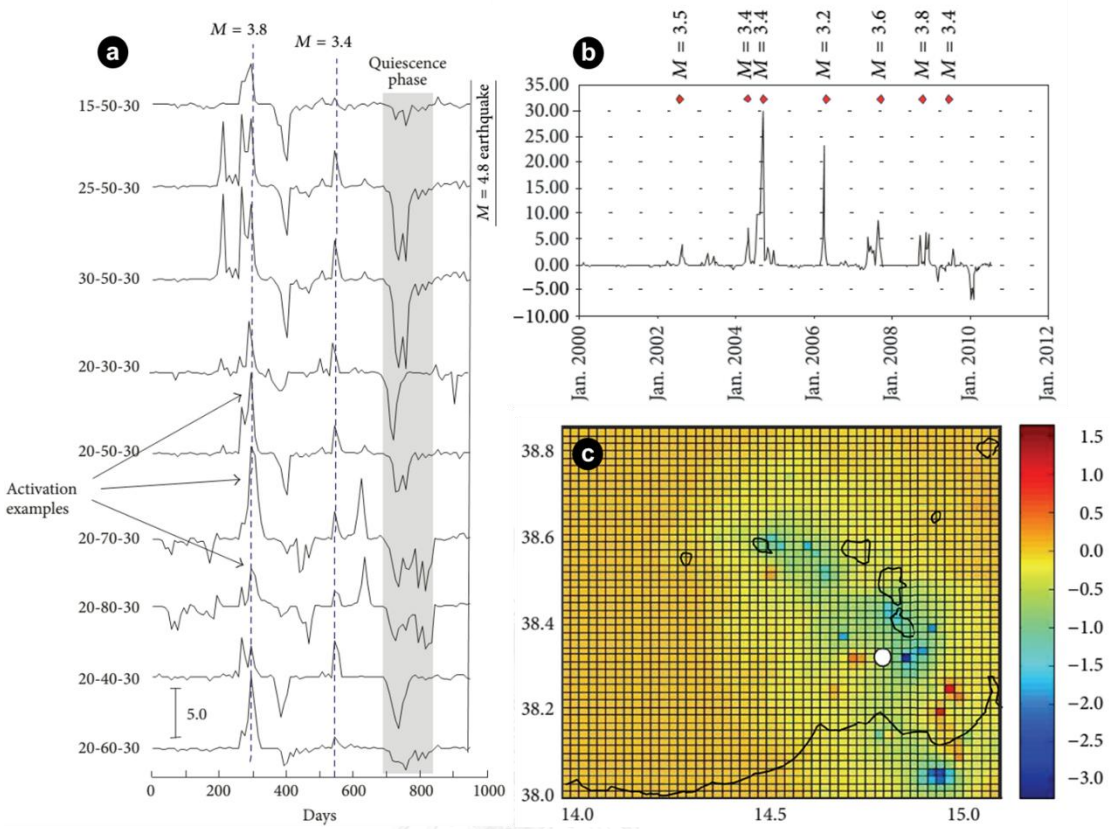

Figure 2.14. The results of a) temporal variation of different RTL parameters (r_0, t_0 and d_0) at the epicenter of the *M*-4.8 Archipalego earthquake on August 16, 2010. RTL curves starting at 1, January, 2008 with duration about 958 days. Some examples of seismic quiescence are indicated by grey shade zone. b) Temporal investigation during January 2000 and August 2010 by using RTL parameters r_0 = 25 km, t_0 = 50 days and d_0 = 30. Red points indicate the occurrence time of the minor earthquakes with $3.2 \leq M \leq 3.8$ located closely (10 – 15 km) to the *M*-4.8 Archipalego earthquake main shock. c) Spatial distribution of *RTL* values in the Aeolian Archipelago region during June 2009 and December 2009. The white point imply the location of the *M*-4.8 Archipalego earthquake epicenter (Gambino et al., 2014).

2.4. Methodology

For evaluate both *Z*-value investigation and *RTL* algorithm in Thailand-Laos-Myanmar borders, in this research, the simplified procedures are generated in 4 parts (Figure 2.15).

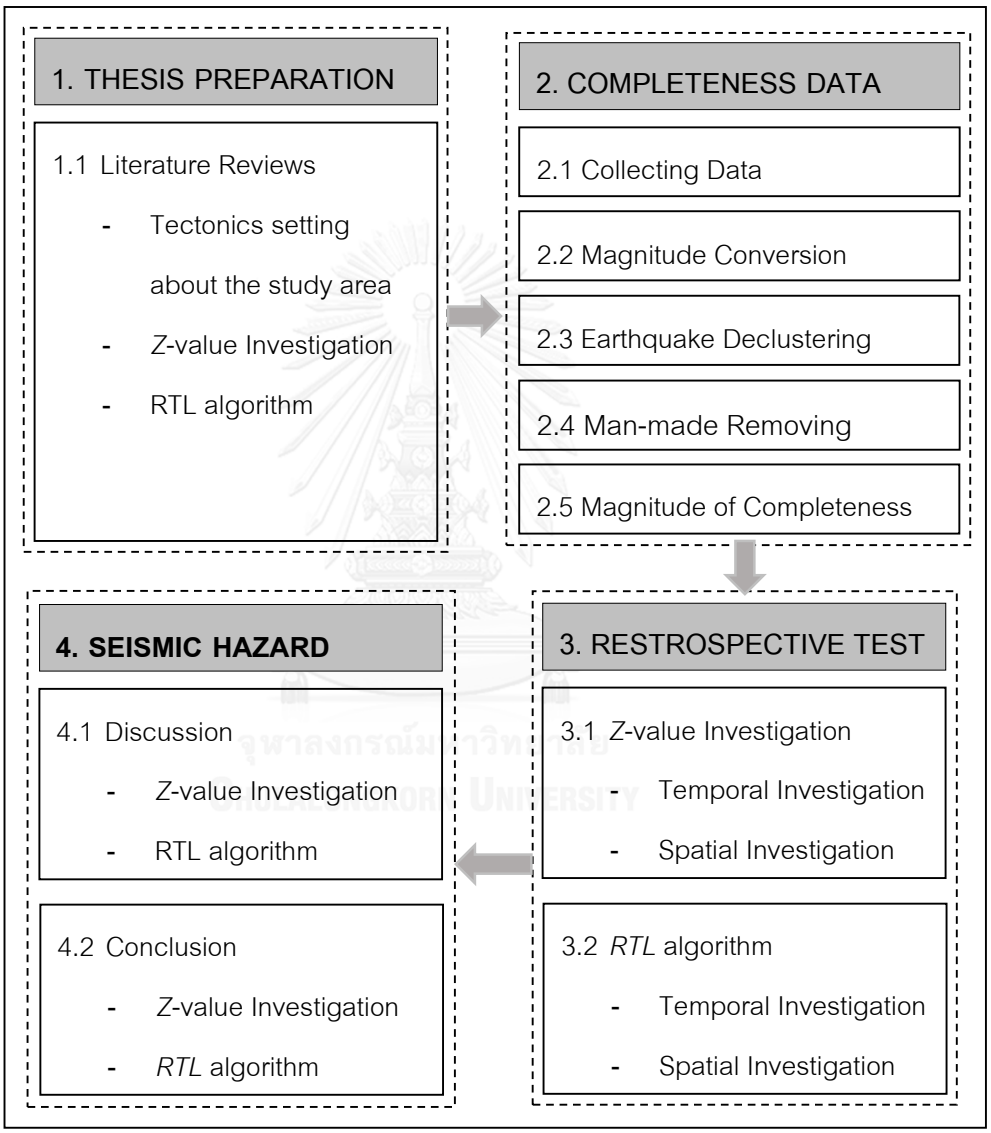

Figure 2.15. Simplified flow chart showing the methodology applied in this study.

According to Figure 2.15., for understanding the methods about the *Z*-value investigation and *RTL* algorithm clearly, at first, the previous works of both techniques were reviewed inclusive the knowledge about tectonic setting of Thailand-Laos-Myanmar borders. Secondly, for the best results, the complete earthquake data is very important. In this part, the algorithms can be defined as below;

i) Data Compiling. Due to the different agency of seismicity sources provided both advantages and disadvantages in each individual seismicity catalogues. Then, in seismology, the collecting seismicity data from several earthquake data sources are very important, for selecting and calibrating the suitable seismicity data source in the study area.

ii) Magnitude Conversion. According to worldwide agencies were reported in the different magnitude scales. Therefore, in order to get a homogeneous seismicity data, all of the earthquake catalogues must be converted in the same magnitude scale before using in the study.

iii) Earthquake Declustering. Although the nature earthquakes consist of foreshock, main shock and aftershock, only main shock is related directly to the tectonics activities. Hence, in order to forecast impending strong earthquake, the calculation should considers only the main shock whereas foreshock and aftershock in seismic data should be removed.

iv) Man-made Removing. Earthquakes are not only caused by the nature, but also caused by human activities, i.e., nuclear explosion, mining, reservoir and so on. Therefore, to prevent an error of artificial earthquake in the calculation, the man-made earthquake should be eliminated from seismicity data.

v) Magnitude of Completeness. Due to the density of seismic station are improved continuously in each era. Then, for screening the unstable magnitude scale which recorded in each earthquake agency. The lowest magnitude scale or magnitude of completeness which indicate 100% of the seismicity in a space-time extent are recorded should be investigated before applying the seismicity catalogues to the any seismicity

investigation. Therefore, the earthquake catalogues which have magnitude scale lower than magnitude of completeness should be removed.

Third part, when the earthquake data are completed, the next algorithm was applied to the data to investigate seismicity quiescence in Thailand-Laos-Myanmar border region by using *Z*-value investigation and *RTL* algorithm. Both methods were calculated retrospective test, in temporal and spatial investigation. The suitable condition in each method was collected for using evaluate the trend of impending earthquakes. Then, the seismic hazard map in each space-time will be generated. After that, the final part is for conclusion and discussion. The result of *Z*-values investigation and *RTL* algorithm were compared and evaluated the forecasting ability in the study area.

CHAPTER III

SEISMICITY DATA AND COMPLETENESS

Earthquake catalogues are one of the most important products of seismology (Woessner and Wiemer, 2005). According to the historical evidence, although the first seismoscope invented by Zhang (Chang) Heng since 132 A.D., the revolution of earthquake studies just provoked after the November 1, 1755 Lisbon earthquake, Portugal, with magnitude more than 8 occurred (Agnew, 2002). Afterward, its take the times nearly 100 years before the early seismograph was generated by Luigi Palmieri in 1855. Then, the number of different seismographs improved continuously, related to the knowhow of earthquake in each era and the discovery of the characteristic types of seismic wave, for example, Body wave, Surface wave, Rayleigh wave, Love wave, etc. According to the magnitude scale mentioned above, at present, there are several magnitude scales created for measuring a specific type of seismic waves. The well-known of earthquake magnitude measurement, i.e., local magnitude (M_L) (Richter, 1935), surface-wave magnitude (M_S) (Gutenberg, 1945), body-wave magnitude (m_b) (Gutenberg and Ritchter, 1956) and moment magnitude (M_w or M) (Hanks and Kanamori, 1979; Kanamori, 1977). Seismologist uses the earthquake catalogues based on these magnitude scales, especially statistical seismology. However, the results found both advantages and disadvantages from each magnitude scale. Furthermore, the lack of seismic station in the past caused the seismicity recorded discontinuous. Therefore, there are a number of researches attempted to improve the seismicity catalogues before applied to their work. In accordance with the reasons above, this work also revised the seismicity catalogues before the calculations of *Z* value and *RTL* algorithm. The homogeneous seismicity catalogues improvement can be showed as topics 3.1 – 3.5.

3.1 Seismicity Investigation

An earthquake catalogue is a list of information which it recorded from each earthquake agency, describing a detail of seismic instrument readings in one earthquake (i.e., name of agency, location of the epicenter, occurrence time, depth of the hypocenter, magnitude scales, and so on, (Table 3.1). Although earthquake catalogues provide a comprehensive database applied for seismicity surveys, this data are not easy to be understand and use. Owning to the products of each earthquake agency have different procedures that start with the configuration of the earthquake network (i.e., a seismic sensor, software, location procedure, magnitude scales, human-selected computational tools, and so on). Therefore, the collecting seismicity data from several earthquake data sources may provide more useful catalogues, which can deploy in seismology (Woessner et al., 2010).

As the results of statistical seismology depend on the number of seismicity data, this work attempted to collect seismicity data in the Thailand-Laos-Myanmar borders (16.76˚ – 22.30˚N and 97.48˚ – 103.16˚E) as much as possible. The results indicate the main earthquake data sources available in this area are from the i) Incorporated Research International Seismological Center (ISC), ii) National Earthquake Information Center (NEIC), iii) Global Centroid Moment Tensor (GCMT), iv) Thai Meteorological Department (TMD) and v) IDC (International Data Center) (Figure 3.1).

These seismicity sources contributed by different networks. However, each network has both advantages and disadvantages themselves in terms of the recording interval, data continuation, and limit of the recordable magnitude range including the type of proposed magnitude scales of their records. For examples, even though NEIC has the longest period of seismicity data and recorded consistently, the seismicity data with $M <$ 2.9 are not reported. ISC has seismicity data with a wider magnitude range than others, however the seismicity data of ISC not stable. TMD has a seismicity catalogue with a widely magnitude range and recorded constantly, nevertheless the duration of seismicity data from TMD are just between 1980 and 2009 only. Even though GCMT have the least

seismicity data, all data from this source were recalculated for making the best seismicity catalogues. Therefore, to improve the quantity and quality of seismicity data, all existing seismicity catalogues (i.e., GCMT, ISC, NEIC, and TMD) are merged by using the assumption from Suckale and Grünthal (2009), for avoiding double-counting earthquake events. Then, the total seismicity data contain 20,699 earthquake events, during 1960.03 and 2015.00 (Figure 3.2).

Table 3.1. Examples of earthquake catalogues occupied by various agencies.

Agency	Lon	Lat	Time (UTC)	Depth (km)	m_b	M_s	M_L	M_w
TMD	97.60	18.95	19/4/2009 06:18:24	10.0	-	-	2.7	-
TMD	99.03	18.95	21/4/2009 15:56:16	10.0	-	1.7	2.7	-
TMD	97.65	18.72	21/4/2009 23:11:29	10.0	-	2.4	1.7	-
TMD	97.87	20.03	29/4/2009 11:39:00	10.0	-	-	3.5	-
ISC	101.61	23.18	04/04/2009 22:03:53	14.6	4.2	3.9	-	-
ISC	95.94	23.82	06/04/2009 16:24:30	36	3.7	-	-	-
ISC	95.03	25.30	17/04/2009 21:14:24	94.1	4.5	-	-	-
ISC	95.08	24.62	26/04/2009 23:10:11	112.0	3.5	-	-	-
NEIC	101.64	22.24	04/04/2009 22:03:52	10.0	4.3	-	-	-
NEIC	95.10	25.32	17/04/2009 21:14:25	104.8	4.6	-	-	-
NEIC	94.54	22.96	29/04/2009 23:31:26	113.5	4.3	-	-	-
IDC	95.07	17.05	20/04/2009 08:44:26	83.6	3.1	3.0	4.0	-
IDC	95.52	22.75	27/04/2009 10:29:36	0	3.2	-	-	-
IDC	23.39	95.68	29/04/2009 10:10:57	0	3.4	-	-	-

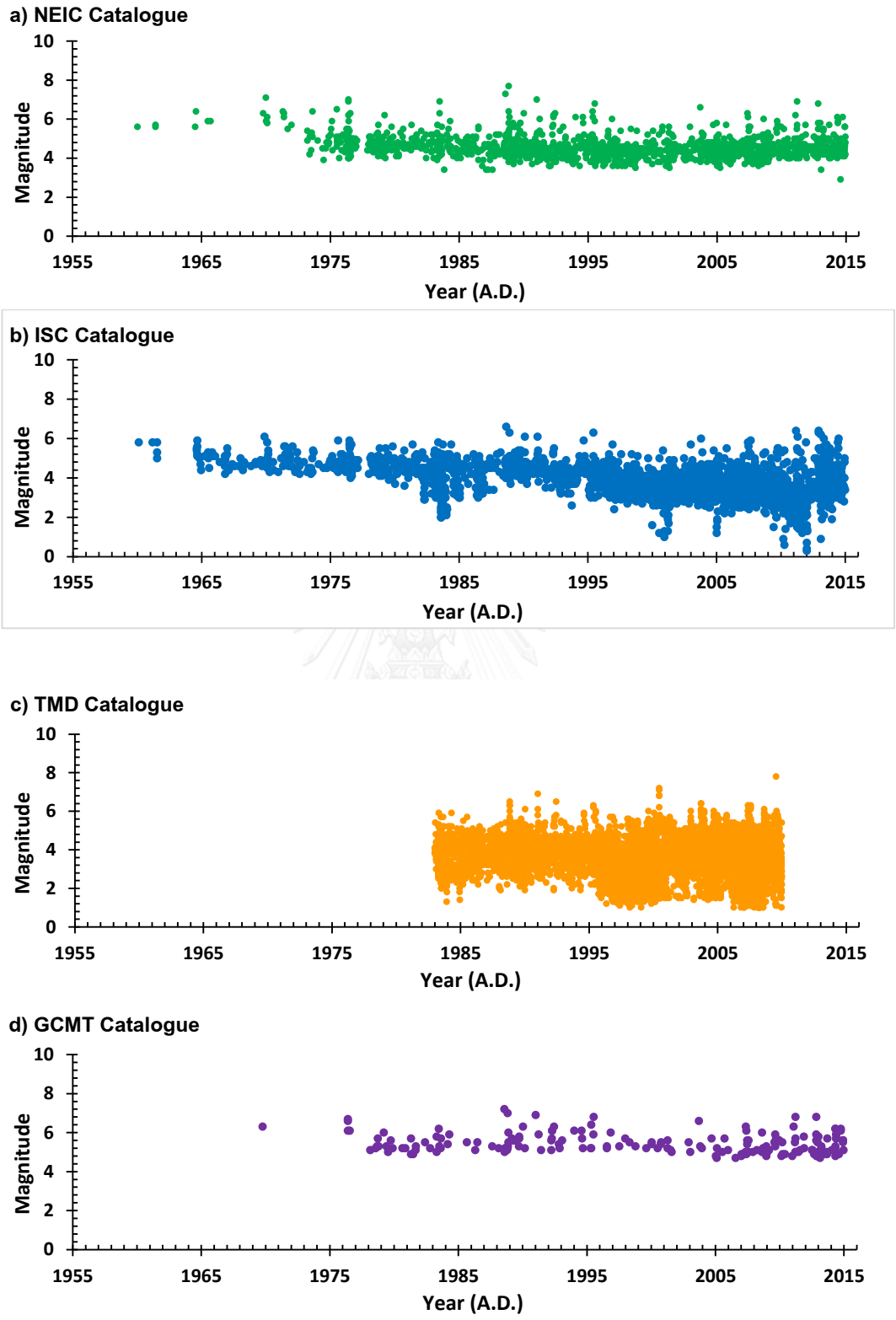

Figure 3.1. Graph showing the relationships between magnitude and time of seismicity recorded from a) NEIC, b) ISC, c) NEIC, d) GCMT.

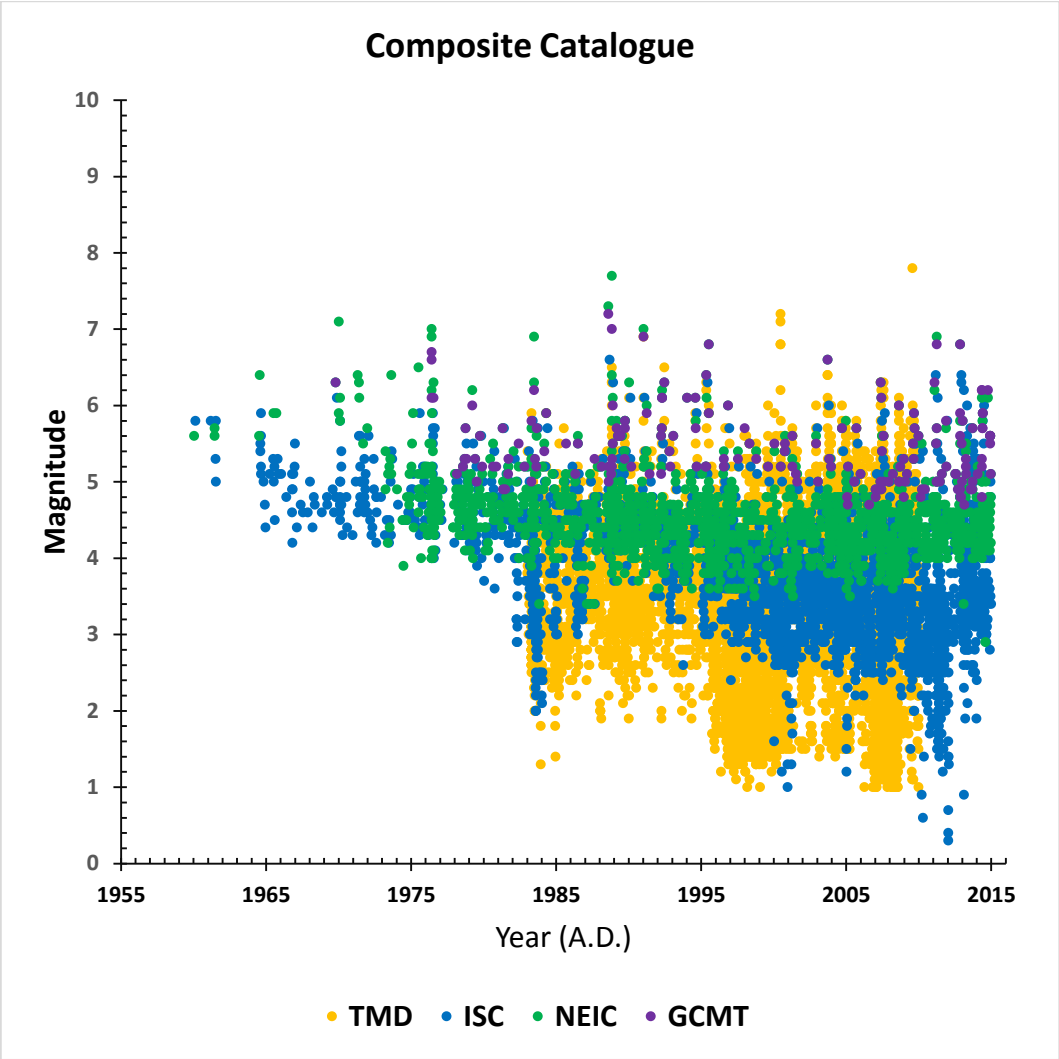

Figure 3.2. Graph showing the comparison of seismicity data from ISC (blue points), TMD (orange points), NEIC (green points), and GCMT (purple points).

3.2 Magnitude Conversion

Because of the local seismicity network (TMD) can record the small shaking events better than the far-field seismicity sources, while the global seismicity networks (i.e., ISC, NEIC, and GCMT) are recordable efficiently with the medium-size and the large-size earthquakes. The magnitude types reported by these agencies are different. The TMD mostly reported M_L, simultaneously the GCMT, NEIC and ISC catalogue record variably the earthquake size in m_b, M_s, and M_w for each earthquake events. According to

each magnitude scale is acquired by a specific hypothesis and diagnostic procedure which have a reasonable report, however there are different value and individual meaning. For explanation these magnitude scale briefly, m_b calculated from the first arrival primary wave (*P*-wave) of a seismogram, M_s and M_L computed from the surface wave and secondary wave (*S*-wave), and the recent magnitude scale (M_w), developed to avoid the error of saturation in other magnitude scale while the large earthquakes occurred (Hanks and Kanamori, 1979; Kanamori, 1977).

Due to the reasons mentioned above, in order to assemble the homologous seismicity data, the seismicity data recorded in Thailand-Laos-Myanmar borders were converted to M_w scale. For simplification, the empirical relationships between the different magnitude scales were developed based on the number of correlation in each case. The investigation of seismicity data in study area indicates that the m_b, M_s and M_w are reported simultaneously in many earthquake events, while there are a few M_L recorded with M_w at the same time. However, there are a lot of earthquake events recorded M_L, m_b and M_s in the meantime. Then, this work attempted to covert M_L to m_b directly. However, although M_L, m_b and M_s were recorded in the meantime, the number of correlation between M_L and m_b is more than the number of correlation between M_L and M_s. Hence, this work determined to convert M_L to m_b before converting m_b to M_w later. Nevertheless, it is notable that the average relationships should be calibrated in polynomial trend line (e.g., Howell (1981); Ottemoller and Havskov (2003)). The empirical relationship equation defined as equations 3.1 to 3.3 and the diagram of seismicity data Thailand-Laos-Myanmar borders after converting to M_w is shown in Figure 3.3.

$$M_w = -0.1188 m_b^{\,2} + 2.1061 m_b - 2.6052 \tag{3.1}$$

$$M_w = -0.0915 M_s^{\,2} + 2.4122 M_s - 5.2206 \tag{3.2}$$

$$m_b = 0.2164 M_L^{\,2} - 0.954 M_L - 4.4467 \tag{3.3}$$

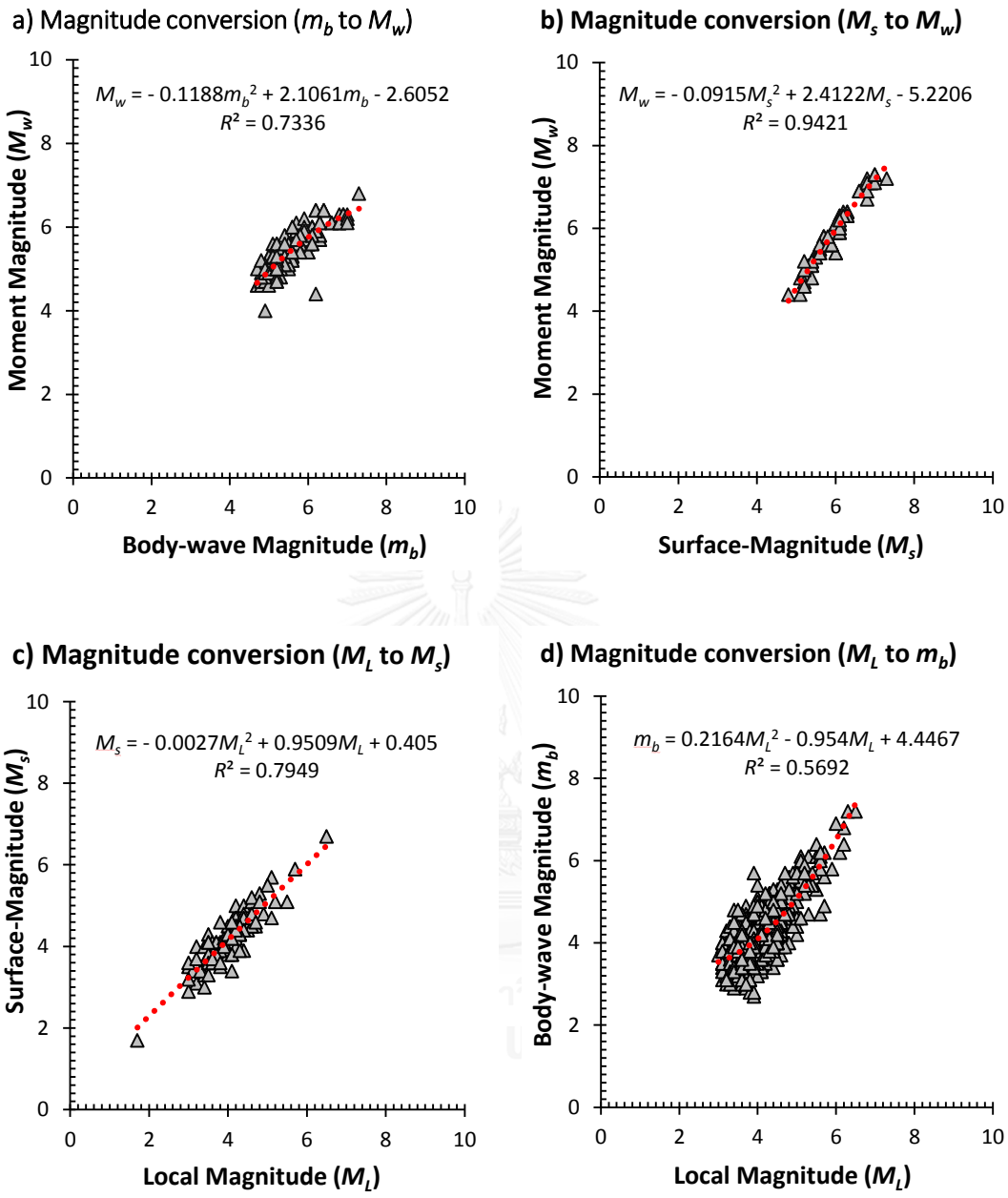

Figure 3.3. Empirical relationships of seismicity data from ISC, a) between body wave magnitude (m_b) and moment magnitude (M_w), b) between surface wave magnitude (M_s) and moment magnitude (M_w), c) between surface wave magnitude (M_s) and Local magnitude (M_L), and d) between Local magnitude (M_L) and body wave magnitude (m_b). Grey Triangles indicate earthquake events and red dash line indicate polynomial trend line calibrated in this study.

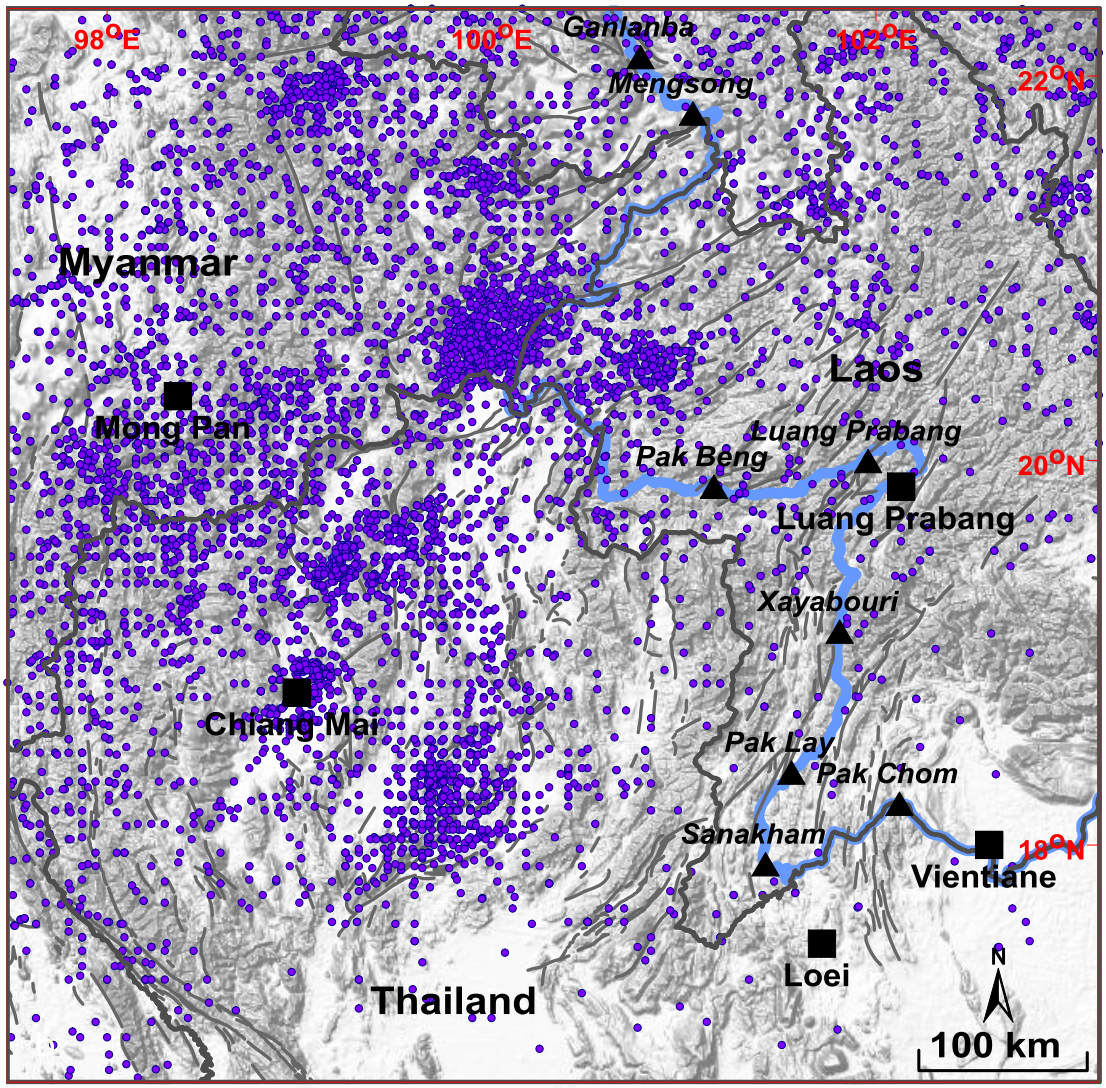

Figure 3.4. Map of Thailand-Laos-Myanmar border region (16.76° – 22.30°N and 97.48° – 103.16°E) showing the distribution of earthquakes during 1960.03 and 2015.00. Blue points indicate the epicenter of main shocks with moment magnitude (M_w) scale.

3.3 Earthquake Declustering

According to Stiphout et al. (2012), in general, seismologists understand earthquake to consist of two types: (1) independent earthquake and (2) dependent earthquake. Independent earthquakes are also called main shock, generated by tectonic loading or stress transients that are not influenced by previous and neighbor earthquakes.

Meanwhile, dependent earthquake are also known as foreshock and aftershock. A foreshock is an earthquake which occurs before the largest seismic event in the same or nearby time and space, while aftershock is a smaller earthquake that occurs following the main shock in the same or neighboring location during the period depended on the magnitude scale (days to years). Although, these second type earthquakes controlled by complex process corresponded to main shock (i.e., seismically-activated, dynamic stress changes, interlock effect and so on), the occurrence mechanisms of dependent earthquake are not stable. Hence, in statistical seismology, seismologists prefer to emphasize on the main shock rather than foreshock and aftershock.

The process of separating and seismicity catalogue into foreshock, main shock, and aftershock, is widely used in statistical seismology and still developed continuously. After Cornell (1968) mentioned that only the main shock can indicate the absolute seismic stress released from the tectonic activities. There are a number of researches supported that the earthquake precursor investigation should be identify and removing foreshock and aftershock within earthquake catalogues before analysis (Gardner and Knopoff, 1974; Palasri, 2006; Petersen et al., 2004). However, this work attempted to use declustering model from Gardner and Knopoff (1974) for filtering dependent earthquakes in Thailand-Laos-Myanmar borders both temporal and spatial distribution. The strongest earthquake in nearby time and space were recognized as the main shock (above the red lines in Figure 3.5). Other earthquake events (below the red lines in Figure 3.5) were recognized as foreshock and aftershock, which they were removed from seismicity catalogues.

After filtering foreshock and aftershock based on Gardner and Knopoff model, the result of declustering found 1,605 clusters of earthquakes from 20,699 events. Among these events, a total of 17,156 events (82.88%) was recognized as dependent earthquake and removed from earthquake catalogue. Then, the declustered seismicity catalogue containing 3,543 events, during 1964.04 and 2014.68. The spatial distribution of seismicity data in Thailand-Laos-Myanmar borders after declustering was indicated in Figure 3.6. Nevertheless, these seismicity data still have the main shock that it occurred by human activities. Thus, in order to obtain a complete autonomous seismicity (i.e., an only main

shock which related directly tectonic activities) distribution, the man-made removing was explained in the next topic.

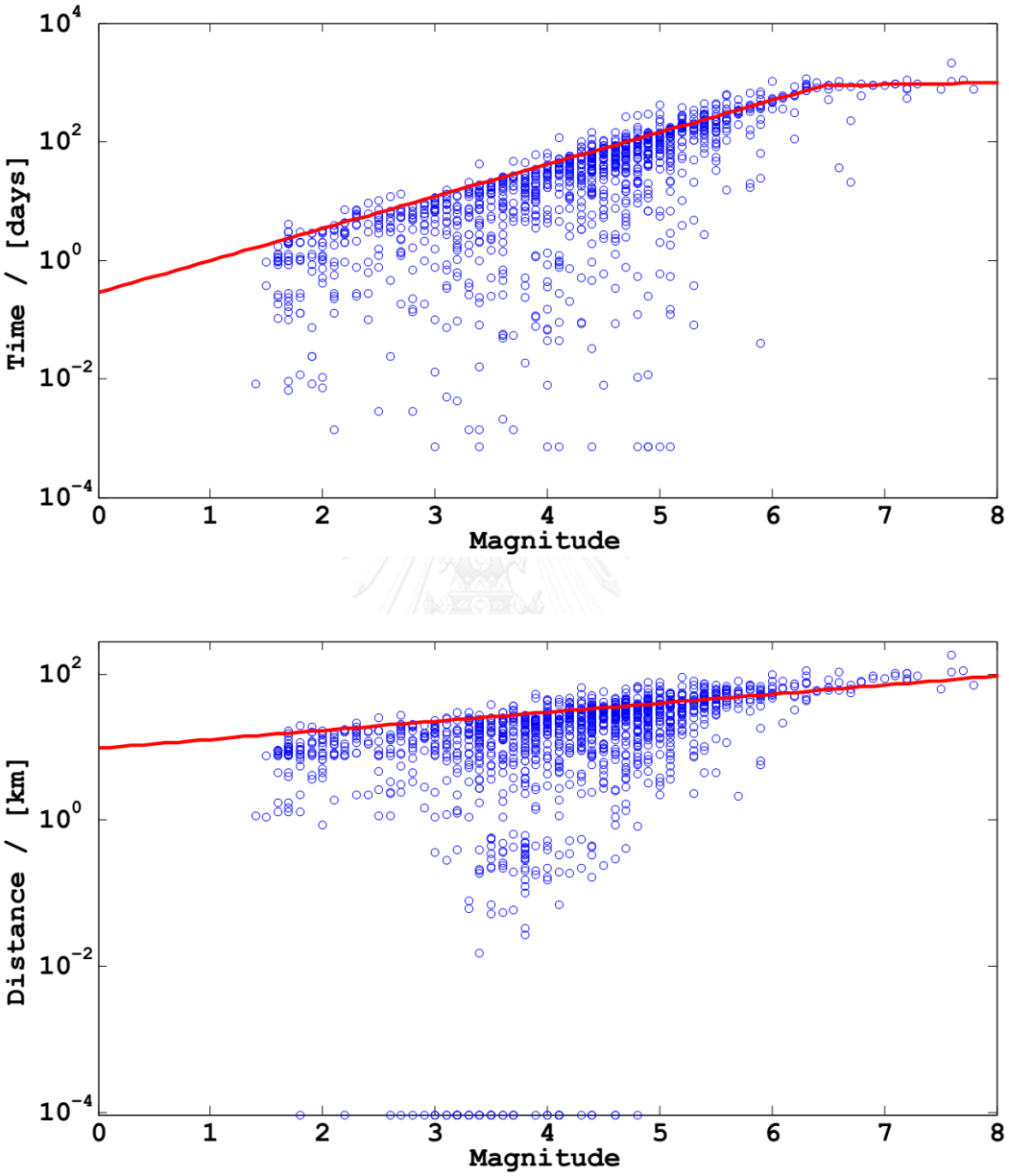

Figure 3.5. The parameters used to filtering foreshocks and aftershocks based on the empirical model from Gardner and Knopoff (1974). (a) Time window and (b) space window. The seismicity data (blue circles) above the red lines of both time and space windows are identified as main shocks.

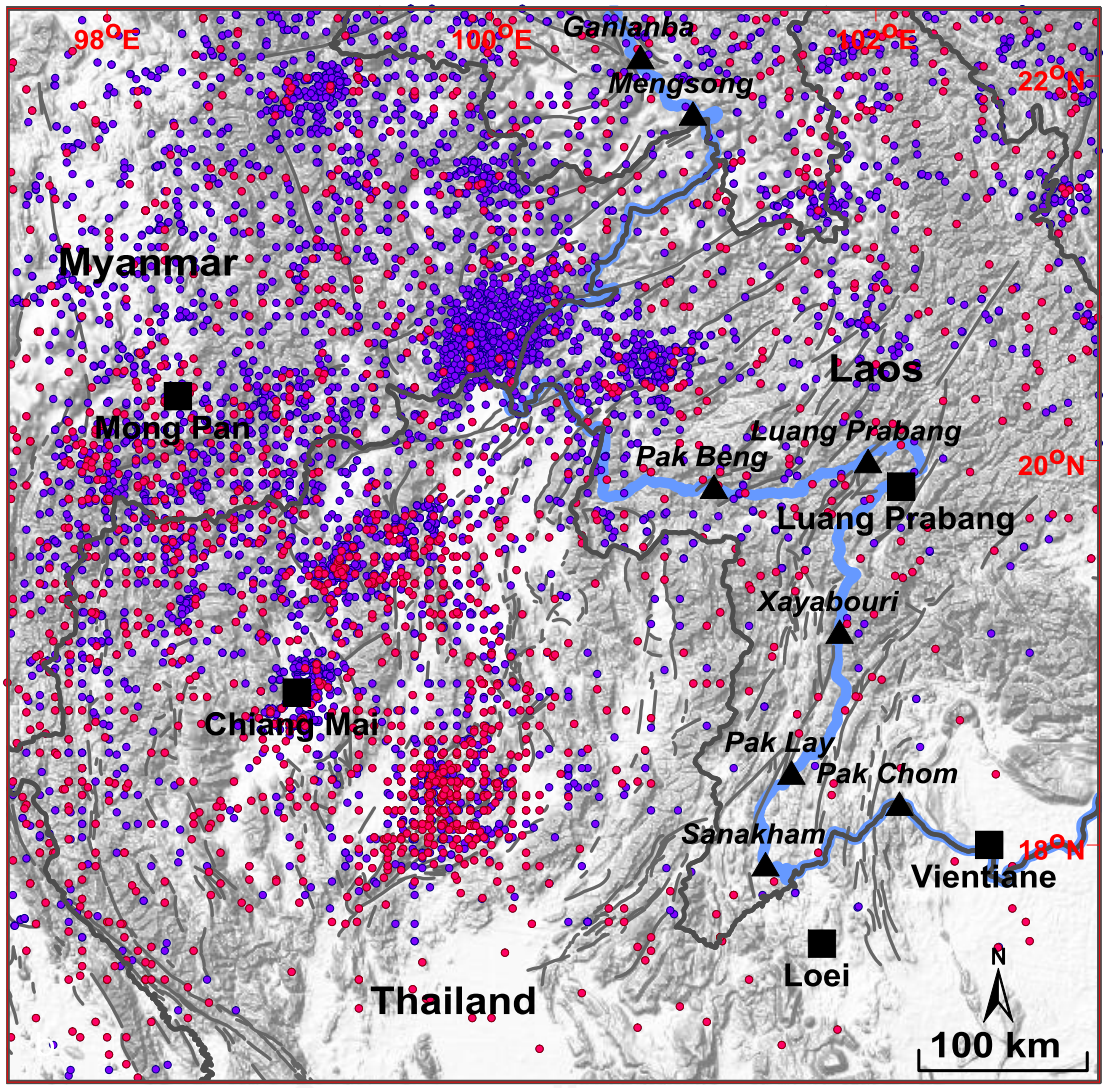

Figure 3.6. Map of Thailand-Laos-Myanmar borders (16.76° – 22.30°N and 97.48° – 103.16°E) showing the distribution of earthquakes during 1964.04 and 2014.68. Blue and red points are the epicenters before and after declustering, using empirical model from Gardner and Knopoff (1974), respectively.

3.4 Man-made Removing

Earthquakes worldwide is not only caused by nature, but also caused by human activities (i.e., nuclear bomb explosions, mining, reservoirs, natural oil and gas extraction, and so on). Moreover, some natural earthquakes do not depend on tectonic activities (i.e., volcanic eruptions, meteor impact, geothermal energy, and etc.). Hence, the identification of artificial earthquakes and earthquake occurred without tectonic activities within seismicity catalogues have been considered in several researches (Habermann, 1982; Habermann, 1983; Habermann and Wyss, 1984; Wyss, 1991; Wyss and Burford, 1985; Zuniga, 1989; Zuniga et al., 2000; Zuniga et al., 2005; Zuniga and Wyss, 1995).

The *GENAS* algorithm (Habermann, 1983; Habermann, 1987) is the useful technique, designed to filter such artificial earthquakes and the earthquake that it is not related to tectonic activities. *GENAS* analyzes and proves significantly change in the seismicity pattern by using the same equation as *Z*-value investigation (equation 2.1), and comparing its results with the seismicity background rate occurred during the period of interested time window. The step is repeated from the beginning to the end of time interval. When the significant seismicity rate changes are found, the seismicity data is highlighted and separated into two sections which are repeatedly investigated in the same pattern. According to Zuniga et al. (2000) and Chouliaras (2009c), the results after applying *GENAS* to seismicity data were indicating the period which outstanding from background rate. The increasing and/or decreasing of seismicity data are investigated, including the magnitude range affected by these changes. Similar to this work, after investigating main shock data in Thailand-Laos-Myanmar borders between 1964.04 and 2014.68 by using *GENAS* algorithm, the results have several periods implied seismicity pattern changes (Figure 3.7).

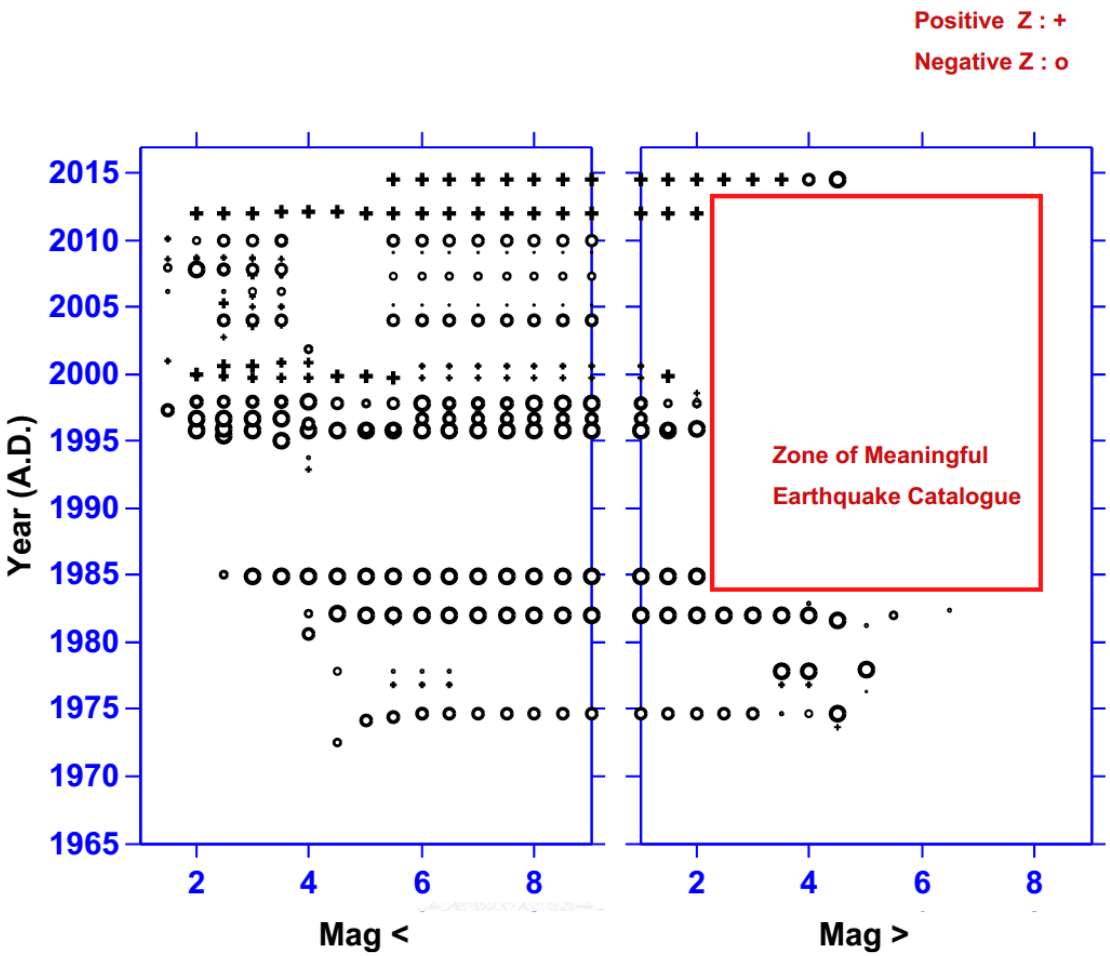

Figure 3.7. Results of seismicity data in Thailand-Laos-Myanmar borders after applying *GENAS* algorithm into the declustered catalogue from 1964.04 to 2014.68 with a magnitude cutoff 1.0. Circles and plus symbols indicate the decreasing and increasing of earthquake detection, respectively. The red box indicates the zone of the meaningful earthquake catalogue, determined to use in the next step.

According to Figure 3.7, the zone of meaningful seismicity data determined during 1981.99 and 2012.16 with the minimum magnitude 2.1. The total of remainder earthquakes in this zone is 2,867 events (Figure 3.8). However, these seismicity data still improved in the next step.

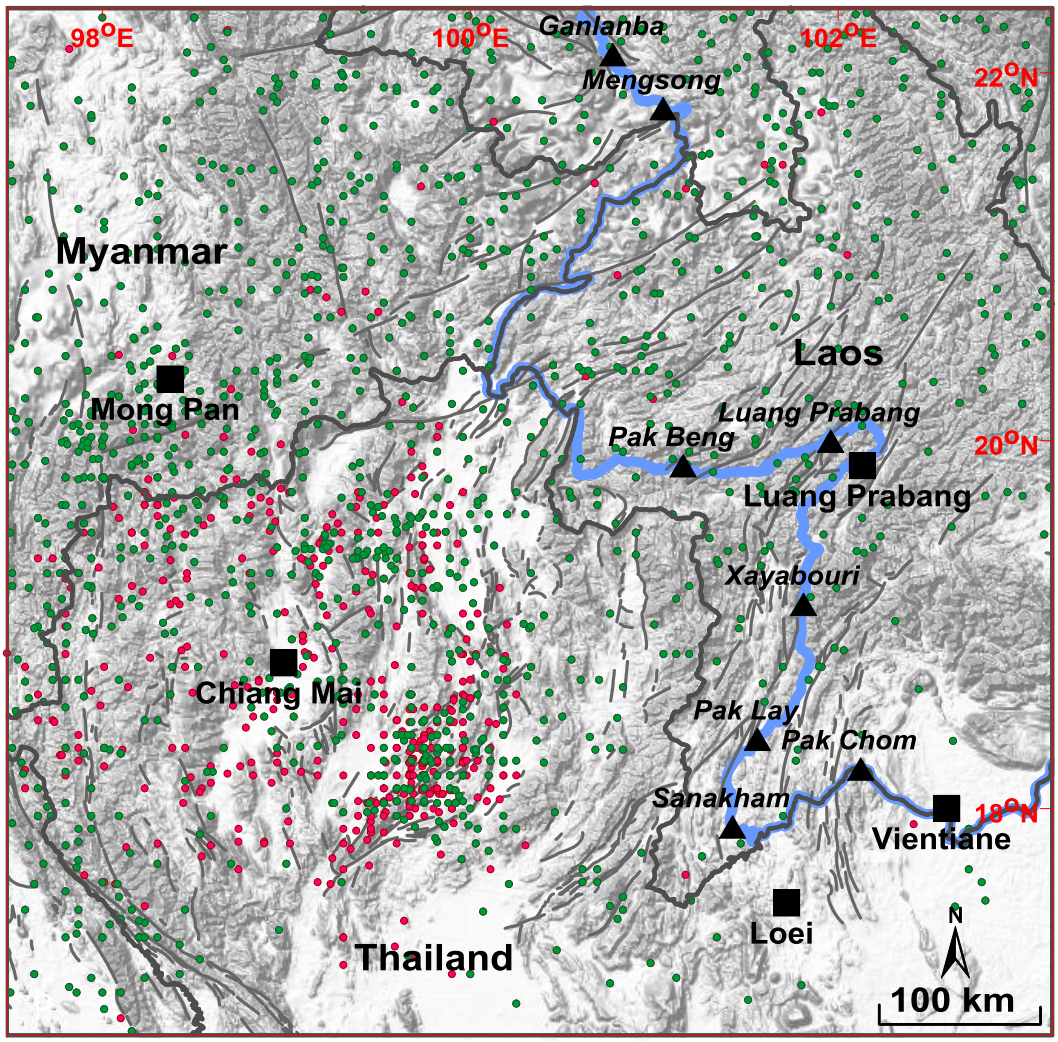

Figure 3.8. Map of Thailand-Laos-Myanmar border region (16.76° – 22.30°N and 97.48° – 103.16°E) showing the distribution of earthquakes during 1981.99 and 2012.16. Red and green points recognized as the epicenter of main shocks before and after eliminated man-made earthquakes by using *GENAS* algorithm proposed previously by Habermann (1983).

3.5 Magnitude of Completeness

Due to the measurement of far-field earthquake stations and the quality of seismic recording instruments can generate the missing gap or the error of measuring earthquakes. Therefore, estimating the magnitude of completeness (M_c) of instrumental earthquake catalogues is an important and required procedure for any earthquake

investigations. M_c is indicated as the minimum magnitude at which 100% of the seismicity in a space-time extent are recorded (Mignan and Woessner, 2012). The assumption to estimate M_c is often calculated by fitting a Gutenberg-Richter (*G-R*) model called the frequency-magnitude distribution (*FMD*) (Gutenberg and Richter, 1944; Ishimoto and Iida, 1939). This model explains the relationship between the frequency of the occurrence and the magnitude of earthquakes which can be defined as equation 3.4 (Gutenberg and Richter, 1944).

$$\log_{10} N = a - bm \tag{3.4}$$

Where *N* is the cumulative number of earthquake with magnitude equal to or larger than *m*, *a* implies the entire earthquake productivity, *b* indicates the relative distribution of small and large seismicity. Earthquake events with magnitude $m < M_c$ are eliminated from seismicity data.

An accurate calculation of M_c is very important. High level of M_c leads to inadequate sampling, by eliminating usable data, meanwhile lower level of M_c brings to erroneous earthquake parameter values and made biased examination, by applying incomplete earthquake data. Therefore, this research attempted carefully to find the suitable M_c in Thailand-Laos-Myanmar borders, by investigating the magnitude of completeness within seismicity data after declustered and man-made cutoff. The results indicate the suitable M_c = 4.4 (Figure 3.9) which it contains 702 main shocks (Figure 3.10).

Consequently, after filtering the non-homogeneous seismicity data, the result found 702 main shocks (3.39%) during 1981.99 and 2012.16 from 20,699 events during 1960.03 and 2015.00. The total of 19,997 events (96.01%) are discarded.

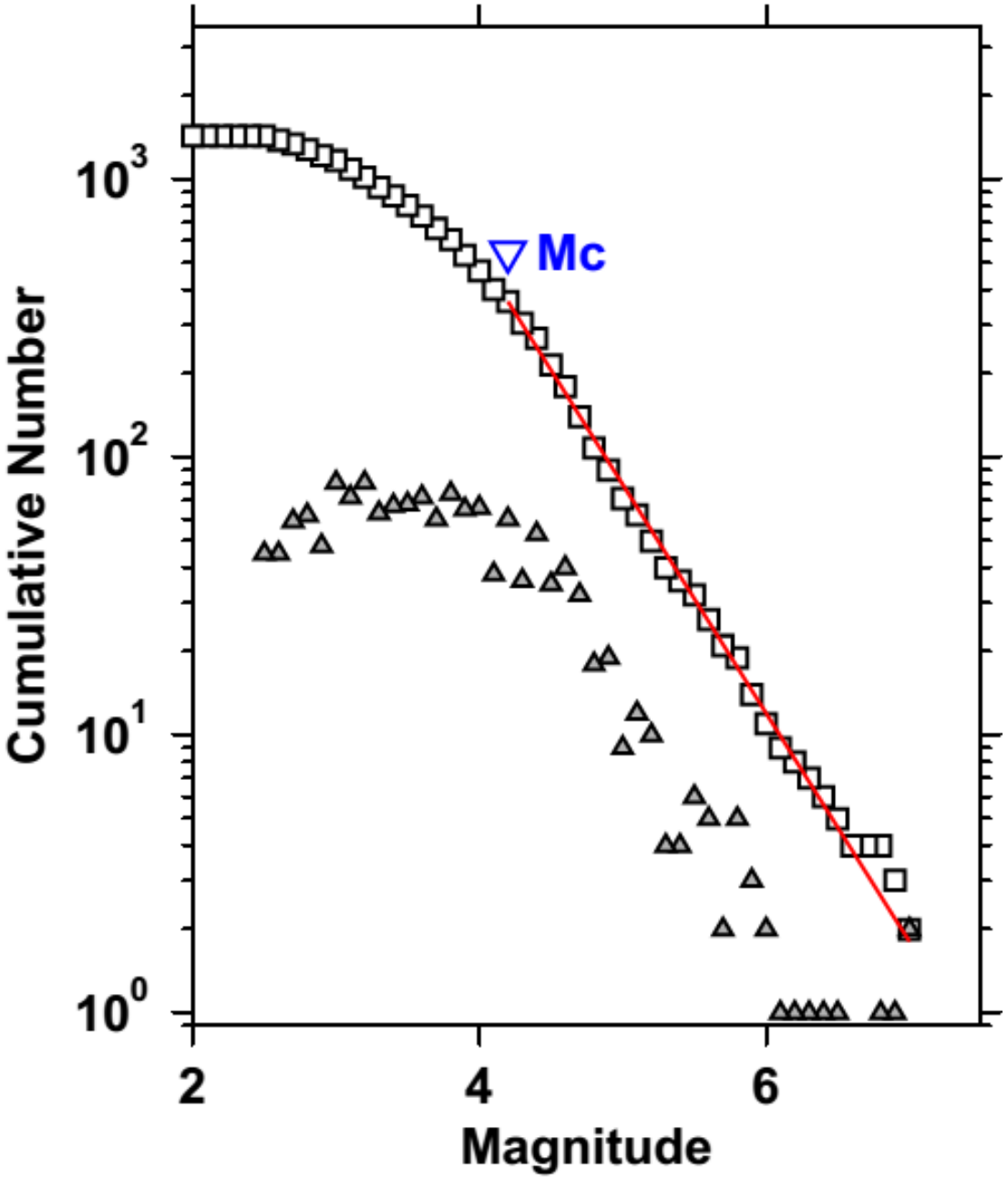

Figure 3.9. The *FMD* of earthquake in Thailand-Laos-Myanmar borders. Triangles shows the total number of seismic data in each magnitude. Squares indicates the cumulative number of earthquakes equal to or larger than each magnitude. The solid red lines are lines of the best fit. M_c is the magnitude of completeness.

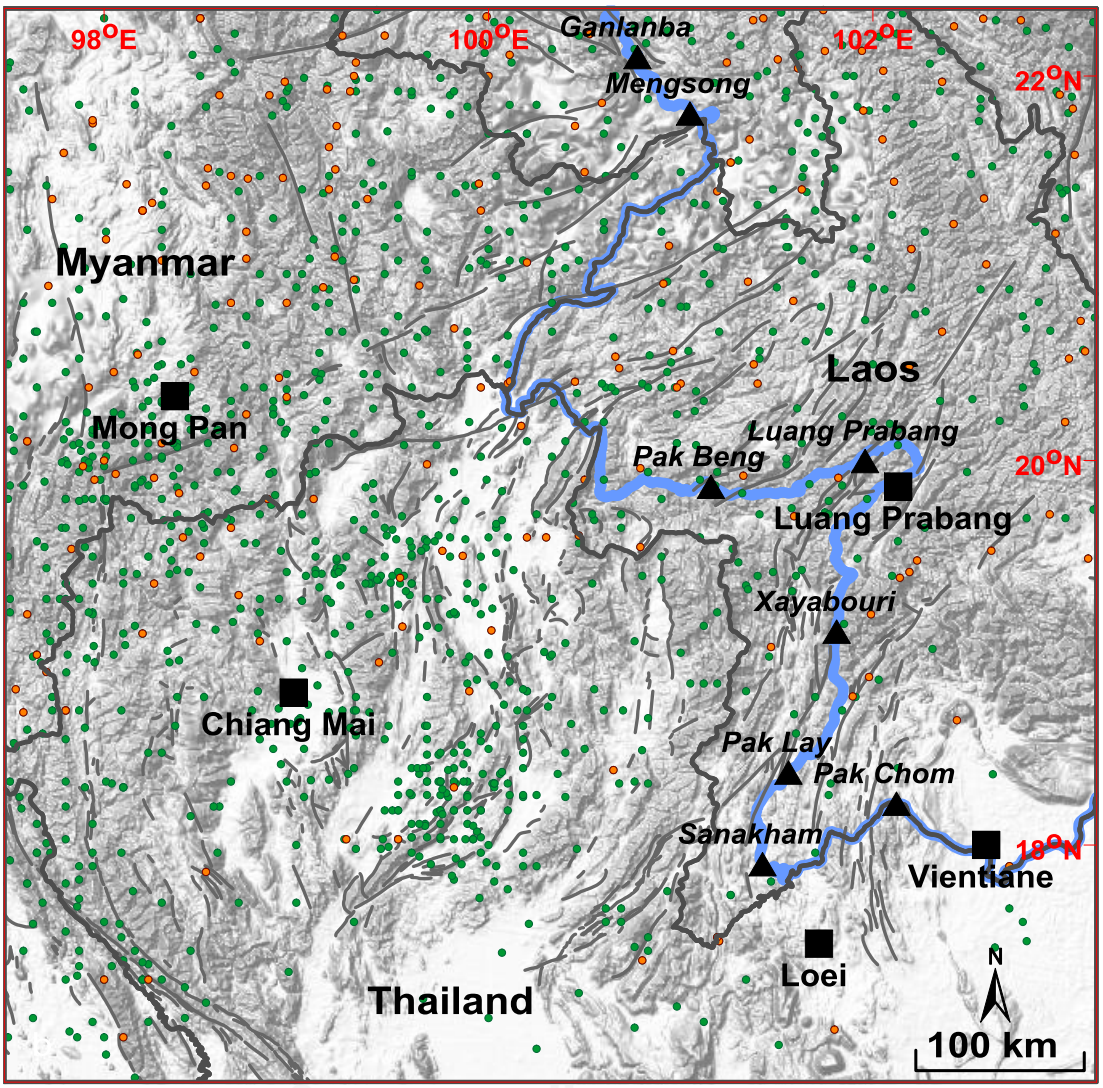

Figure 3.10. Map of Thailand-Laos-Myanmar border region (16.76° – 22.30°N and 97.48° – 103.16°E) showing the distribution of earthquakes after filtering the completeness seismicity data during 1981.99 and 2012.16. Green and orange points indicate the epicenter of main shocks before and after eliminating the epicenter of main shocks, which have moment magnitude scale (M_w) less than 4.4.

CHAPTER IV

SEISMICITY RATE CHANGE

After synthesis the completeness of seismicity data, the existing seismicity catalogues were applied to the retrospective tests in space and time by using seismicity rate changes (*Z*-value investigation) to investigate the seismicity precursors before the occurrences of 8 strong earthquakes ($M_w \geq 6.0$) which occurred in Thailand-Laos-Myanmar borders (16.76° – 22.30°N and 97.48° – 103.16°E) (Table 4.1). For the calculation, this work varies the *Z* parameters including the number of events (*n*) calculated from 25 to 150 with spacing every 25 events, time window (T_w) varied from 0.5 to 15 years with spacing every 0.5 years. Therefore, there were 6 x 30 = 180 characteristic conditions considered mainly (see appendix A). The suitable condition is arbitrary collected by the best result in temporal investigation and spatial investigation as explained in topics 4.1 and 4.2.

4.1 Temporal Investigation

According to the results of varied conditions, the main characteristic conditions cannot indicate seismicity anomalies prior to all strong earthquakes clearly. Consequently, this work decided to calculate *Z* value in subordinate scales, based on the group of characteristic parameters which provide good results. Then, the suitable characteristic parameter of *Z* values were determined as the number of events (*n*) = 50 and the time window (T_w) = 1.2 years.

For simplification the temporal investigation by this condition, the investigate area is calculated over a radius of 300 km around the study area, divided by a grid from latitude 13.97°N - 25.17°N and longitude 94.68°E - 105.88°E, with an interval of 0.2° gridded spacing. Thus, the total number of nodes is 3,250. In each grid node, a circle is drawn around by radius (*r*) that was increased until it includes a total of epicenters of *n* = 50. However, this study have fixed the limit of radius *r* = 250 km. The radius of more than 250

km will be cutoff because this area do not have many seismicity data, for preventing the meaningless of anomaly. Afterward, the cumulative number of earthquakes event versus time is plotted for every grid node, starting at a time t_0 (December 28, 1981) and ending at a time t_e (February 28, 2012). A time window is placed, starting at T_s and ending at $T_s + T_w$, where $t_0 \leq T_s \leq T_s + T_w \leq t_e$. T_w value of 1.2 years is used here, and T_s is moved forward in steps period of 0.04 years (~14 days). Then, in each interval position the Z value is calculated, generating the Long Time Average (LTA) function defined by Wiemer and Wyss (1994), which measures the significance of the difference between the mean seismicity rate R_w within the window T_w , and the background rate R_{bg} which is defined here as the equation 2.1.

After the seismicity rate change calculation, the results of the retrospective temporal investigation found 5 seismicity precursor from 8 strong earthquake events (62.5%) (Table 4.1).

Table 4.1. List of strong earthquake ($M_w \geq 6.0$) calculated by using Z parameter n = 50 events and T_w = 1.2 years. The parameters Z, Q_s, and Q-time indicate maximum of Z value at the epicenter of earthquake, starting time of seismic quiescence, and the duration between starting time of seismic quiescence and the occurrence time of main shock, respectively.

No	Lon (Deg)	Lat (Deg)	Date	Time (UTC)	Depth (km)	M_w	Z	Q_S (year)	Q-time (year)
1	102.58	21.36	24/6/1983	09:07	49.0	6.9	-	-	-
2	99.62	21.79	23/4/1984	22:30	17.0	6.3	-	-	-
3	99:06	20.32	28/9/1989	21:52	15.0	6.2	-	-	-
4	99.22	21.89	11/7/1995	21:46	15.0	6.8	3.0	1985.83	9.7
5	101.90	18.77	7/6/2000	21:48	33.0	6.5	6.0	1993.08	7.4
6	100.89	20.52	16/5/2007	08:56	12.6	6.3	6.9	2003.93	3.4
7	100.00	21.49	23/6/2007	08:17	16.1	6.1	7.0	1999.52	8
8	100.02	20.62	24/3/2011	13:55	13.2	6.8	6.8	2008.53	2.7

According to Table 1.1., the M_w-6.9 earthquake on June 6, 1983, the M_w-6.3 earthquake on April 23, 1984, and the M_w-6.2 earthquake on September 28, 1989 cannot calculate by *Z*-value investigation because there are insufficient seismicity data. However, the calculation of the M_w-6.8 earthquake on July 11, 1995, the M_w-6.5 earthquake on June 7, 2000, the M_w-6.3 earthquake on May 16, 2007, the M_w-6.1 earthquake on June 23, 2007 and the M_w-6.8 earthquake on March 24, 2011 can provide the cumulative number of *Z* values corresponding with impending strong earthquakes (Figure 4.1). The explanations of temporal variation can describe as follows;

i) According to Figure 4.1a, although the M_w-6.8 earthquake on July 11, 1995 found several phases of *Z* value peaks, the starting quiescence stage of this event was determined at 1985.83 (9.7 years before the main shock of the M_w-6.8 earthquake), because at this time, the *Z* curve at the epicenter of M_w-6.8 main shock indicates the highest peak with a maximum of *Z* values at this location = 3.0.

ii) Based on Figure 4.1b, the M_w-6.5 earthquake on June 7, 2000 detect the peaks of *Z* value started at 1987.25 and 1993.08. Even though both of peak have the same *Z* value (maximum *Z* value at the epicenter location = 6.0). The starting seismic quiescence stage was determined at 1993.08, because this peak was developed nearest to the occurrence time of main shock (7.4 years before the M_w-6.5 main shock occurred).

iii) Regarding to Figure 4.1c, the *Z* curve of the M_w-6.3 earthquake on May 16, 2007 shows the 4 durations of seismicity quiescence stage. These quiescence stages have the same *Z* value (maximum *Z* value at the main shock = 6.9). However, this work determined the duration of latest peak which it started at 2003.93 is the starting point of quiescence stage (3.4 years before the occurrence of the M_w-6.3 earthquake main shock), because the occurrence time of quiescence stage developed closely to the main shock.

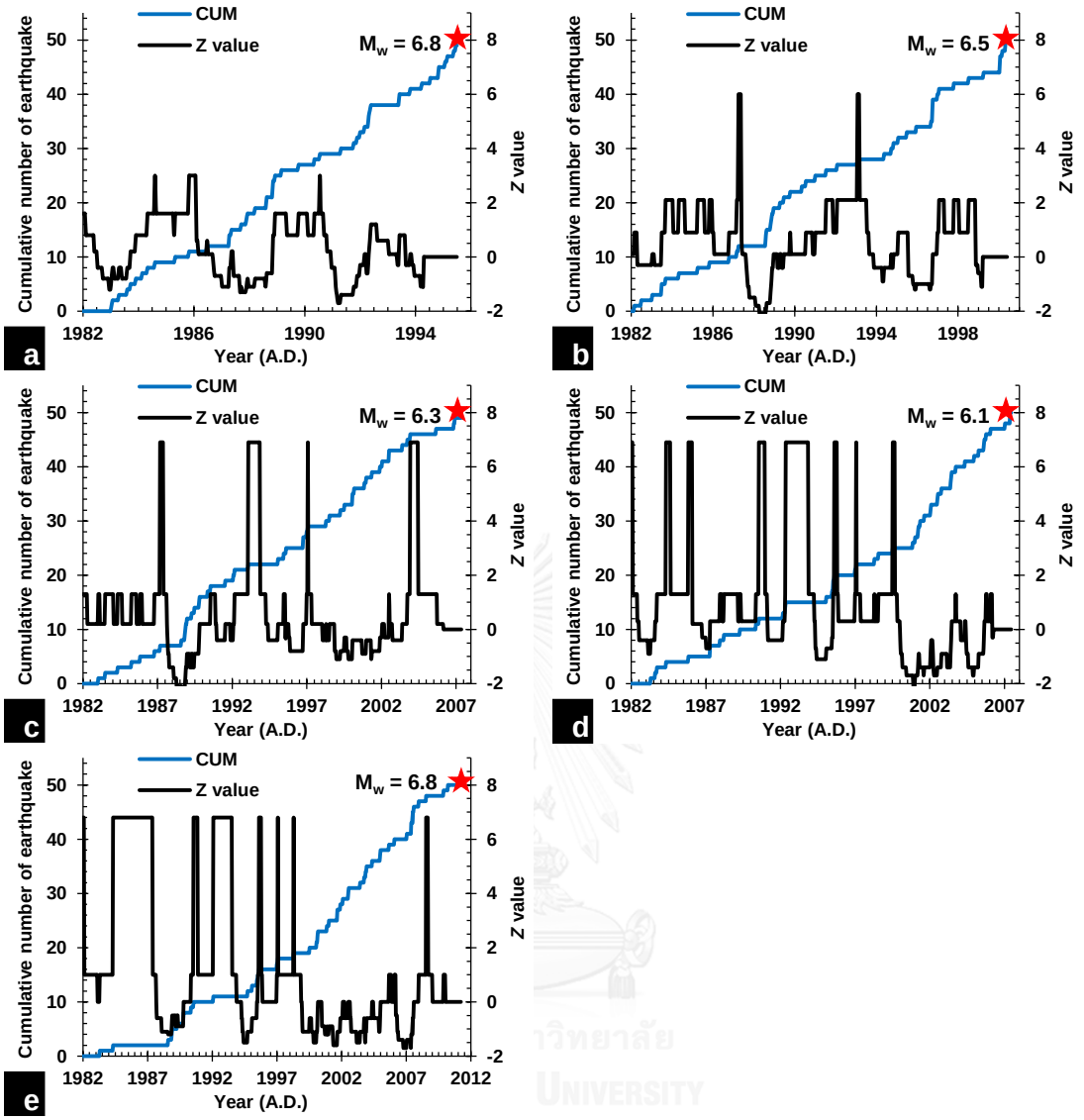

Figure 4.1. Cumulative number of earthquake and *Z* value plot versus time interval of the (a) M_w-6.8 earthquake on July 11, 1995, (b) M_w-6.5 earthquake on June 7, 2000, (c) M_w-6.3 earthquake on May 16, 2007, (d) M_w-6.1 earthquake on June 23, 2007, and (e) M_w-6.8 earthquake on March 24, 2011. The blue line implies the increasing of cumulative number of earthquakes during the focused time period. The thick black line indicates the Long-Term Average (*LTA*) function, displaying seismicity rate changes (*Z*-value investigation) relating the mean rate within the time interval in the calculable strong earthquake. Red Stars indicate the occurrence time of main shocks.

iv) According to Figure 4.1d, the *Z* parameter of the M_w-6.1 earthquake on June 23, 2007 shown the 8 duration of the seismic quiescence stages. These quiescence stage have the same *Z* value (maximum *Z* value at the epicenter = 7.0). However, based on the same reasons mentioned in ii) and iii), this work determined the occurrence of the latest peak that started in 1999.52 as the starting point of quiescence stage (8 years before the occurrence of the M_w-6.1 earthquake main shock).

v) Finally, in Figure 4.1e, the *Z* value of the M_w-6.8 earthquake on March 24, 2011 indicate the 8 durations of seismicity quiescence stages. These quiescence stages have the equal of *Z* values (maximum *Z* value at the location of the M_w-6.8 earthquake = 6.8). However, this work decided to choose the occurrence of the latest peak, which started in 2008.53 as the starting point of quiescence stage (2.7 year before the main shock of the M_w-6.8 earthquake on March 24, 2011 occurred), because the similar reasons mentioned in ii), iii) and iv).

4.2 Spatial Investigation

In order to constrain the potential of the *Z*-value investigation for detecting the earthquake precursor in intermediate-term and short-term in Thailand-Laos-Myanmar borders. This work applied also spatial investigation to investigate the upcoming strong earthquake in this area. The retrospective map shows the *Z* values in the area of latitude 16.76°N to 22.30°N and longitude 97.48°E to 103.16°E. The *Z* value of each node and each time slice indicating the seismicity rate change at that node. Positive and negative *Z* values represent that the seismicity rate is lower, and higher, than the mean rate, respectively. The positive of *Z* values represents the decreasing of earthquake in the study area (seismic quiescence). As the number of effective grid nodes is 3,250 for each time slice, and since there are more than 750 time slices, the total number of effective grid nodes, where *Z* values were calculated, are more than 2,437,500. The results of spatial investigation at the starting time of seismicity quiescence explained as follows;

i) The spatial distribution of the M_w-6.8 earthquake on July 11, 1995 indicate the seismicity quiescence anomaly covered widely around 350 km^2 over the eastern part of

Myanmar (including cities i.e., Mongyan, Kengtung, Monghpyak, Mongyawng, Mong Ho-pung, Bok Hsopnam), the Southern Yunnan, China and the northern part of Laos (including cities Pak Beng and Houay Xay). The anomaly area locate on the 4 fault zones, for examples, Nam Ma (Morley, 2007), Jinghong (Lacassin et al., 1998), Menglian (Lacassin et al., 1998) and Mengxing (Lacassin et al., 1998) fault zones The location of maximum Z value (Z_{max} = 6.8) situate on Monyawng city (21.27˚N, 100.29˚E) with the group of high Z value belt pose in the north-west of Z_{max} location and passing through Mengxing and Nam Ma fault zones. However, the epicenter of the M_w-6.8 earthquake on July 11, 1995 located at the north-west of Kengtung city (21.89˚N, 99.22˚E) far from the location of Z_{max} area around 150 km (Figure 4.2).

ii) The spatial map of the M_w-6.5 earthquake on June 7, 2000 shows the seismicity quiescence anomaly generated dimly around 300 km^2 over the eastern part of Myanmar (including cities i.e., Mongyan, Kengtung, Monghpyak, Mongyawng, Mong Ho-pung, Bok Hsopnam), northwestern part of Laos (including cities, i.e., Vientiane, Pak Lai, Phonsavan, Luang Prabang and Pak Beng) and some area in the northeastern part of Thailand (including cities, Nan, Uttaradit and Phayao). Moreover, the anomaly area locate in a number of fault zones between Thailand and Laos and Myanmar. The zone of high Z value ($Z \geq 6.0$) developed lengthily from the eastern part of Myanmar to the southern part of Laos and the northern part of Thailand, passing through Mengxing, Nam Ma, Mae Ing (Fenton et al., 2003) fault zones (Figure 4.3).

iii) The spatial map of the M_w-6.3 earthquake on May 16, 2007 shows the seismicity quiescence anomaly developed widely with high Z value, posing in a long belt with the distance more than 700 km started from the northern part of Thailand to the northern part of Laos (including well-known cities i.e., Chiang Mai, Chiang Rai, Phayao, Nan, Pak Beng, Luang Prabang) (Figure 4.4). The anomaly area covered on a number of fault zones between Thailand and Laos. However, the epicenter of the M_w-6.3 earthquake on May 16, 2007 (20.52˚N, 100.89˚E) located at the Mae Ing fault zones which it has positive Z value = 6.9 (High Z value zone). Nevertheless, the zone of high Z values ($Z \geq 6.0$) developed

continuously from the northern of Thailand to the northern of Laos with the distance more than 600 km.

iv) The spatial distribution of the M_w-6.1 earthquake on June 23, 2007 indicate the seismicity quiescence anomaly covered straightly around 600 km over the eastern part of Myanmar (i.e., Mongyan, Kengtung, Monghpyak, Mongyawng, Mong Ho-pung, and Bok Hsopnam cities), the Southern Yunnan, China and the northern part of Laos (including cities Muang Ou Tai and Muang Khoa). The anomaly of quiescence area located on Jinghong and Mengxing fault zones. The Z_{max} = 7.1 situate around Kengtung and Bok Hsopnam city (21.37˚N, 100.48˚E) with the group of high Z value belt posing in the east of Z_{max} location and passing to Mengxing fault zones. The epicenter of the M_w-6.1 earthquake located at the north-west of Kengtung city (21.49˚N, 100.00˚E) that it is closely to the location of Z_{max} area around 150 km (Figure 4.5).

v) The spatial distribution of the M_w-6.8 earthquake on March 24, 2011 indicate the seismicity quiescence anomaly covered widely around 400 km^2 over the eastern part of Myanmar (i.e., Mongyan, Kengtung, Monghpyak, Mongyawng, Mong Ho-pung, and Bok Hsopnam cities), the northern part of Thailand (including cities i.e., Chiang Mai, Chiang Rai and Nan) and the northern of Laos (including cities Pak Beng, Luang Prabang and Xaignabouli). The anomaly of quiescence area locate in Mengxing fault zones and Wan Na-awn fault zones (Pailoplee et al., 2009b). The Z_{max} zone (Z_{max} = 6.8) situate around Monghpyak city (20.57 ˚N, 99.68 ˚E and 20.77 ˚N, 99.88 ˚E) with the group of high Z value belt posing in the north-west of Z_{max} location and passing through the Chiang Rai, Mengxing and Wan Na-awn fault zones. The epicenter of the March 24, 2011 M_w-6.8 earthquake located among the location of high Z value zone ($Z \geq 6.0$), at Monghpyak city (20.62˚N, 100.02˚E) (Figure 4.6).

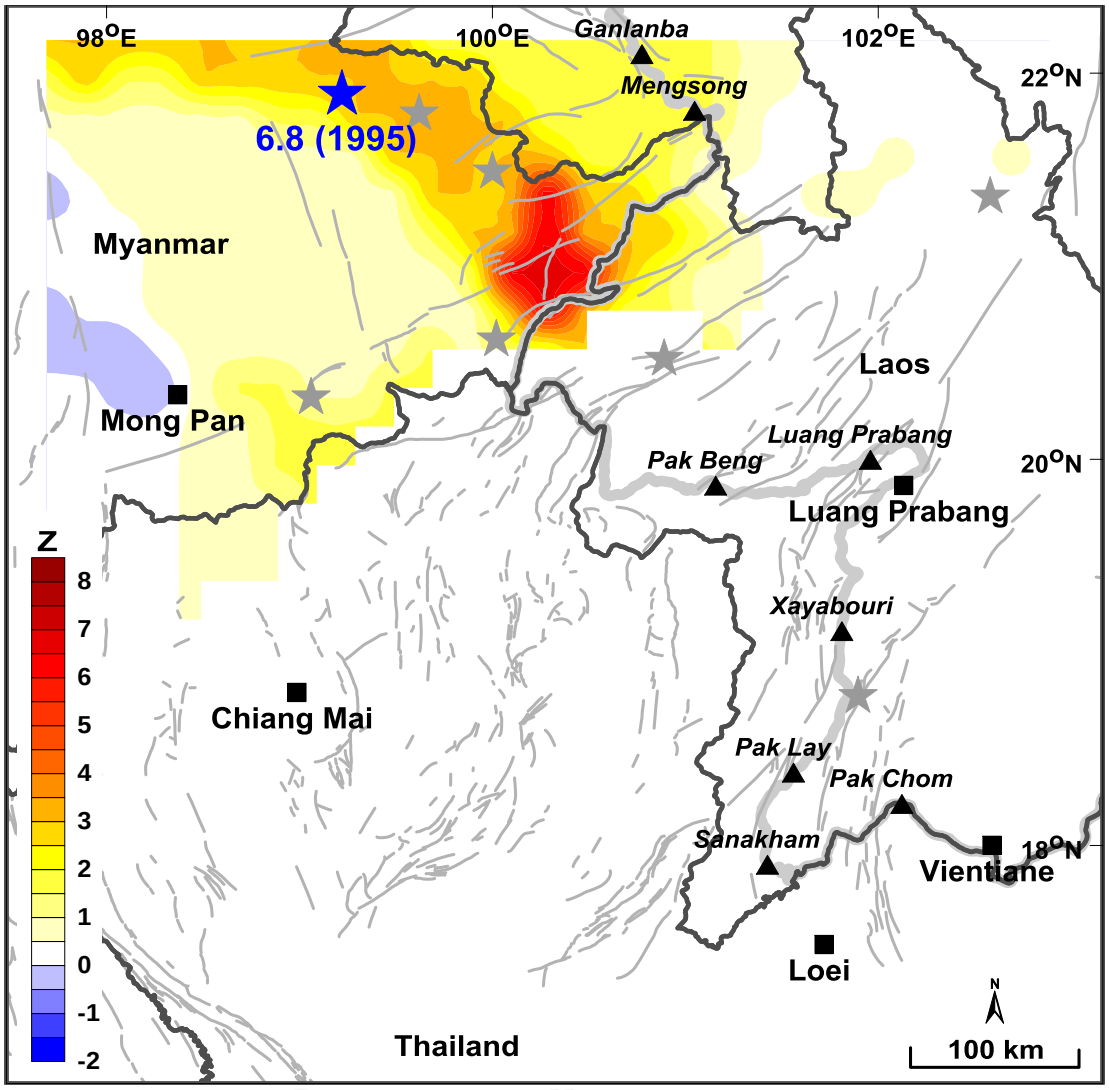

Figure 4.2. Map of Thailand-Laos-Myanmar borders showing spatial distribution of *Z* values at the time slice of seismic quiescence stage A.D. 1985.83, 9.7 years before the occurrences of the M_w-6.8 earthquake on July 11, 1995. The scale on the left corresponds to the *Z* value, a red shade (positive *Z* value) and blue shade (negative *Z* value) represents a decrease and increase in the seismicity rate, respectively. The epicenter of the M_w-6.8 earthquake (21.89˚N, 99.22˚E) is shown as a blue star. The grey stars show the epicenters of all 8 events utilized for retrospective test.

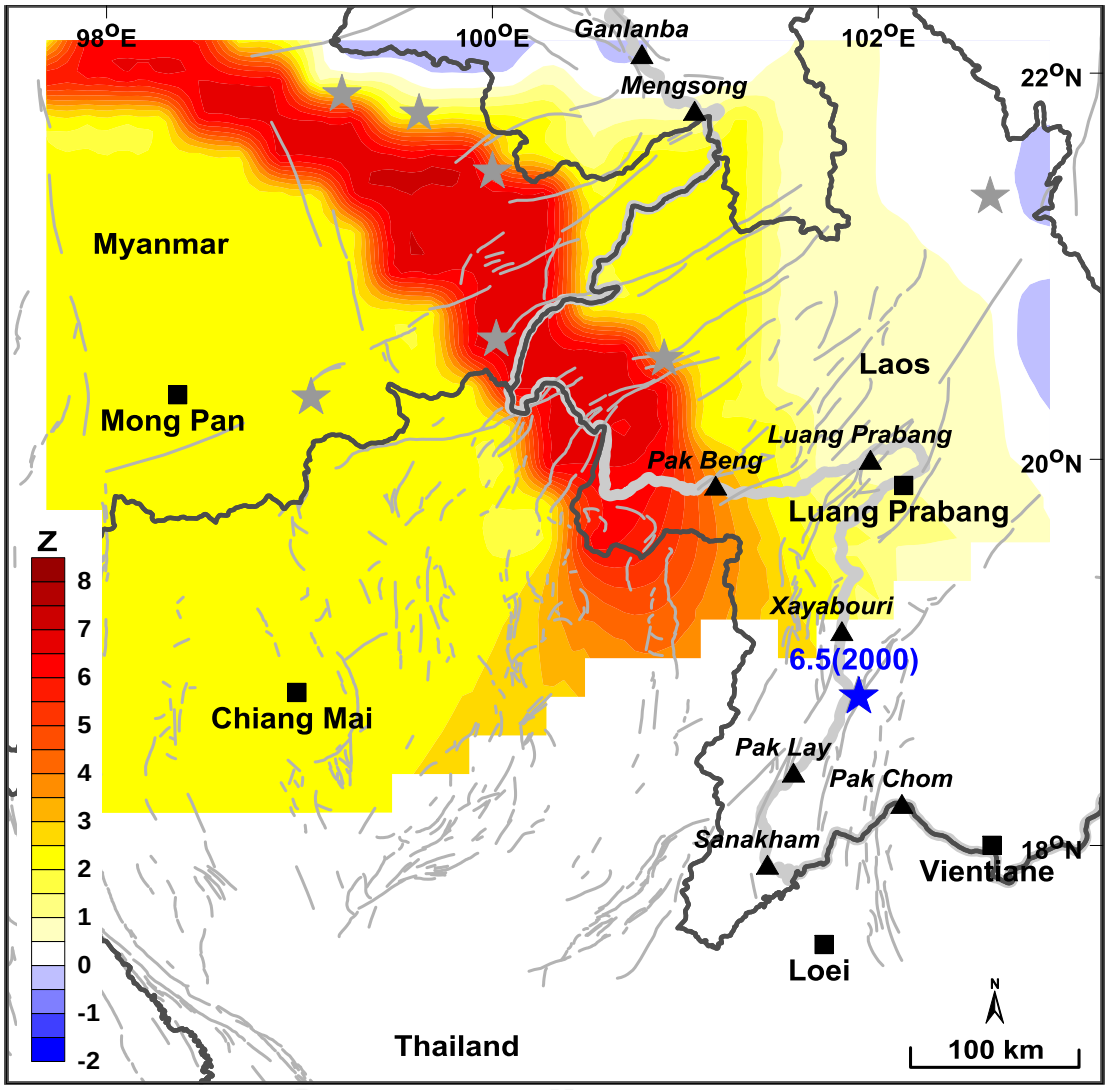

Figure 4.3. Map of Thailand-Laos-Myanmar borders showing spatial distribution of *Z* values at the time slice of seismic quiescence stage A.D. 1999.03, 7.4 years before the occurrences of the M_w-6.5 earthquake on June 7, 2000. The scale on the left corresponds to the *Z* value, a red shade (positive *Z* value) and blue shade (negative *Z* value) represents a decrease and increase in the seismicity rate, respectively. The epicenter of the M_w-6.5 earthquake (18.77˚N, 101.90˚E) is shown as a blue star. The grey stars show the epicenters of all 8 events utilized for retrospective test.

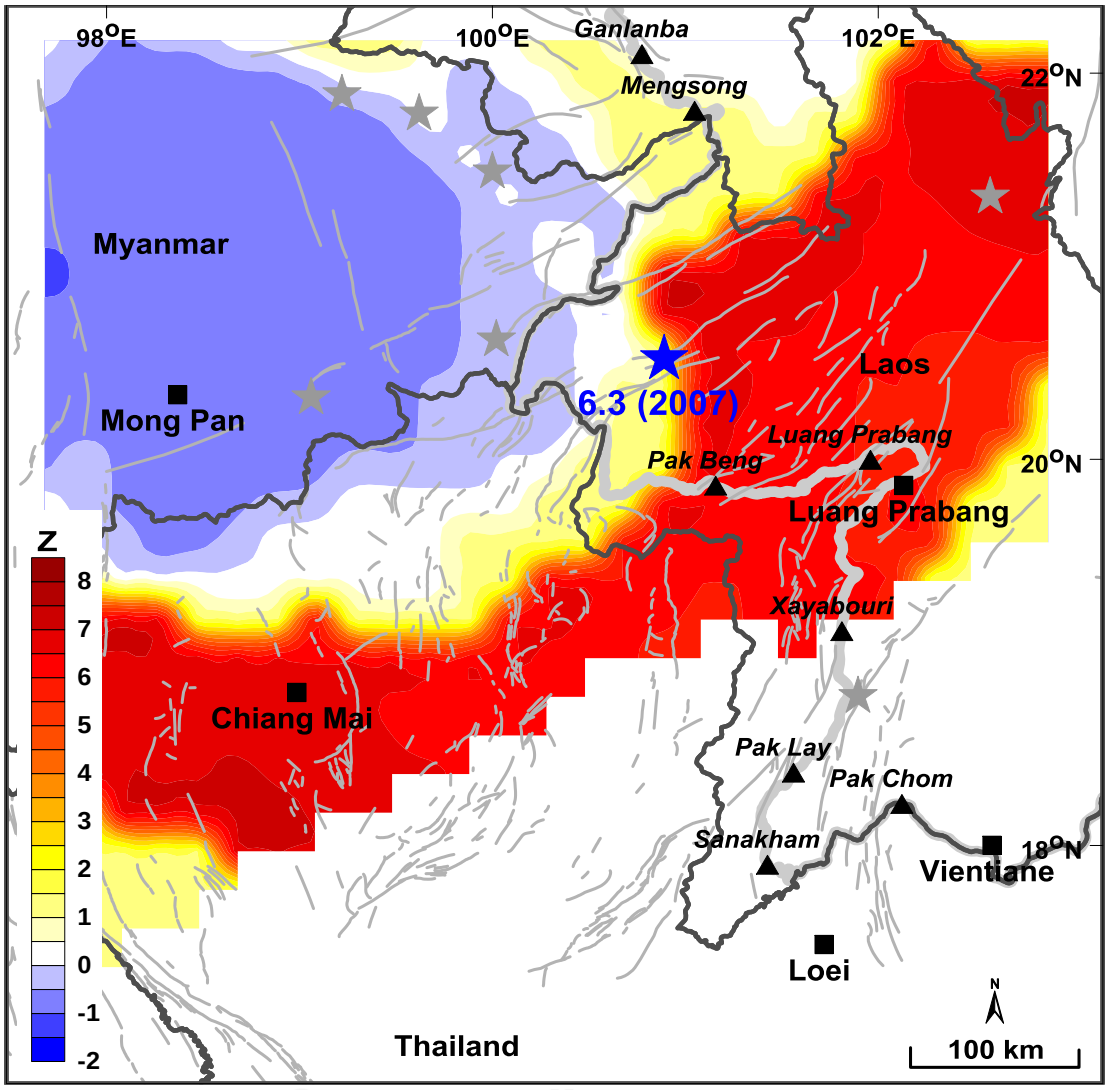

Figure 4.4. Map of Thailand-Laos-Myanmar borders showing spatial distribution of *Z* values at the time slice of seismic quiescence stage A.D. 2003.93, 3.4 years before the occurrences of the M_w-6.3 earthquake on May 16, 2007. The scale bar on the left corresponds to the *Z* value, a red shade (positive *Z* value) and blue shade (negative *Z* value) represents a decrease and increase in the seismicity rate, respectively. The epicenter of the M_w-6.3 earthquake (20.52˚N, 100.89˚E) is shown as a blue star. The grey stars show the epicenters of all 8 events utilized for retrospective test.

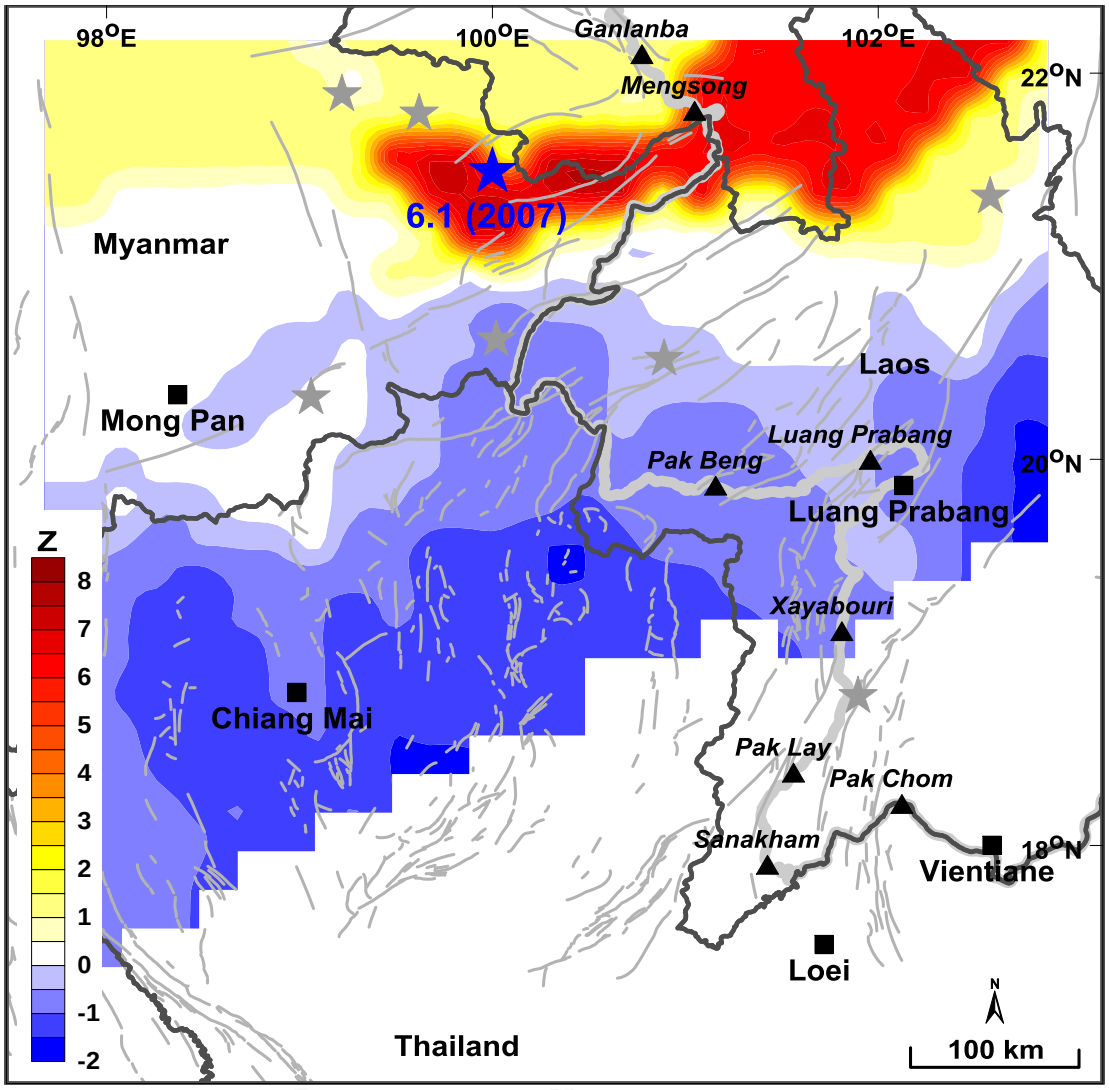

Figure 4.5. Map of Thailand-Laos-Myanmar borders showing spatial distribution of *Z* values at the time slice of seismic quiescence stage A.D. 1999.52, 8 years before the occurrences of the M_w-6.1 earthquake on June 23, 2007. The scale on the left corresponds to the Z value, a red shade (positive *Z* value) and blue shade (negative *Z* value) represents a decrease and increase in the seismicity rate, respectively. The epicenter of the M_w-6.1 earthquake (21.49˚N, 100.00˚E) is shown as a blue star. The grey stars show the epicenters of all 8 events utilized for retrospective test.

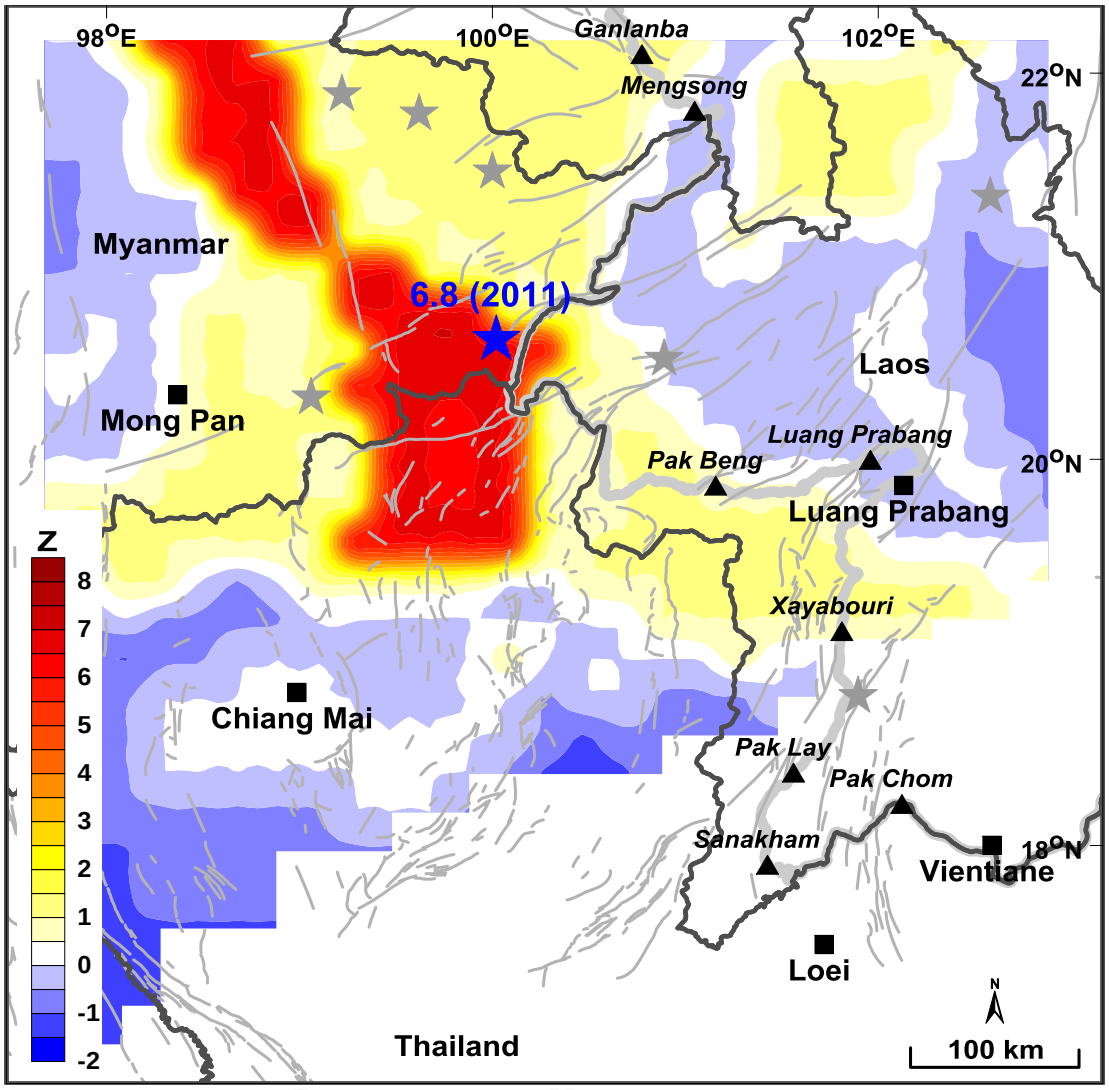

Figure 4.6. Map of Thailand-Laos-Myanmar borders showing spatial distribution of *Z* values at the time slice of seismic quiescence stage A.D. 2008.53, 2.7 years before the occurrences of the M_w-6.8 earthquake on March 24, 2011. The scale bar on the left corresponds to the *Z* value, a red shade (positive *Z* value) and blue shade (negative *Z* value) represents a decrease and increase in the seismicity rate, respectively. The epicenter of the M_w-6.8 earthquake (20.62˚N, 100.02˚E) is shown as a blue star. The grey stars show the epicenters of all 8 events utilized for retrospective test.

Remark: According to Figure 4.3, although the temporal investigation of the retrospective test can detect seismic quiescence at the location of the main shock, the result of retrospective spatial investigation don't shows the anomaly cover the epicenter. The unreasonable result of this case study caused by the spatial investigation of *Z* don't shows the result if the collecting radius at each grid node more than 250 km. Then, the M_w-6.5 main shock (18.77°N, 101.90°E) occurred outside the anomaly zone within the southeast direction of the mentioned anomalies and the distance, approximate 100 km because the node around the epicenter which collecting radius more than 250 km were not indicated quiescence stage.

CHAPTER V

REGION-TIME-LENGTH ALGORITHM

In order to constrain the *Z* value obtained from the previous chapter, this work investigate the seismicity pattern changes in Thailand-Laos-Myanmar borders by using the *RTL* algorithm as well. The *RTL* investigation also implements the same completeness seismicity data used in the previous *Z* value investigation. The retrospective tests were investigated in space and time prior to 8 strong earthquakes ($M_w \geq 6.0$) which occurred in Thailand-Laos-Myanmar borders (16.76° – 22.30°N and 97.48° – 103.16°E) (Table 5.1). The goal of this chapter is finding the suitable characteristic *RTL* parameter (r_0 and t_0, resembling to R_{max} and T_{max}, respectively) which can detect earthquake precursor impending to strong earthquakes. Then, this work varies the characteristic *RTL* parameters including the characteristic distance r_0 from 40 to 150 with spacing every 5 km, and characteristic time-span t_0 from 0.5 to 5 years with spacing 0.05 years. Hence, 22 x 80 = 1,980 characteristic *RTL* conditions were considered mainly (Appendix B). The suitable characteristic *RTL* parameter is in arbitrary collected by the best result in both temporal and spatial investigations as explained in topics 5.1 and 5.2.

5.1 Temporal Investigation

As the results of varied conditions, it seems to be that the characteristic distance r_0 = 120 km ($R_{max} = 2r_0$ = 240 km) and the characteristic time-span t_0 = 2 ($T_{max} = 2t_0$ = 4 years) successful to find out concurrently the irregular seismic activity, i.e., anomalous value of *RTL*, or it can determine as the suitable characteristic *RTL* parameters.

For simplification the temporal investigation by this *RTL* condition, the investigate area is calculated over radius 300 km around the study area, divided by a grid from latitude 13.97°N - 25.17°N and longitude 94.68°E - 105.88°E, with an interval of 0.2° gridded spacing. Thus, the total number of nodes is 3,250 (same as the total nodes of *Z* values). In each grid node, a circle is drawn around by the radius of R_{max} = 240 km. The

earthquakes occurred inside radius R_{max}, during the time window T_{max} = 4 years are selected. Then, the *RTL* algorithm was evaluated by changing the calculated time at a step of 14 days, starting at the beginning of available seismicity data through the occurrence time of earthquake considered. Nevertheless, in order to avoid the erroneous calculation of *RTL* algorithm, this work determined the minimum of the number of events inside the radius (n) = 30 events, the *RTL* value which calculated less than 30 earthquake events are eliminated. Afterward, the *RTL* values in each node are normalized between -1 and 1 of *RTL* scores. The results of *RTL* values are plotted versus time at every grid node, for identifying the significance of the difference between the background seismicity rates. The result of the temporal investigation by using *RTL* algorithm applied prior to strong earthquakes, found 5 seismicity precursor from 8 strong earthquake events (62.5%, same as *Z*-value investigation) (Table 5.1).

Table 5.1. List of strong earthquake ($M_w \geq 6.0$) calculated by using characteristic *RTL* parameter r_0 = 120 and t_0 = 2. The parameters *RTL*, Q_s, and *Q*-time indicate minimum of *RTL* value at the epicenter of each strong earthquake, starting time of seismic quiescence, and the duration between starting time of seismic quiescence and the occurrence time of main shock, respectively.

No	Lon (Deg)	Lat (Deg)	Date	Time (UTC)	Depth (km)	M_w	*RTL*	Q_S (year)	*Q*-time (year)
1	102.58	21.36	24/6/1983	09:07	49.0	6.9	-	-	-
2	99.62	21.79	23/4/1984	22:30	17.0	6.3	-	-	-
3	99:06	20.32	28/9/1989	21:52	15.0	6.2	-	-	-
4	99.22	21.89	11/7/1995	21:46	15.0	6.8	-0.68	1992.39	3.1
5	101.90	18.77	7/6/2000	21:48	33.0	6.5	-0.90	2000.06	0.4
6	100.89	20.52	16/5/2007	08:56	12.6	6.3	-0.65	2003.93	3.4
7	100.00	21.49	23/6/2007	08:17	16.1	6.1	-0.65	1995.65	11.8
8	100.02	20.62	24/3/2011	13:55	13.2	6.8	-1.00	2007.58	3.7

According to temporal investigation of *RTL*, it reveals that the M_w-6.9 earthquake on June 6, 1983, the M_w-6.3 earthquake on April 23, 1984, and the M_w-6.2 earthquake on September 28, 1989 cannot calculated *RTL* value, because there are insufficient seismicity data. Nevertheless, the computation of the However, the calculation of the M_w-6.8 earthquake on July 11, 1995, the M_w-6.5 earthquake on June 7, 2000, the M_w-6.3 earthquake on May 16, 2007, the M_w-6.1 earthquake on June 23, 2007 and the M_w-6.8 earthquake on March 24, 2011 can provide the temporal variation of *RTL* value corresponding with impending strong earthquakes (Figure 5.1). The explanations of temporal variation can be described as follow;

i) Based on Figure 5.1a, the normalized *RTL* curve of the M_w-6.8 earthquake on July 11, 1995 epicenter rather developed straightly along background value until it found the seismic quiescence started in 1992.31. After that, the *RTL* parameters decreased immediately and reach its minimum in 1992.39 (minimum *RTL* value= - 1.0). After then, the *RTL* curve raised rapidly to background value in 1992.77 and has develop along the mean rate again until the occurrence of main shock (2.76 years after the quiescence posed).

ii) According to Figure 5.1b, the normalized *RTL* curve at the M_w-6.5 earthquake on June 7, 2000 location generated straightly along the mean value between 1984.56 and 1992.73. Afterward, the curve has a little variation during 1992.74 and 2000.02 before it decreased instantly to the bottom in 2000.6 (minimum *RTL* = - 0.96). This earthquake occurred in 2000.36, in the duration of seismicity quiescence.

iii) Regarding to Figure 5.1c, the normalized *RTL* parameter of the M_w-6.3 earthquake on May 16, 2007 identified the variant development along the *RTL* graph. This *RTL* curve indicates 3 quiescence stage (started at 1989.79 – 1991.81, 1991.89 – 1992.73 and 2003.24 – 2004.28) and 3 activation stage (started at 1987.36 – 1988.97, 1993.58 – 1995.65 and 1995.76 – 1996.76). However, the precursor stage of this event determined at the quiescence stage between 2003.24 and 2004.28 because this duration indicates the most different *RTL* value from the background rate (minimum *RTL* value = - 0.80).

Therefore, the M_w-6.3 main shock occurred with a time delay of 3.09 years after the end of quiescence stage.

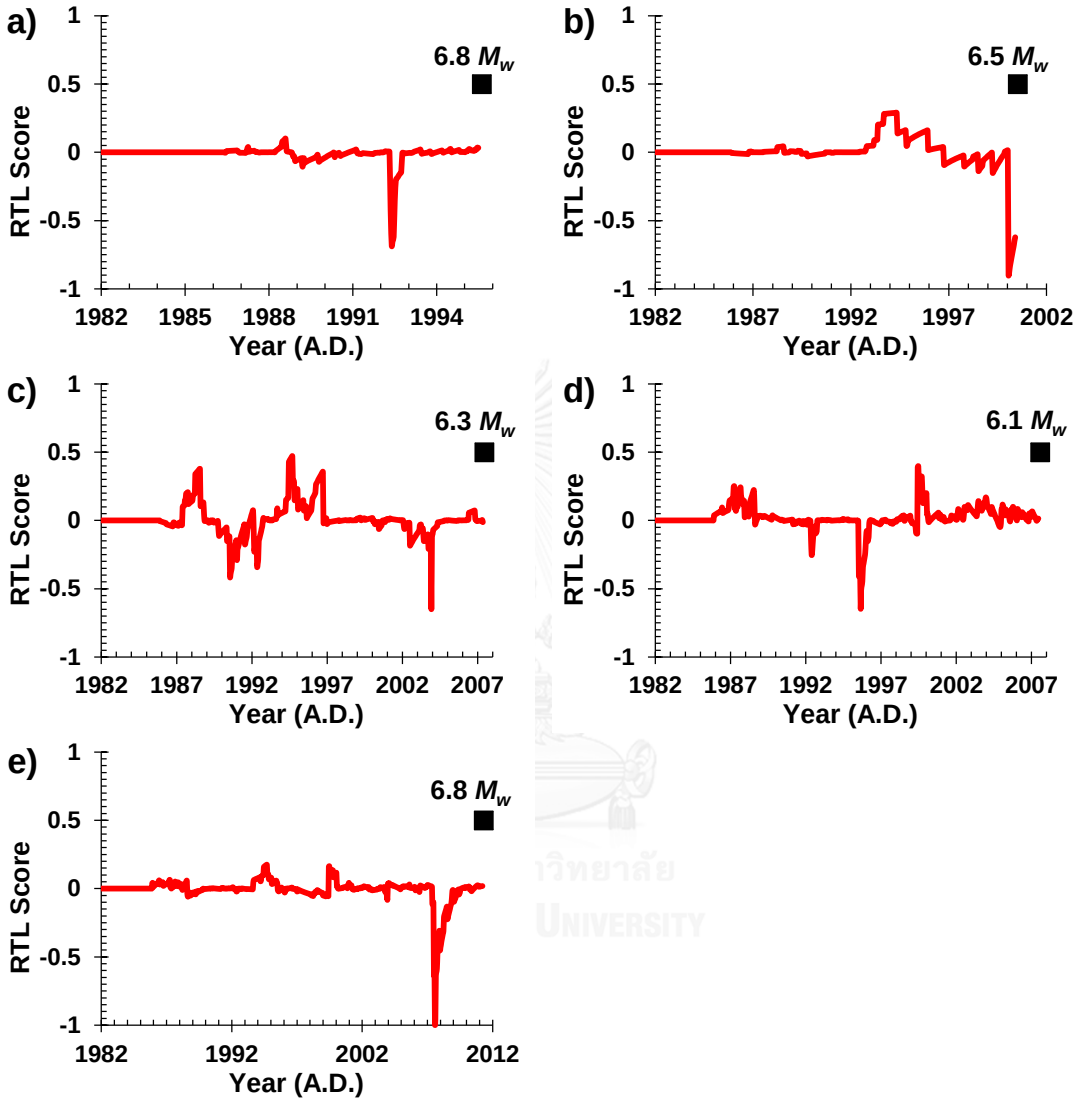

Figure 5.1. Temporal variation of *RTL* values plot versus time interval of the (a) M_w-6.8 earthquake on July 11, 1995 (21.89˚N, 99.22˚E), (b) M_w-6.5 earthquake on June 7, 2000 (18.77˚E, 101.90˚N), (c) M_w-6.3 earthquake on May 16, 2007 (20.52˚N, 100.89˚E), (d) M_w-6.1 earthquake on June 23, 2007 (21.49˚N, 100.00˚E), and (e) M_w-6.8 earthquake on March 24, 2011 (20.62˚N, 100.02˚E). The red line implies the *RTL* value during the focused time period. The black square indicates the occurrence time of each earthquake.

iv) Based on Figure 5.1d, the normalized *RTL* value plotted versus time of the M_w-6.1 earthquake on June 23, 2007 location identify the seismicity quiescence start decreasing in 1995.49 and reached its minimum in 1995.65 (minimum *RTL* = - 0.66). After that, the normalized *RTL* parameter increased and return to the normal stage in 1996.53 until 1999.18. Then, the normalized *RTL* value indicates activation stage started in 1999.25 – 2000.21 with a maximum *RTL* value = 0.40. After the activation stage, the *RTL* curve has a small variants 7.27 years before the occurrence of the main shock.

v) In final case in Figure 5.1e, the normalized *RTL* curve at the M_w-6.8 earthquake on March 24, 2011 epicenter indicate seismic quiescence clearly from the background seismicity rate. The decreasing start at 2007.35 and reach its minimum at 2007.58 before returning gradually to the background rate at 2009.57, the normal stage has a duration of 1.66 years before the occurrence of main shock.

5.2 Spatial Investigation

In order to support the potential of the *RTL* algorithm for short-term and intermediate-term earthquake forecasting. This research used also spatial investigation to identify the seismicity precursor of the upcoming strong earthquake in the Thailand-Laos-Myanmar borders. The retrospective spatial distribution indicates the *RTL* parameter in the area of latitude 16.76°N to 22.30°N and latitude 97.48°E to 103.16°E. The normalized *RTL* value in each grid node and each time slice is calculated by using the *Q*-parameter as mentioned as equation 2.6. The results of *Q*-parameter are indicate the seismicity rate variation around each node area. Negative and positive *RTL* values imply that the earthquake activities are lower, and higher, than the background rate, respectively. The positive of *RTL* value implies the increasing of earthquake in the study area (seismicity activation) and the negative of *RTL* value implies the decreasing of earthquake activities in the study area (seismicity quiescence).

As the number of effective grid nodes is 3,250 for each time slice, and since there are more than 750 time slices, the total number of effective grid nodes, where *RTL* values were calculated, are more than 2,437,500. The results of spatial investigation between the duration of seismicity quiescence stage described as follows;

i) The spatial distribution of the M_w-6.8 earthquake on July 11, 1995 indicates the seismicity quiescence anomaly covered widely around 300 km^2 over the Eastern Myanmar (around 150-km southwestern part of the Mengsong city) and some area in the southern part of Yunnan, China. The anomaly area locates on the 3 fault zones, for examples, Jinghong (Lacassin et al., 1998), Mengxing and Nam Ma fault zones. The location of minimum *RTL* value situated on Kengtung city (21.37˚N, 99.69˚E) and close to Jinghong fault zones. However, the epicenter of the July 11, 1995 M_w-6.8 earthquake located at the north-west of Kengtung city (21.89˚N, 99.22˚E) far from the location of the minimum *RTL* zone around 100 km (Figure 5.2).

ii) The spatial map of the M_w-6.5 earthquake on June 7, 2000 shows the seismicity quiescence anomaly generated dimly around 300 km^2 over the northwestern of Laos (including cities, i.e., Vientiane, Pak Lai, Phonsavan, Luang Prabang and Pak Beng) and some area in the northeastern Thailand (including cities, Nan, Uttaradit and Phayao). The anomaly area locates in the vicinity of 3 fault zones, for examples, Dein Bein Fu (Zuchiewicz et al., 2004), Nam Peng (Charusiri et al., 1999) and Loei-Petchabun Suture fault zones (Lepvrier et al., 2004). The location of minimum *RTL* value situated on Pak Beng city (19.97˚N, 100.89˚E) and close to Nam Peng fault zone. However, the epicenter of the June 7, 2000 M_w-6.5 earthquake located at the south-east of Pak Beng city (18.77˚N, 101.90˚E) far from the location of minimum *RTL* area around 180 km (Figure 5.3).

iii) The spatial map of the M_w-6.3 earthquake on May 16, 2007 represented the seismicity quiescence anomaly developed dimly around 300 km^2 over the Northern of Thailand (including cities, i.e., Chiang Rai, Phayao, Nan, Uttaradit, Lampang and Phrae) and some area in the north of Laos (including cities, Pak Beng and Houay Xay). The anomaly area located on the 4 fault zones, for examples, Pha Yao (Fenton et al., 2003), Mae Ing, Mae Chan (Fenton et al., 2003) and Chiang Rai fault zones (Pailoplee et al.,

2009b). The location of minimum *RTL* value situated on Chiang Rai city (20.18˚N, 100.08˚E) and close to Chiang Rai fault zone. However, the epicenter of the May 16, 2007 M_w-6.3 earthquake located at the north-east of Chiang Rai city (20.52˚N, 100.89˚E) far from the location of minimum *RTL* zone around 125 km (Figure 5.4).

iv) The spatial map of the M_w-6.1 earthquake on June 23, 2007 indicated the seismicity quiescence anomaly posed around 300 km along the eastern of Myanmar (including cities, i.e., Bok Hsopnam, Mongyawng, Kengtung, Mongyan and Ta-kaw) to the southern of Yunnan, China. The anomaly area located in the Jinghong fault zone. The location of minimum *RTL* value situated on Mongyan city (22.17˚N, 99.08˚E) and close to Jinghong fault zone. However, the epicenter of the June 23, 2007 M_w-6.1 earthquake located at the south of Mongyan city (21.49˚N, 100.00˚E) with the distance from the location of minimum *RTL* area to the location of epicenter around 50 km (Figure 5.5).

v) The spatial map of the M_w-6.8 earthquake on March 24, 2011 implied the seismicity quiescence anomaly covered around 350 km^2 over of eastern part of Myanmar (including cities, i.e., Bok Hsopnam, Mongyawng, Kengtung, Mongyan and Ta-kaw), the northern of Thailand (including cities, i.e., Chaing Mai and Chiang Rai), the northern part of Laos (including cities, Houay Xay and Luang Namtha). The anomaly area located on the 2 fault zones, for examples, southern part of Mae Chan and Wan Na-awn fault zone. The location of minimum *RTL* value situate on the northern of Chiang Mai city (19.57˚N, 99.28˚E) and close to Mae Chan fault zone. However, the epicenter of the March 24, 2011 M_w-6.8 earthquake locate at the south-west above Chiang Mai city (20.62˚N, 100.02˚E) with the distance from the location of minimum *RTL* area to the location of epicenter around 150 km (Figure 5.6).

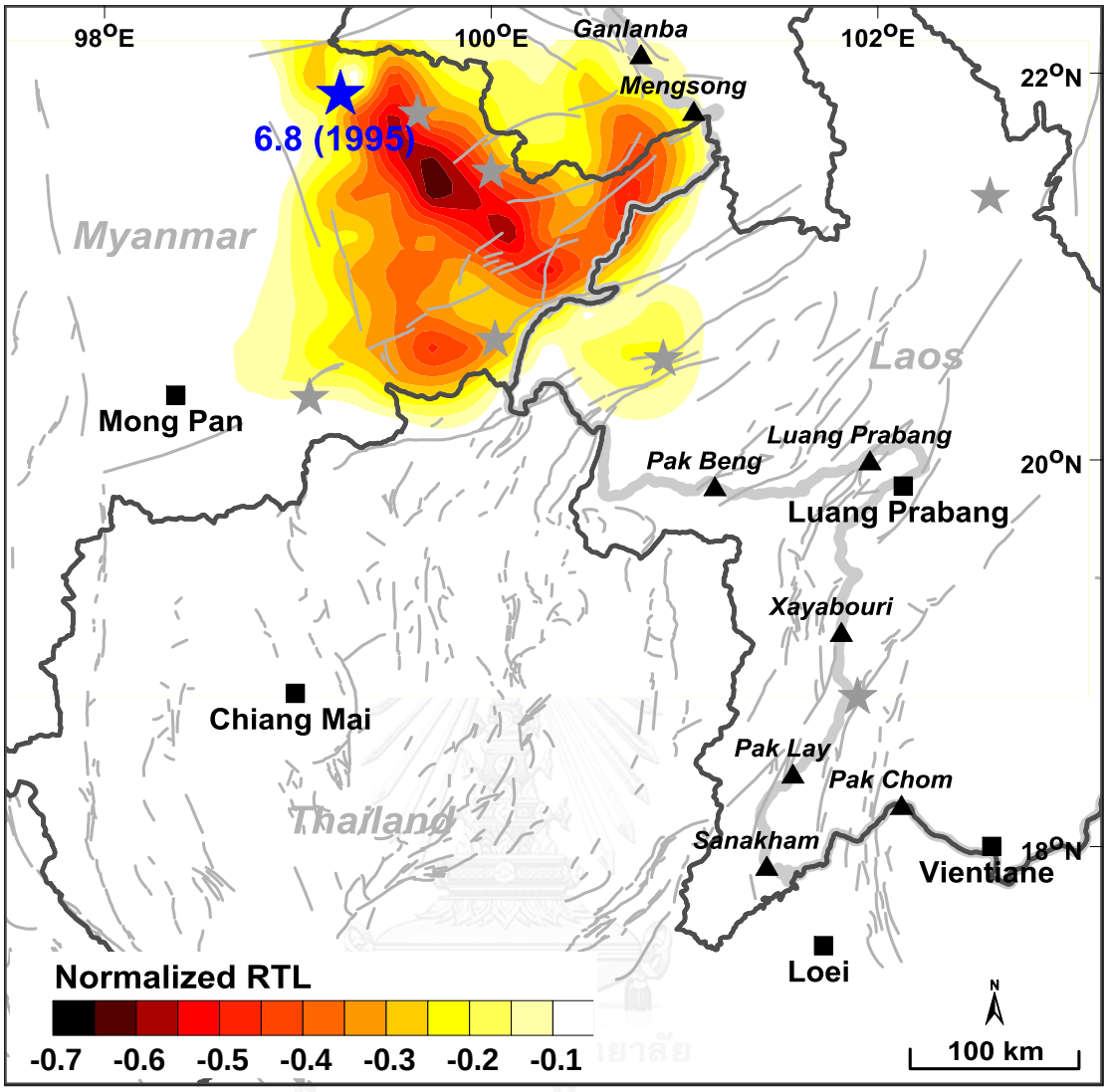

Figure 5.2. Map of Thailand-Laos-Myanmar borders showing spatial distribution of *RTL* values, at the duration of seismicity quiescence stage between 1992.35 and 1992.85, 2.68 years before the occurrences of the M_w-6.8 earthquake on July 11, 1995. The scale on the left corresponds to the *RTL* value in units of normalized standard deviation. A red shade (negative *RTL* score) and blue shade (positive *RTL* score) represents a decrease and increase in the seismicity rate, respectively. The epicenter of the M_w-6.8 earthquake (21.89˚N, 99.22˚E) is shown as a blue star. The grey stars show the epicenters of all 8 events utilized for retrospective test.

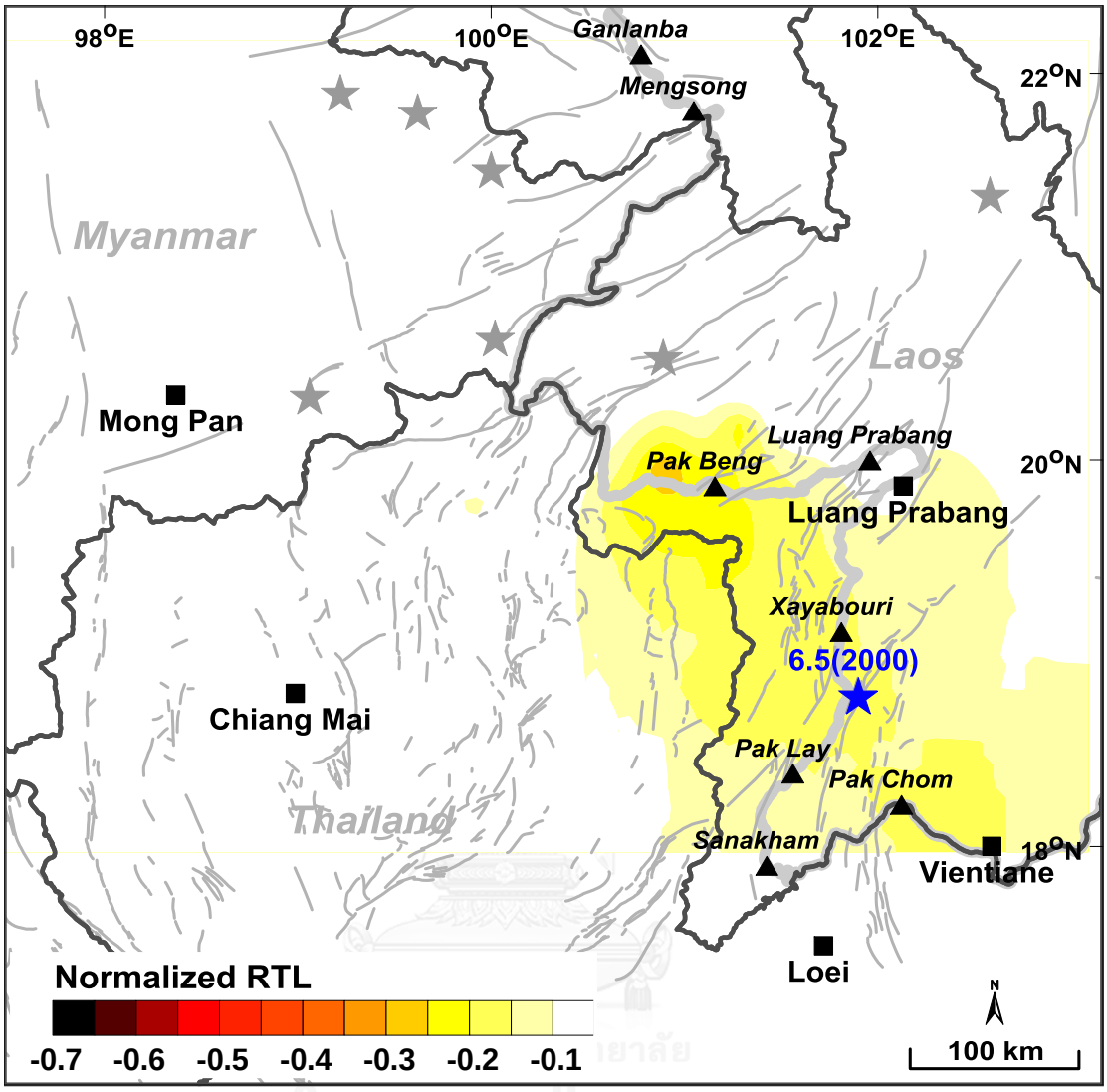

Figure 5.3. Map of Thailand-Laos-Myanmar borders showing spatial distribution of *RTL* values, at the duration of seismicity quiescence stage between 2000.06 and 2000.40, 0.03 years before the occurrences of the M_w-6.5 earthquake on June 7, 2000. The scale on the left corresponds to the *RTL* value in units of normalized standard deviation. A red shade (negative *RTL* score) and blue shade (positive *RTL* score) represents a decrease and increase in the seismicity rate, respectively. The epicenter of the M_w-6.5 earthquake (18.77˚E, 101.90˚N) is shown as a blue star. The grey stars show the epicenters of all 8 events utilized for retrospective test.

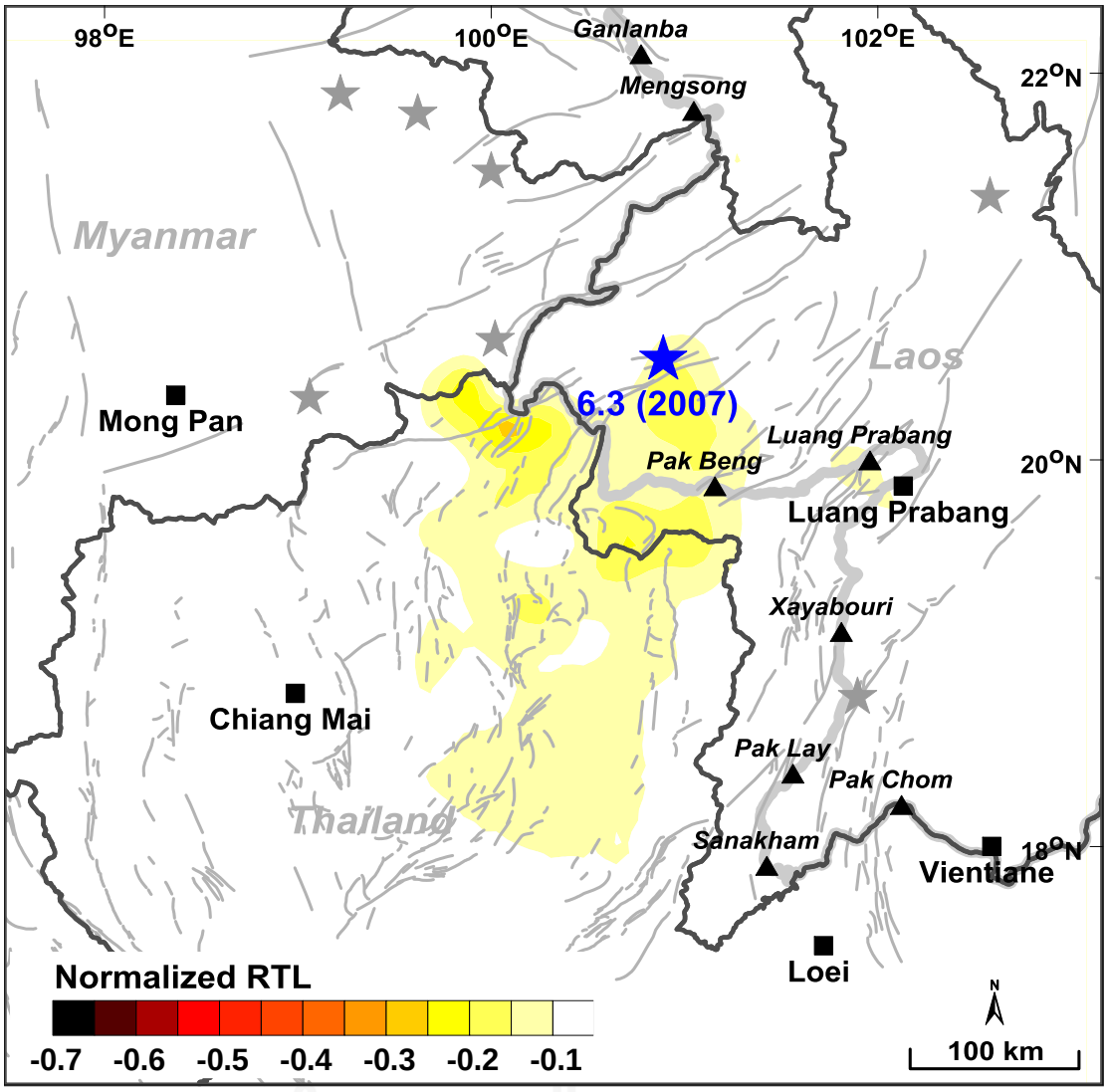

Figure 5.4. Map of Thailand-Laos-Myanmar borders showing spatial distribution of *RTL* values, at the duration of seismicity quiescence stage between 2003.93 and 2004.81, 2.56 years before the occurrences of M_w-6.3 earthquake on May 16, 2007. The scale on the left corresponds to the *RTL* value in units of normalized standard deviation. A red shade (negative *RTL* score) and blue shade (positive *RTL* score) represents a decrease and increase in the seismicity rate, respectively. The epicenter of the M_w-6.3 earthquake (20.52˚N, 100.89˚E) is shown as a blue star. The grey stars show the epicenters of all 8 events utilized for retrospective test.

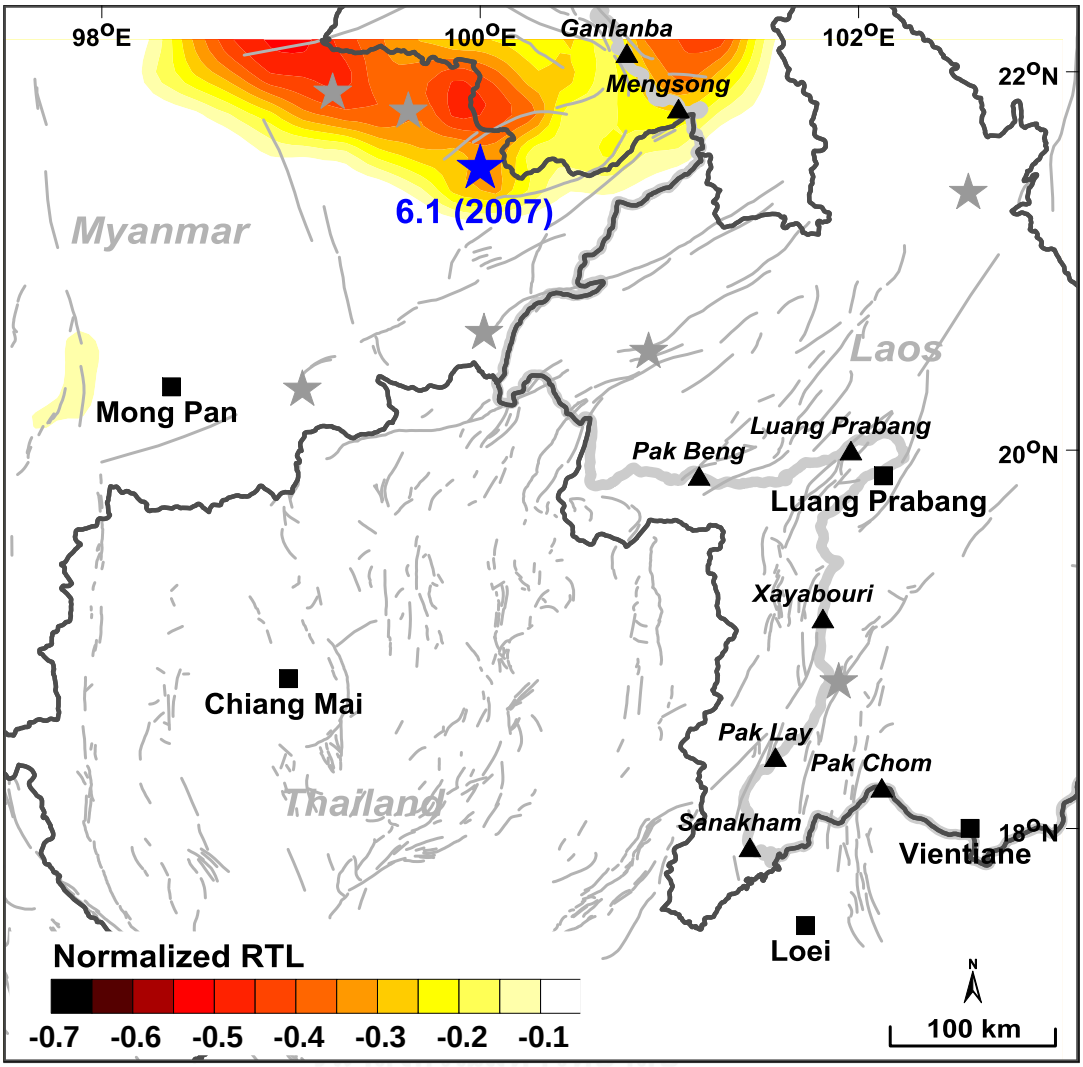

Figure 5.5. Map of Thailand-Laos-Myanmar borders showing spatial distribution of *RTL* values, at the duration of seismicity quiescence stage between 1995.45 and 1996.26, 11.22 years before the occurrences of the M_w-6.1 earthquake on June 23, 2007. The scale on the left corresponds to the *RTL* value in units of normalized standard deviation. A red shade (negative *RTL* score) and blue shade (positive *RTL* score) represents a decrease and increase in the seismicity rate, respectively. The epicenter of the M_w-6.1 earthquake is shown (21.49˚N, 100.00˚E) as a blue star. The grey stars show the epicenters of all 8 events utilized for retrospective test.

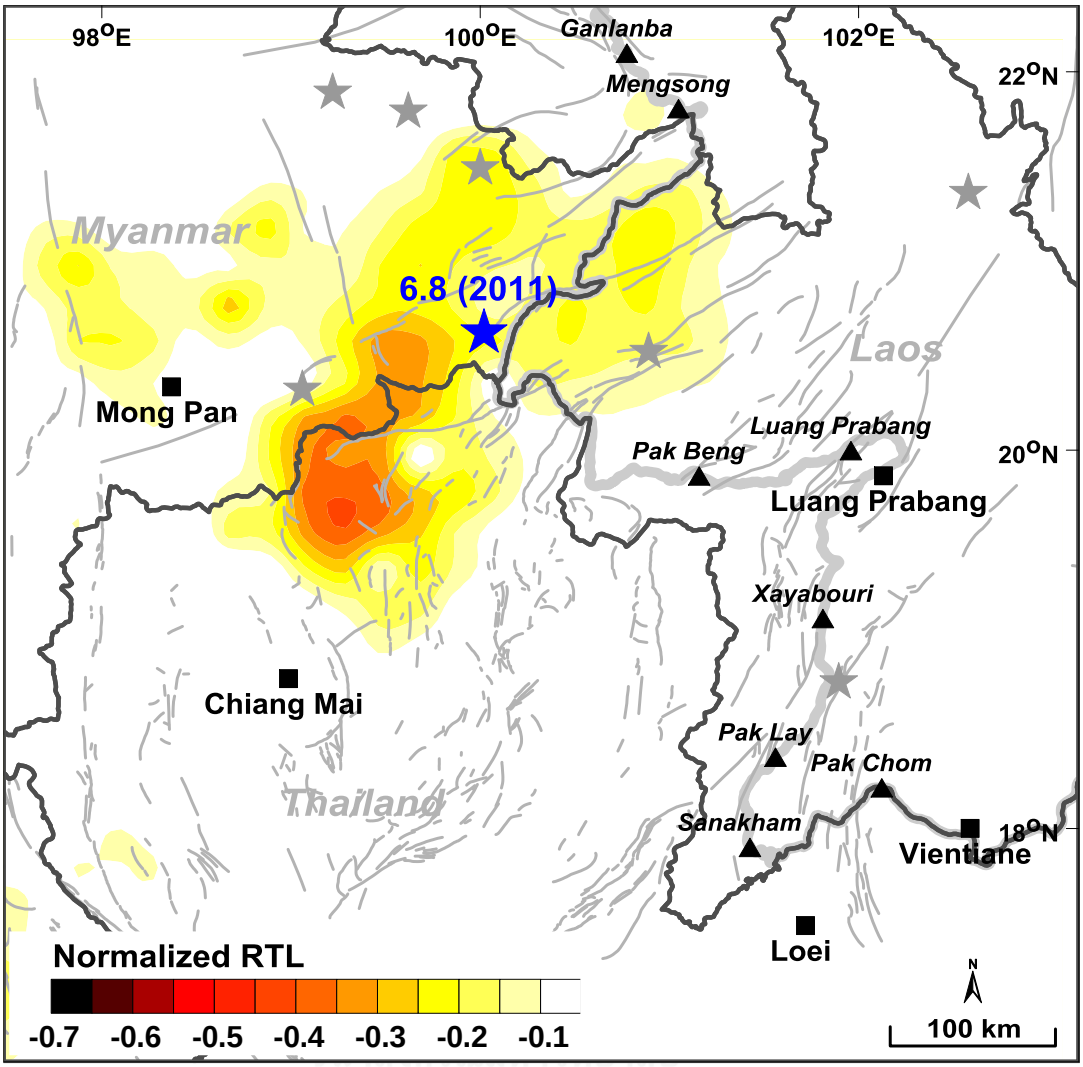

Figure 5.6. Map of Thailand-Laos-Myanmar borders showing spatial distribution of *RTL* values, at the duration of seismicity quiescence stage between 2007.38 and 2009.57, 1.66 years before the occurrences of March 24, 2011 M_w-6.8 main shock. The scale on the left corresponds to the *RTL* value in units of normalized standard deviation. A red shade (negative *RTL* score) and blue shade (positive *RTL* score) represents a decrease and increase in the seismicity rate, respectively. The epicenter of the M_w-6.8 earthquake (20.62˚N, 100.02˚E) is shown as a blue star. The grey stars show the epicenters of all 8 events utilized for retrospective test.

CHAPTER VI

DISCUSSION

In order to support that the seismicity rate change (*Z* value) and *RTL* algorithm can be utilized as earthquake forecaster tools in Thailand-Laos-Myanmar borders. In this chapter, the results in previous chapters were considered in together and compare with the previous researches which corresponded to this study. The comparison of rational results was described as follows:

6.1 Completeness of Earthquake Data

Because the seismicity data used in the statistical seismology should have homogeneous database. The existing seismicity catalogues after the procedures of earthquake data improvement should contain only the main shock which directly related to tectonic activities (excluding foreshock, aftershock, man-made earthquake, and the maximum magnitude which seismic instrument cannot recorded 100%). In order to constrain the results of completeness of seismicity data, several works were attempted to observe the relationships of cumulative number of earthquakes against time. The results indicated that the trend line of cumulative number versus time or magnitude scales are more smooth and reformed to the straight line after the individual process such as earthquake declustering, man-made cutoff, magnitude of completeness (Bachmann, 2001; Chouliaras, 2009c; Katsumata, 2011a; Katsumata and Sakai, 2013; Rudolf-Navarro et al., 2010; Santi Pailoplee et al., 2013). Therefore, this work also observed the cumulative number of earthquakes against time in each procedure of completeness of seismicity data. At first, the cumulative number curve of the total seismicity data represents the flat trend line generated between 1960 and 1983. After that, although the cumulative curve raised gradually until 2012, at this time the curve showed irregularities of cumulative number until the end of the data. Secondly, the cumulative number curve after declustering indicates the flat trend line during 1964 and 1974. Afterward, the cumulative

curve developed gradually until the end of the data. The overall trend line of declustered seismicity catalogues seems to be straighter than the previous one. Next, the cumulative number curve after removing the man-made earthquake does not show the flat trend line. Moreover, the cumulative number curve increased gradually as a straight line during time-span. Finally, the cumulative number rate of the main shock data with magnitude scales at least 4.4 indicate the trend of straight line also develop smoothly along the function of time. Even if both of the cumulative number of earthquake events before and after eliminating M_c show the developing as a straight line, the slope of the cumulative number curve after M_c seem to be better than before. Consequently, the seismicity data improvement in each procedure in Chapter III lead to the completeness of earthquake catalogues in Thailand-Laos-Myanmar borders. Then, it can mention that the seismicity catalogues before applying to *Z* value and *RTL* algorithm investigation are the reliable and meaningful for any seismicity investigation (Figure 6.1 and Figure 6.2).

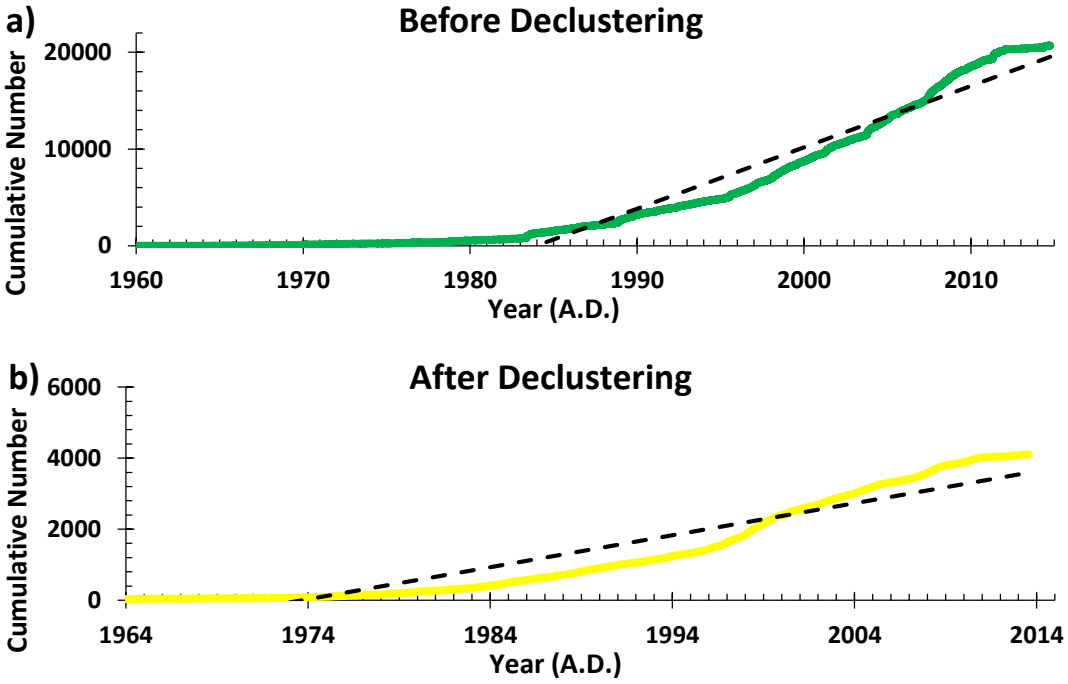

Figure 6.1. The cumulative number of earthquakes in Thailand-Laos-Myanmar borders plotted against time. a) Before declustering. b) After declustering. Dash lines indicate linear trend line.

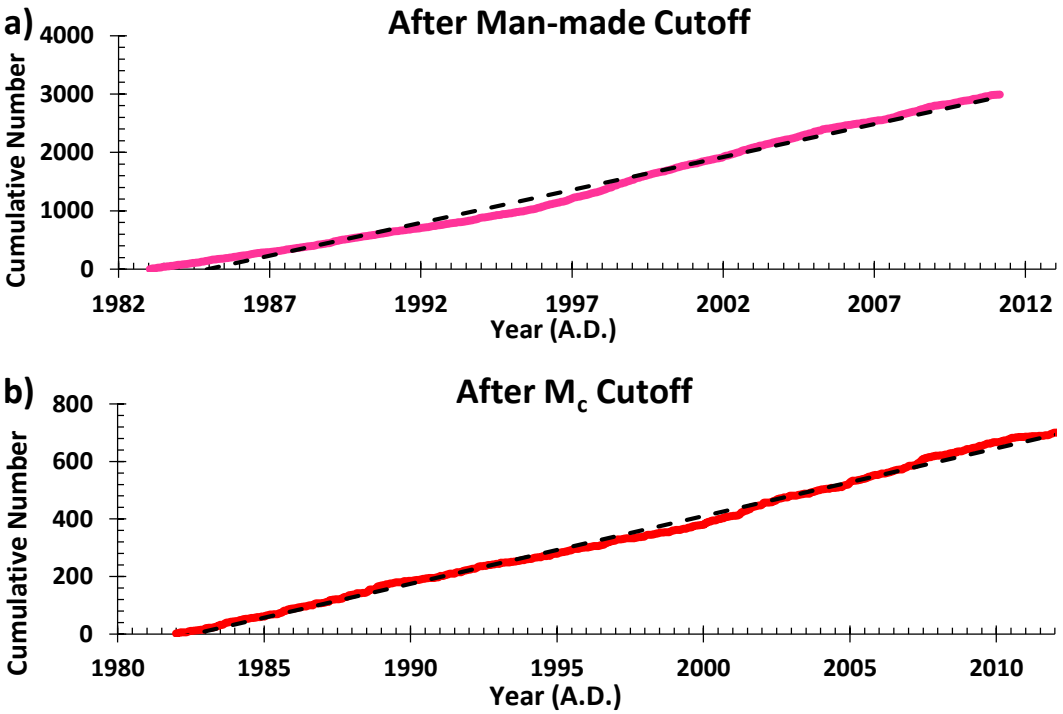

Figure 6.2. The cumulative number of earthquakes in Thailand-Laos-Myanmar borders plotted against time. a) After man-made cutoff and b) after magnitude of completeness cutoff. Dash lines indicate linear trend line.

6.2 The Starting Time of Seismic Quiescence

In order to support the *Z*-value investigation and *RTL* algorithm have potential to evaluate seismic precursors before the occurrence of an earthquake in the short-term and intermediate-term, this work also compared the calculable duration time between starting time of seismic quiescence and the occurrence time of the main shock (*Q*-time) from both techniques with the previous researches. At the beginning, after review the previous researches of *Z* value, the *Z*-value investigation can categorize the forecasting duration in 2 groups. The first group is short-term and intermediate-term investigation (months - 10 years) because mostly previous studies indicated the duration of Q-time varied in the range of 0.75 – 7.00 years (Chouliaras, 2009a; Katsumata, 2011a; Katsumata and Sakai, 2013; Murru et al., 1999; Öztürk and Bayrak, 2009). The second group is the long-term

investigation (more than 10 years) because there is only one research indicate the quiescence detection more than 20 years (Katsumata, 2011b). However, the results after calculated *Z* value in Thailand-Laos-Myanmar borders indicate the detection time of quiescence varied in the zone of intermediate-term. The quiescence detection time of M_w-6.3 earthquake on May 16, 2007 and the M_w-6.8 earthquake on March 24, 2011 which located inside the *Q*-time range of previous studies. Therefore, according to the reasons mentioned above, the quiescence detection time of this work which is calculated by the *Z*-value investigation are effective for intermediate-term forecasting (Figure 6.3).

Secondly, after review the previous researches of *RTL* algorithm, all previous research reported that the *RTL* investigation can classify the forecasting duration as short-term and intermediate-term (Chen and Wu, 2006; Gambino et al., 2014; Gentili, 2010; Huang, 2004; Huang, 2005; Huang and Sobolev, 2002; Huang et al., 2001; Sobolev and Tyupkin, 1997). These previous studies indicate the detection of quiescence time, which is calculated by *RTL* algorithm varied between 1.00 and 5.00 years. In the same way as the previous works, the duration time between the starting time of seismic quiescence and the occurrence time of the main shock for the M_w-6.8 earthquake on July 11, 1995, the M_w-6.5 earthquake on June 7, 2000, the M_w-6.3 earthquake on May 16, 2007, and the M_w-6.8 earthquake on March 24, 2011 developed in the same duration as previous studies. Due to the quiescence detection time of M_w-6.1 earthquake on June 23, 2007 was found in the duration of long-term forecasting, however the quiescence detection time of this event occur closely to the period of intermediate-term earthquake forecasting. Then, regarding to the rationale mentioned above, the quiescence detection time of this work which is calculated by *RTL* algorithm is also effective for intermediate-term forecasting the same as mentioned above with a *Z*-value investigation (Figure 6.4).

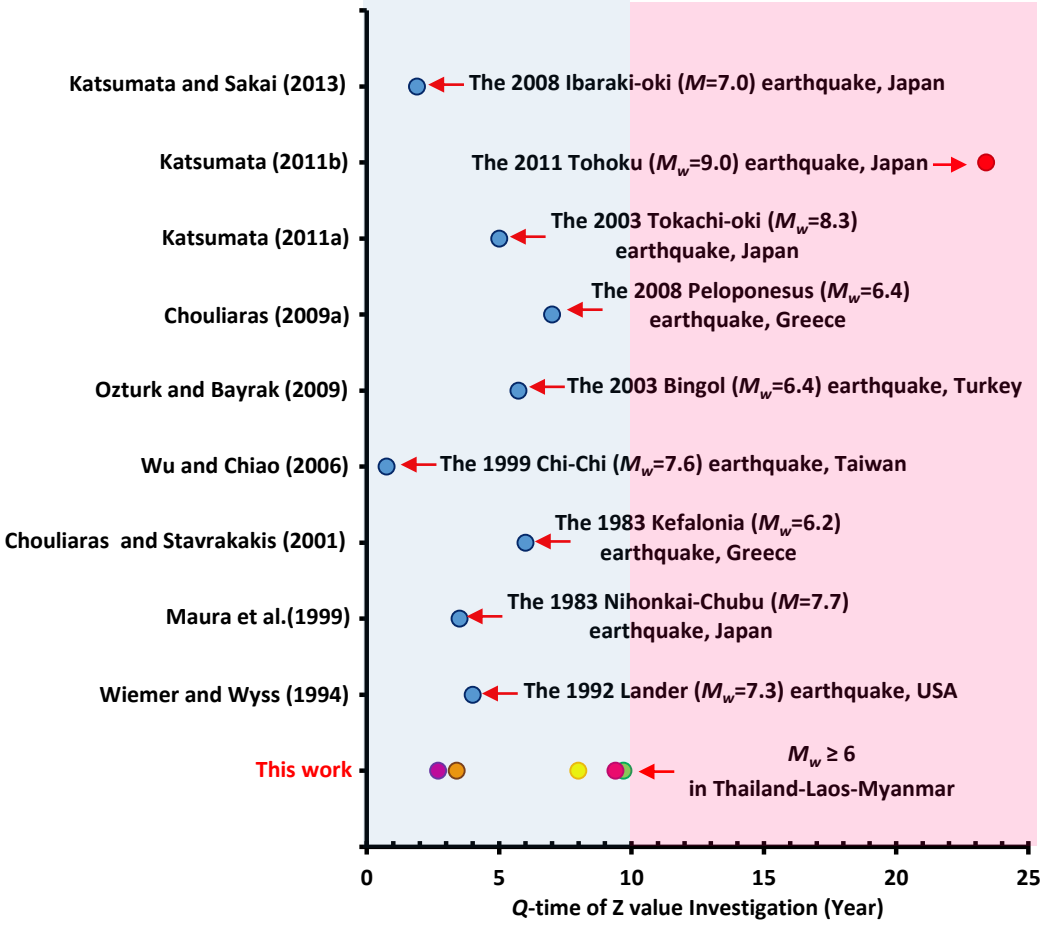

Figure 6.3. The duration time between starting time of seismic quiescence and the occurrence time of the main shock of strong earthquake (*Q*-time), calculated by *Z*-value investigation. Blue circles indicate seismic quiescence detection time of previous works in short-term and intermediate-term forecasting. Red circle indicates seismic quiescence detection time of previous work in long-term forecasting. Blue shaded area is the zone of short-term and intermediate-term forecasting time, pink shaded area is the zone of long term forecasting time. The quiescence detection time of the M_w-6.8 earthquake on July 11, 1995, the M_w-6.5 earthquake on June 7, 2000, the M_w-6.3 earthquake on May 16, 2007, the M_w-6.1 earthquake on June 23, 2007 and the M_w-6.8 earthquake on March 24, 2011 are represented by a green circle, yellow circle, orange circle, pink circle, and purple circle, respectively.

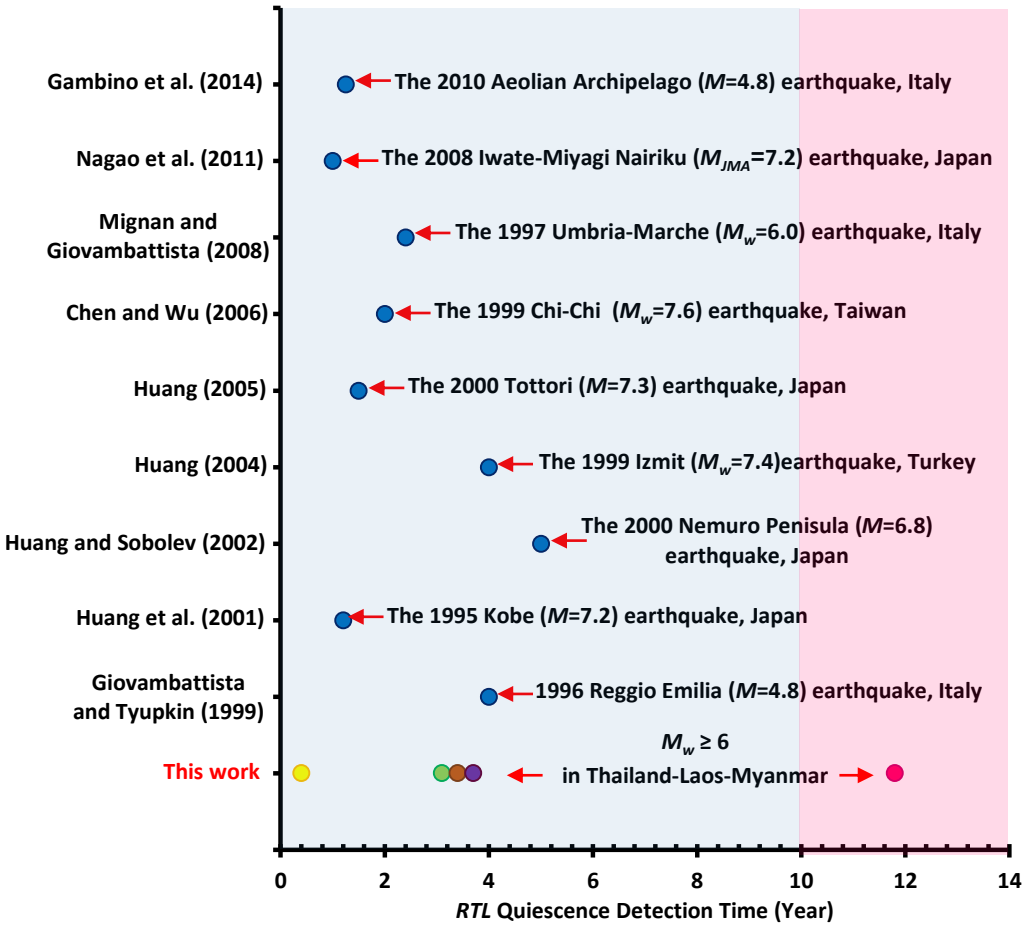

Figure 6.4. The duration time between the starting time of seismic quiescence and the occurrence time of the main shock of strong earthquake (*Q*-time), investigated by *RTL* algorithm. Blue circles indicate seismic quiescence detection time of previous works in short-term and intermediate-term forecasting. Red circle indicates seismic quiescence detection time of previous work in long-term forecasting. Blue shaded area is the zone of short-term and intermediate-term forecasting time, pink shaded area is the zone of long term forecasting time. The quiescence detection time of the M_w-6.8 earthquake on July 11, 1995, the M_w-6.5 earthquake on June 7, 2000, the M_w-6.3 earthquake on May 16, 2007, the M_w-6.1 earthquake on June 23, 2007 and the M_w-6.8 earthquake on March 24, 2011 are represented by a green circle, orange circle, yellow circle, pink circle, and purple circle, respectively.

6.3 The Precursor Parameters Comparison

In addition to constrain the results of both methods, this work attempted to compare the Z anomalies with the previous research works. The previous studies indicated that the Z value at the location of main shock varied between Z = 2.5 and Z = 7.4, while the results of maximum Z value at the location of the calculable strong earthquake of this work showed the Z value are in the same range of Z value of previous works. Although the event of the M_w-6.8 earthquake on July 11, 1995 generated Z value = 3.0, the other calculable strong earthquakes generated high Z value (Figure 6.5).

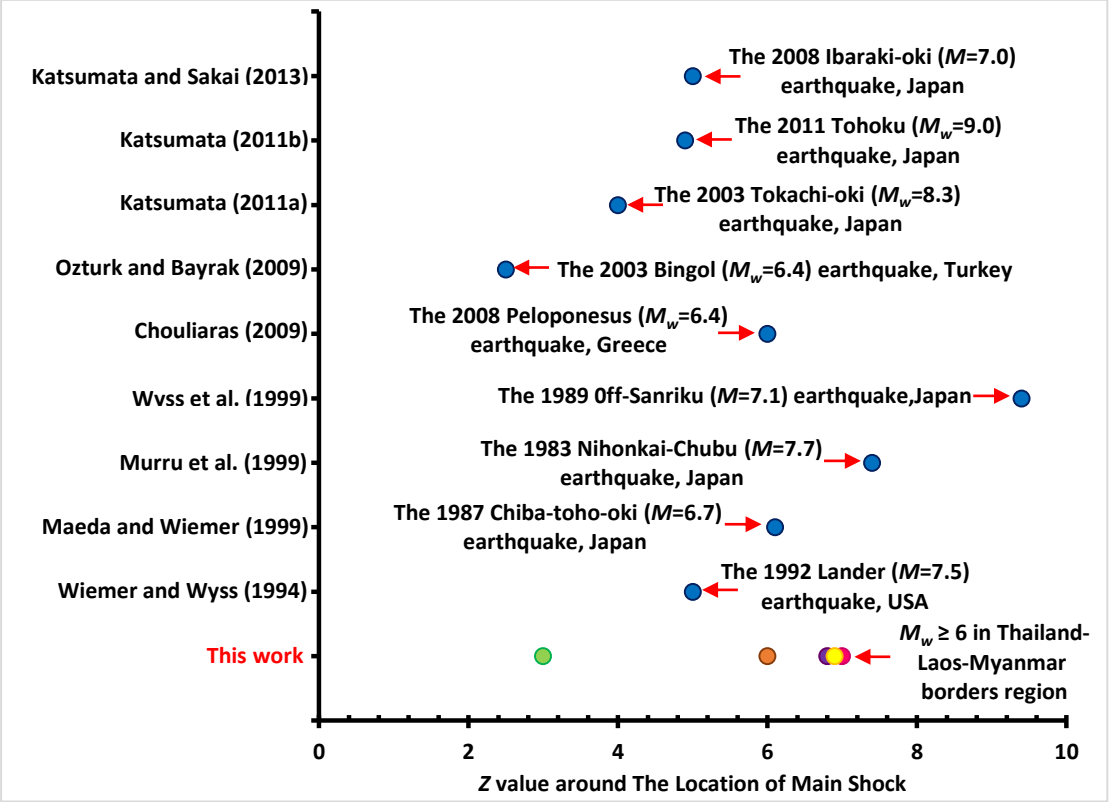

Figure 6.5. The Z value comparison between this work and previous research works. Blue circles indicate Z value of previous works. The Z value of the M_w-6.8 earthquake on July 11, 1995, the M_w-6.5 earthquake on June 7, 2000, the M_w-6.3 earthquake on May 16, 2007, the M_w-6.1 earthquake on June 23, 2007 and the M_w-6.8 earthquake on March 24, 2011 represented by a green circle, orange circle, yellow circle red circle, and purple circle, respectively.

Therefore, it can mention that the *Z*-value investigation in Thailand-Laos-Myanmar border by using *Z* parameter n = 50 and T_w = 1.2 can generate the *Z* value at the location of strong earthquake clearly and all of *Z* values in this work are noticeable and obvious.

Regarding to *RTL* algorithm, the *RTL* anomalies obtained in this study cannot compare with the previous works because several previous studies did not normalized the *RTL* values. However, the *RTL* curve of retrospective temporal investigation indicated the similar results as previous works (some events are better). Hence, it can conclude that the *RTL* investigation in Thailand-Laos-Myanmar border by using characteristic parameter r_0 = 120 and t_0 = 2 can generate the *RTL* value at the location of strong earthquake clearly and all of *RTL* values in this work are prominent as well.

6.4 Comparison between *Z* and *RTL* Values

Theoretically, the more values of positive *Z* and negative RTL, the more quiescence were detected. Therefore, in order to constrain the obtained result, both Z and RTL values of individual cased study was plotted as shown in Figure 6.6.

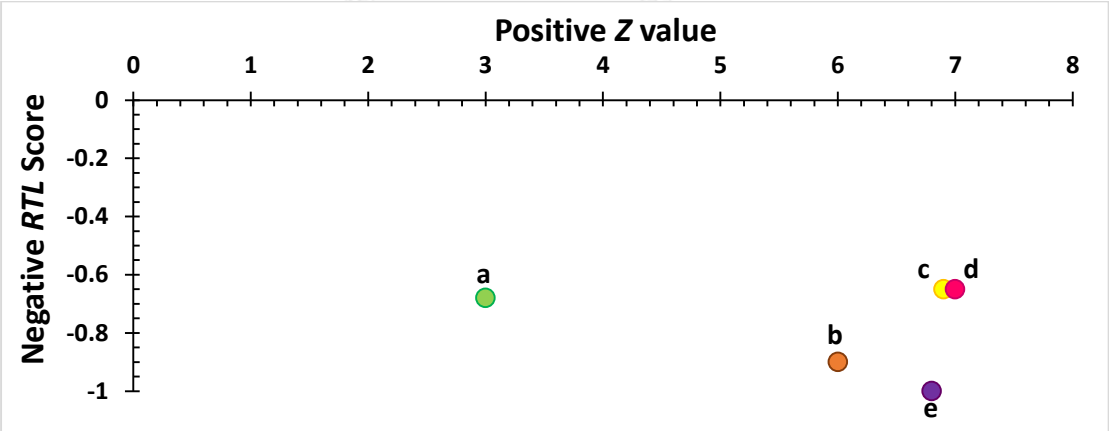

Figure 6.6. The comparison between *Z* and *RTL* value prior to the a) M_w-6.8 earthquake on July 11, 1995 (green circle), b) M_w-6.5 earthquake on June 7, 2000 (orange circle), c) M_w-6.3 earthquake on May 16, 2007 (yellow circle), d) M_w-6.1 earthquake on June 23, 2007 (pink circle) and e) M_w-6.8 earthquake on March 24, 2011 (purple circle).

According to Figure 6.6., almost all results of this work are significant in term of the positive value of *Z*, conform to the negative value of *RTL*. While there is only the M_w-6.8 earthquake on July 11, 1995 generated low positive *Z* value, it created very low *RTL* value as well. This error may be caused by the lack of earthquake data for investigation of *Z* value in that occurrence time. Therefore, based on reasons introduced above, it can mention that the *Z* and *RTL* value investigation in Thailand-Laos-Myanmar borders are interrelated.

6.5 Evolution of Seismic Quiescence Stage

Regarding to the results of the temporal variations of *Z* values, there are several flat parts occurred along cumulative number curves. These flat parts lead to the developing of several *Z* peaks (seismic quiescence periods) along the time-span. These complications cause by the interruptions of seismic quiescence which come from the vicinity severe earthquakes, especially the zone of low seismicity data because it made the collecting radius in each node wider. However, when the *Z* peak developed, the main shock was occurred subsequently after that. Then, the latest dominant *Z* peak, which no main shock occurred should be monitored (Figure 6.7).

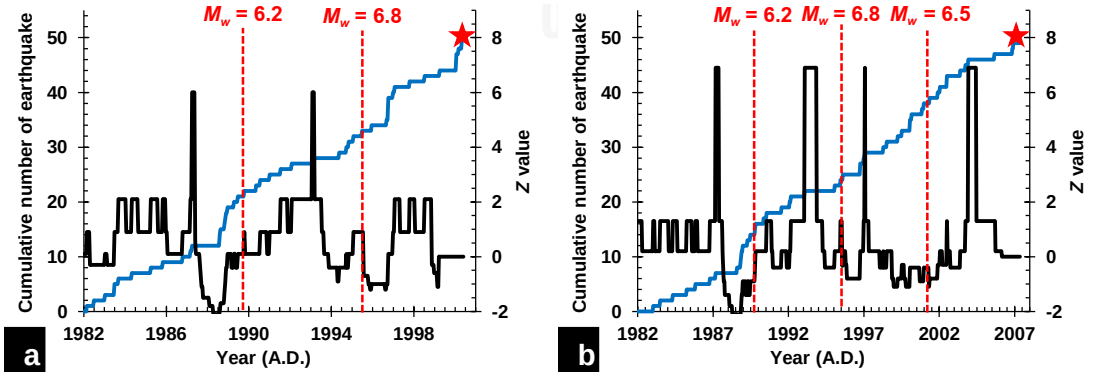

Figure 6. 7. The examples temporal variation of the a) M_w-6.5 earthquake on June 7, 2000 and b) M_w-6.3 earthquake on May 16, 2007. Red dashed indicate the occurrence time of vicinity earthquakes, black triangles indicate the occurrence time of main shocks.

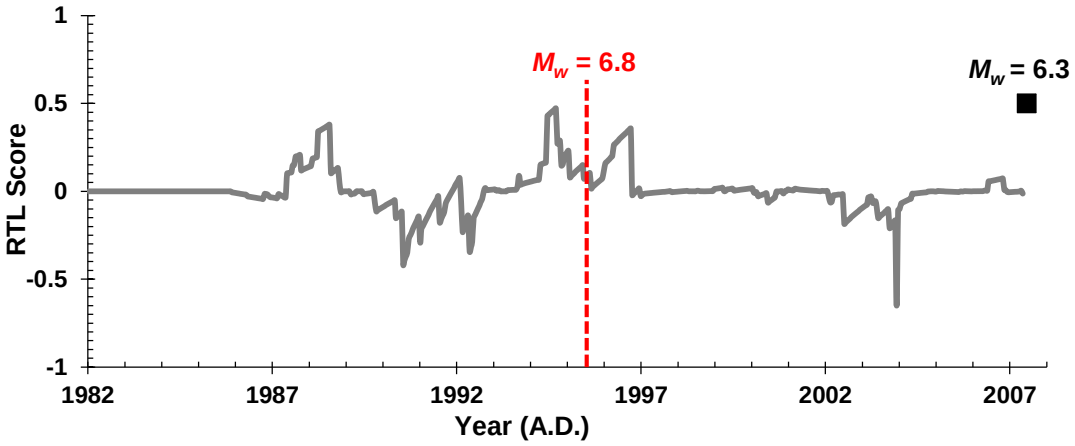

Figure 6.8. The examples temporal *RTL* variation of the M_w-6.3 earthquake on May 16, 2007. Red dashed indicate the occurrence time of vicinity earthquake. Black square indicate the occurrence time of the main shock.

Furthermore, the observation of *Z* curves and *RTL* curves indicate that the occurrence time of main shocks not only arise immediately in the quiescence stage, but also occurred after the end of quiescence duration with the variation of the time period. For explanation the time delayed of the results of both methods, the duration between the end of quiescence time and the occurrence time of main shock were analyzed. However, the quiescence stages of *Z* value are developed for a short while before return to the normal stage, similar to previous studies. Then, the time delay of *Z* value was considered at the occurrence of quiescence time until the occurrence of the main shock. During *Z*-value investigation, there is no strong earthquakes occurred in the duration of quiescence time. The main shock of the M_w-6.8 earthquake on July 11, 1995, the M_w-6.5 earthquake on June 7, 2000, the M_w-6.3 earthquake on May 16, 2007, the M_w-6.1 earthquake on June 23, 2007, and the M_w-6.8 earthquake on March 24, 2011 occurred with the time delay = 9.7 years, 7.4 years, 3.4 years, 8 years, and 2.7 years, respectively. A uniform time delay after the detection quiescence stage was also informed by previous Z value studies, i.e., Wu and Chiao (2006) studied the M_w-7.6 Chi-Chi (Taiwan) earthquake on September 20, 1999, the results show the seismic quiescence anomalies started in January 1999, 9 months before the occurrence time of the main shock. Wu et al. (2008) analyzed the

seismicity characteristics prior to the M_w-6.8 Chengkung (Taiwan) earthquake on December 10, 2003, the results indicate the quiescence stage generated around the end of 2001, 2 years before the main shock occurs. Katsumata (2011) investigated the precursory seismicity pattern changes before the M_w-8.3 Takachi-oki (Japan) earthquake on 26 September 2003, the results indicate seismic quiescence anomalies started around the beginning of 1999 until the main shock occurs. More examples of time delay investigated by *Z* value are indicated in Figure 6.3

Among the temporal variation, the RTL algorithm calculated in this work indicate mostly RTL curve have time delay after quiescence stage before the main shock as well. The main shock of the M_w-6.8 earthquake on July 11, 1995, the M_w-6.3 earthquake on May 16, 2007, the M_w-6.1 earthquake on June 23, 2007, and M_w-6.8 earthquake on March 24, 2011 have time delay = 2.6 years, 3.09 years, 7.27 years, and 1.66 years. A similar time delay after the quiescence stage was also informed by previous *RTL* algorithm studies, e.g., Sobolev and Tyupkin (1999) reported that the investigation of the *M*-7 northern Gulf of Kamchatka (Russia) earthquake on December 5, 1997 have seismic quiescence stage, following with seismic activation stage and time delay of main shock about 1.5 years subsequent the end of the seismic activation phase; Huang and Sobolev (2002) analyzed the seismicity rate changes before the M_w-6.8 Nemuro Peninsula (Japan) earthquake on January 28, 2000, the results indicated seismic quiescence anomalies started in 1995 with its duration time about 1.5 years until the end of 1996, after then, the seismic activation stage appeared with the period around 0.7 year and returned to the normal stage around 2.5 years before main shock occurs; Gambino et al. (2014) investigated seismicity characteristic before the M_w-4.8 Aeolian Archipelago (Italy) earthquake on the August 16, 2010, the results detected seismic quiescence stage started around 1.25 years before the main shock with its duration approximately about 6 - 7 months and returned to the normal stage without an seismic activation stage (time delayed around 7 months before the occurrence of main shock. More examples in term of time delay duration which investigated by *RTL* algorithm similarly to the results are expressed in Figure 6.4.

As the results mentioned above, although it seems to be that the time delay of the *Z*-value investigation have a longer period than *RTL* algorithm investigation, both methods still detected seismic precursor impending to the strong earthquake. Moreover, even though the existence stage of time delay which mentioned above makes it hard to estimate and determine the occurrence time accurately in short-term and intermediate-term earthquake forecasting, the investigation of seismicity pattern changes by both techniques may provide useful information for forecasting future earthquake.

6.6 Prospective Area of the Upcoming Earthquake Source

Although the limit of seismicity data, this research cannot create a present day map by *Z*-value investigation and *RTL* algorithm, in order to constrain the *Z* and *RTL* evaluated in this work, the obtain results were compared with *b*-value of *FMD* by Pailoplee et al. (2013). Seismotectonically, the lower *RTL* and higher *Z* value implied the higher of seismic quiescence. Meanwhile, the lower *b* of *FMD* relates empirically to higher stress accumulated. After comparing all methods mentioned above, the results revealed that at the same duration of time close to the end 2010, the regions indicate comparatively low *RTL* and high *Z* (this study) quite conform to the comparatively low of low *b* mentioned by Pailoplee et al. (2013) (Figure 6.9). The overlap anomalous areas developed around 350 km^2 with a NW-SE direction, covered mostly in the eastern part of Myanmar (i.e., Kentung, Mongsat, Monghpyak, Mongyawng and Bok Hsopnam), some parts of the northern Thailand (i.e., Chiang Mai, Chiang Rai, Phayao and Nan) and some areas in the northern Laos (i.e., Bokeo, Luang Namtha and Xainabouli). Then, after these anomalies occurs, there were two strong earthquakes posed in the southeast Kentung city, Myanmar (M_w-6.8 earthquake on March 24, 2011) and in the Mae Lao district, southwestern part of Chiang Rai, Thailand (M_w-6.2 earthquake on March 5, 2014). It is interpreted that the high *Z* value and low-*RTL* areas mentioned above act presently as the quiescence area which might be risked by the upcoming strong-to-major earthquake, including i.e., i) some areas

in the northern part of Laos (i.e., Bokeo, Luang Namtha and Xainabouli), and ii) eastern part of Myanmar (Shan state, for example, Ta-kaw, Mongpan). Then, some earthquake mitigation plan should be arranged in this area.

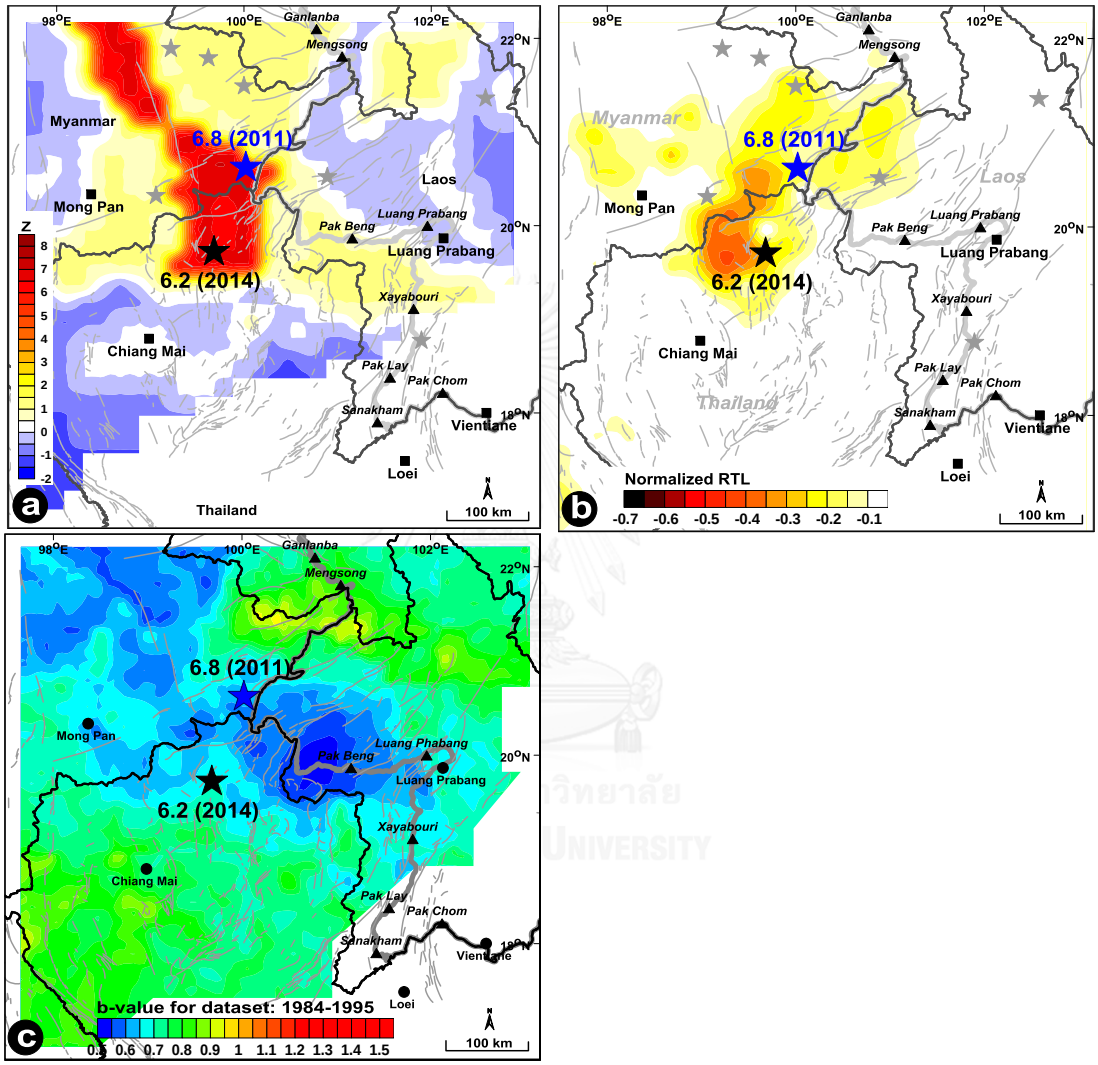

Figure 6.9. Spatial distribution of a) *Z* values evaluate at the time slice 2008.53, b) *RTL* values mapped during 2010.28 – 2010.36 time span, and c) *b* values analyze from the seismicity data recorded during 1984 – 2010, modified after Pailoplee et al. (2013). Blue and black star indicate the M_w-6.8 earthquake on March 24, 2011 and M_w-6.2 earthquake on March 5, 2014, respectively.

6.7 Stochastic Test of *Z* Value and *RTL* Score

According to Huang (2005), in order to constrain that the anomalous areas of *Z* value and *RTL* algorithm investigation are not involved the random phenomena of earthquake occurrence, the statistical method call stochastic test is recognized here. For explaining the details of stochastic test, at first, the random seismicity catalogues (e.g., N = 10,000) were produced by randomizing the space (longitude and latitude) and time of earthquake data. Afterward, for each random catalogue, the *Z* value and *RTL* parameter were computed at the location of main shock of the investigated strong earthquake (see Tables 4.1 and 5.1). The identical criteria applied in the computations for the real catalogue were chosen in the investigations. After quantifying the positive anomaly of *Z* value and the negative anomaly of the *RTL* parameter, one can consider whether *Z* and *RTL* anomaly appear or not. Eventually, one can analyze the *Z* value and *RTL* parameters at the location of main shock for all random catalogues and estimate the probability of occurrence of *Z* and *RTL* anomaly. Based on Huang (2005), in order to corroborate that the *Z* and *RTL* anomalies are not synthesized, the expected probability of the observed *Z* and *RTL* anomalies before the occurrence of strong earthquake should be nearly 0.

After investigating stochastic of the positive *Z* and the negative *RTL* anomalies, the results indicated that the probability of the *Z* value is higher than that obtained from the *RTL* algorithm. Statistically, it can mention that the anomalies of *RTL* algorithm are more significant than the anomalies of *Z* parameter. The detailed study of stochastic of *Z* value and *RTL* parameter impending to the occurrence strong earthquake in Thailand-Laos-Myanmar border shown in Figures 6.10 and 6.11. Therefore, using *RTL* algorithm analysis precursory seismicity rate change in Thailand-Laos-Myanmar borders generate more reliable anomalies than *Z*.

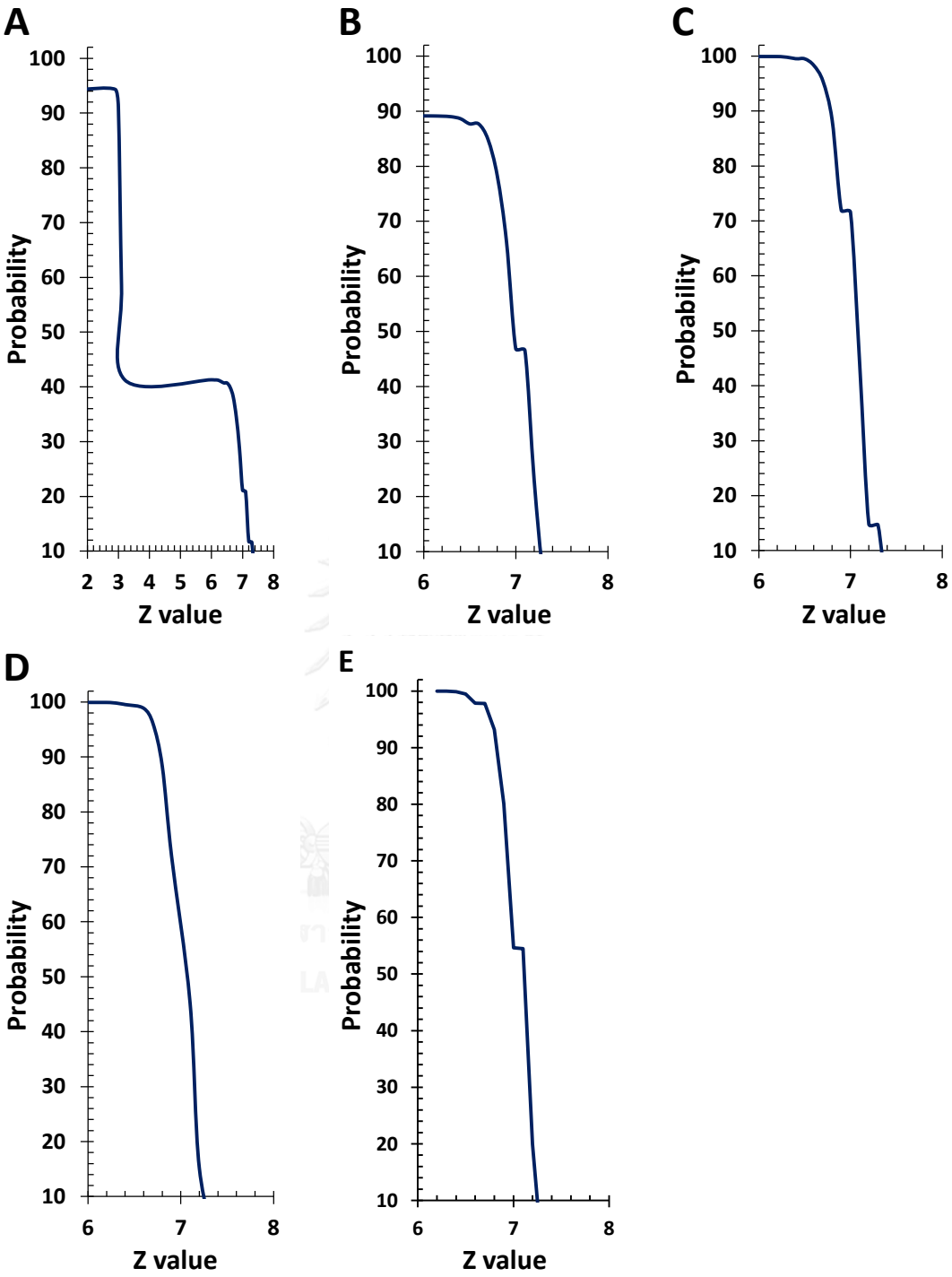

Figure 6.10. Stochastic tests of *Z* value at the epicenters of the a) M_w-6.8 earthquake on July 11, 1995, b) M_w-6.5 earthquake on June 7, 2000, c) M_w-6.3 earthquake on May 16, 2007, d) M_w-6.1 earthquake on June 23, 2007 and e) M_w-6.8 earthquake on March 24, 2011.

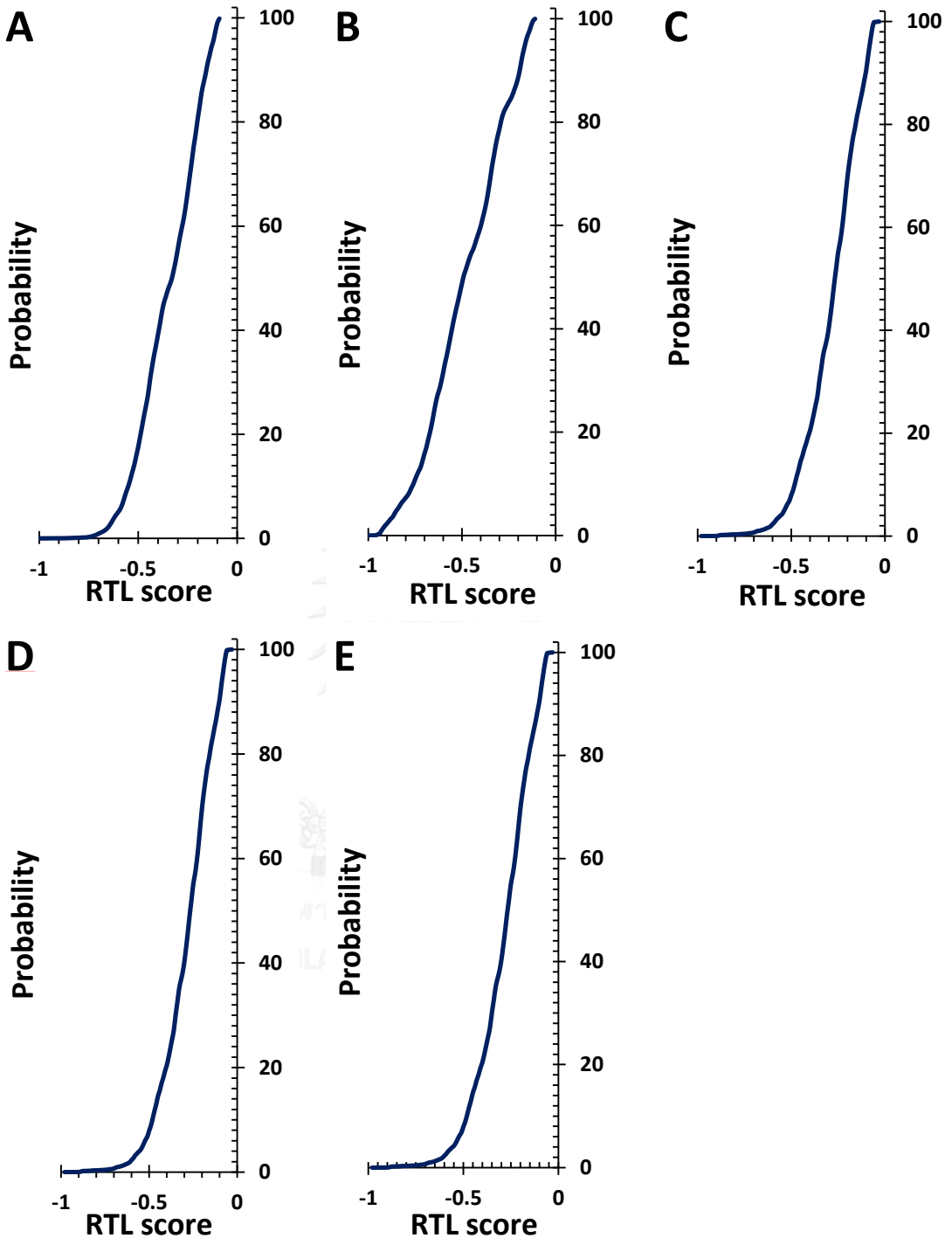

Figure 6.11. Stochastic tests of *RTL* values at the epicenters of the a) M_w-6.8 earthquake on July 11, 1995, b) M_w-6.5 earthquake on June 7, 2000, c) M_w-6.3 earthquake on May-16, 2007, d) M_w-6.1 earthquake on June 23, 2007 and e) M_w-6.8 earthquake on March 24, 2011.

6.8 Correlation Coefficient of *RTL* Algorithm

Regarding to several studies of *RTL* algorithm which mentioned that the characteristic parameters (r_0 and t_0) affect directly to the *RTL* investigation (Chen and Wu, 2006; Huang, 2004; Huang and Sobolev, 2002; Huang et al., 2001). Therefore, in order to observe such changes, this work repeated the *RTL* calculations by using the different characteristic *RTL* parameters, subsequently plotted the results of *RTL* curves at each conditions for considering the suitable characteristic *RTL* parameters. Furthermore, after varied that conditions, this research also computes the correlation coefficient in each condition of strong earthquake for determining whether the values of two variables are associated. For simplification briefly, the suitable condition r_0 = 120 km and t_0 = 2 years were calculated for correlation coefficient by comparison with different RTL conditions which increase/decrease r_0 = 25 km and increase/decrease t_0 = 0.5 years from the suitable characteristic *RTL* parameter used in this study. Then, the significance in each correction coefficient was considered by using Pearson correlation coefficient *r* (*P*-value). If the *P*-value probability is lower than the conventional 5% ($P < 0.05$) the correlation coefficient is called statistically significant. Hence, the maximum level of *P*-value for determining whether the anomalies are random samples or normal distribution was set as 0.05, based on Bendat and Piersol (2000).

After evaluating the correlation coefficient in each strong earthquake which found anomalous areas in the study area, the statistical analysis implied that mostly the conditions listed in Table 6.1 correlated at a significance of 0.05. The explanations of correlation coefficients in each strong earthquake which have anomaly in the study area can be described as follow;

i) Due to the calculation correlation coefficient of the M_w-6.8 earthquake on July 11, 1995, the condition i) r_0 = 95 km, t_0 = 2 years ii) r_0 = 120 km, t_0 = 1.5 years and r_0 = 120 km and t_0 = 3 years are significant to the suitable condition with *P*-value < 0.05. Moreover, even though the condition r_0 = 95 km, t_0 = 2 years seem to have very low value of correlation coefficient (correlation coefficient < 0.30), it still significant with *P*-value < 0.05 as well. However, the results of the condition r_0 = 145 km, t_0 = 2 years indicate that it

is not significant to the suitable condition. The problem may come from the low density of the earthquake data in that year. More R_{max} but less seismicity data may provide the very large anomalous areas which can affect to the results of correlation analysis not significant.

ii) Regarding to the calculation correlation coefficient of the M_w-6.5 earthquake on June 7, 2000, the M_w-6.3 earthquake on May 16, 2007, the M_w-6.1 earthquake on June 23, 2007 and the M_w-6.8 earthquake on March 24, 2011 the condition i) r_0 = 95 km, t_0 = 2 years ii) r_0 = 120 km, t_0 = 1.5 years and r_0 = 120 km and t_0 = 3 years and iv) r_0 = 145 km, t_0 = 2 years are significant to the suitable condition with *P*-value < 0.05. Although the different *RTL* characteristic condition of the M_w-6.5 earthquake on June 7, 2000 and the M_w-6.8 earthquake on March 24, 2011 indicated high (correlation coefficient > 0.70 – 0.90) and very high (correlation coefficient > 0.90 – 1.00) correlation with suitable condition, the M_w-6.3 earthquake on May 16, 2007 and the M_w-6.1 earthquake on June 23, 2007 showed the moderated correlation coefficient (correlation coefficient > 0.50 – 0.70). This result may be caused by the epicenter of the M_w-6.3 earthquake on May 16, 2007 and the M_w-6.1 earthquake on June 23, 2007 are locate nearly in space and time. Then, the quiescence area of both earthquakes may interrupt each other. However, it can mention that the suitable condition r_0 = 120 km and t_0 = 2 years has potential to investigate earthquake precursor. Furthermore, this can support that the anomaly of seismic quiescence, which was detected before a strong and major earthquakes in Thailand-Laos-Myanmar borders is not an artificial anomaly due to the selections of characteristic *RTL* parameters.

In order to constrain the result of correlation coefficient, this work also plots the *RTL* score against time in each strong earthquake. The results from this analysis reveal that, even though the characteristic *RTL* parameters r_0 and t_0 was changed, almost seismic quiescence stages are started in the same duration. These can constrain that the seismic quiescence stages, which was investigated before a strong earthquake in Thailand-Laos-Myanmar borders is not a fortuitous calculation due to the selections of

characteristic *RTL* parameters. The temporal variations of varying different characteristic *RTL* parameters were indicated in Figures 6.12 - 6.16.

Table 6.1. Correlation of RTL values between different characteristic parameters r_0 and t_0 of the i) M_w-6.8 earthquake on July 11, 1995, ii) M_w-6.5 earthquake on June 7, 2000, iii) M_w-6.3 earthquake on May 16, 2007, iv) M_w-6.1 earthquake on June 23, 2007 and v) M_w-6.8 earthquake on March 24, 2011. Case A represents the suitable values of independent characteristic parameters that we used for investigate precursory seismicity changes before the strong and major earthquake, case B represents the different characteristic RTL parameters that we used for comparison with suitable condition.

i) The M_w-6.8 earthquake on July 11, 1995

Cases	A	r_0 = 120 km, t_0 = 2.0 years			
	B	r_0 = 95 km	r_0 = 145 km	t_0 = 1.5 Years	t_0 = 2.5 Years
Correlation between A and B		0.16	0.04	0.71	0.91
P-value		0.003383	0.500797	<0.00001	<0.00001

ii) The M_w-6.5 earthquake on June 7, 2000

Cases	A	r_0 = 120 km, t_0 = 2.0 years			
	B	r_0 = 95 km	r_0 = 145 km	t_0 = 1.5 Years	t_0 = 2.5 Years
Correlation between A and B		0.84	0.71	0.95	0.95
P-value		<0.00001	<0.00001	<0.00001	<0.00001

iii) The M_w-6.3 earthquake on May 16, 2007

Cases	A	r_0 = 120 km, t_0 = 2.0 years			
	B	r_0 = 95 km	r_0 = 145 km	t_0 = 1.5 Years	t_0 = 2.5 Years
Correlation between A and B		0.68	0.66	0.68	0.64
P-value		<0.00001	<0.00001	<0.00001	<0.00001

iv) The M_w-6.1 earthquake on June 23, 2007

Cases	A	r_0 = 120 km, t_0 = 2.0 years			
	B	r_0 = 95 km	r_0 = 145 km	t_0 = 1.5 Years	t_0 = 2.5 Years
Correlation between A and B		0.57	0.51	0.61	0.85
P-value		<0.00001	<0.00001	<0.00001	<0.00001

v) The M_w-6.8 earthquake on March 24, 2011

Cases	A	r_0 = 120 km, t_0 = 2.0 years			
	B	r_0 = 95 km	r_0 = 145 km	t_0 = 1.5 Years	t_0 = 2.5 Years
Correlation between A and B		0.87	0.82	0.82	0.90
P-value		<0.00001	<0.00001	<0.00001	<0.00001

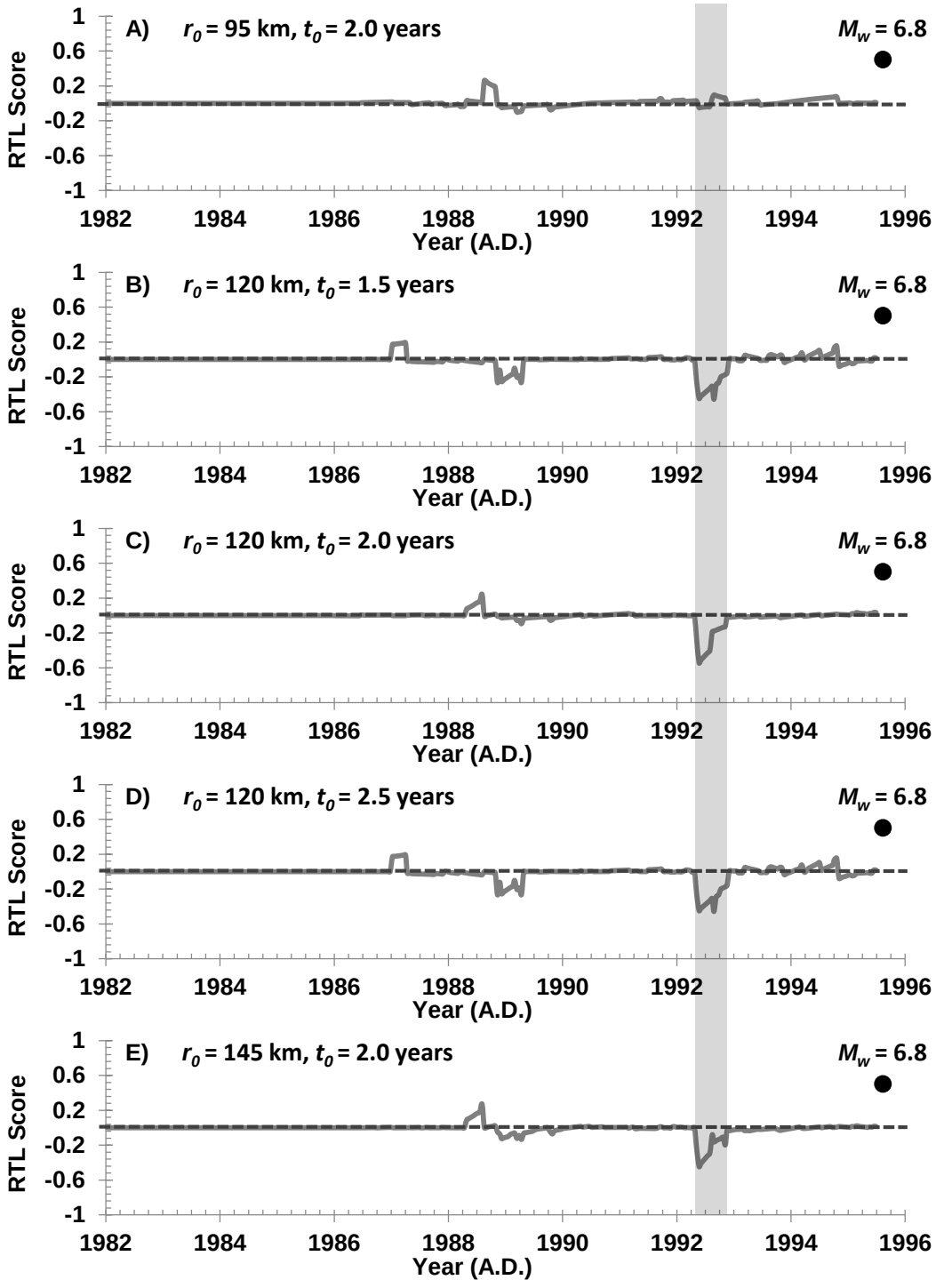

Figure 6.12. Temporal variation of *RTL* scores (grey lines) evaluate from different characteristic parameter. Black circles denote the occurrence time of the M_w-6.8 earthquake on July 11, 1995. Grey shade indicated the duration of quiescence which is used to generate spatial distribution in Figure 5.2.

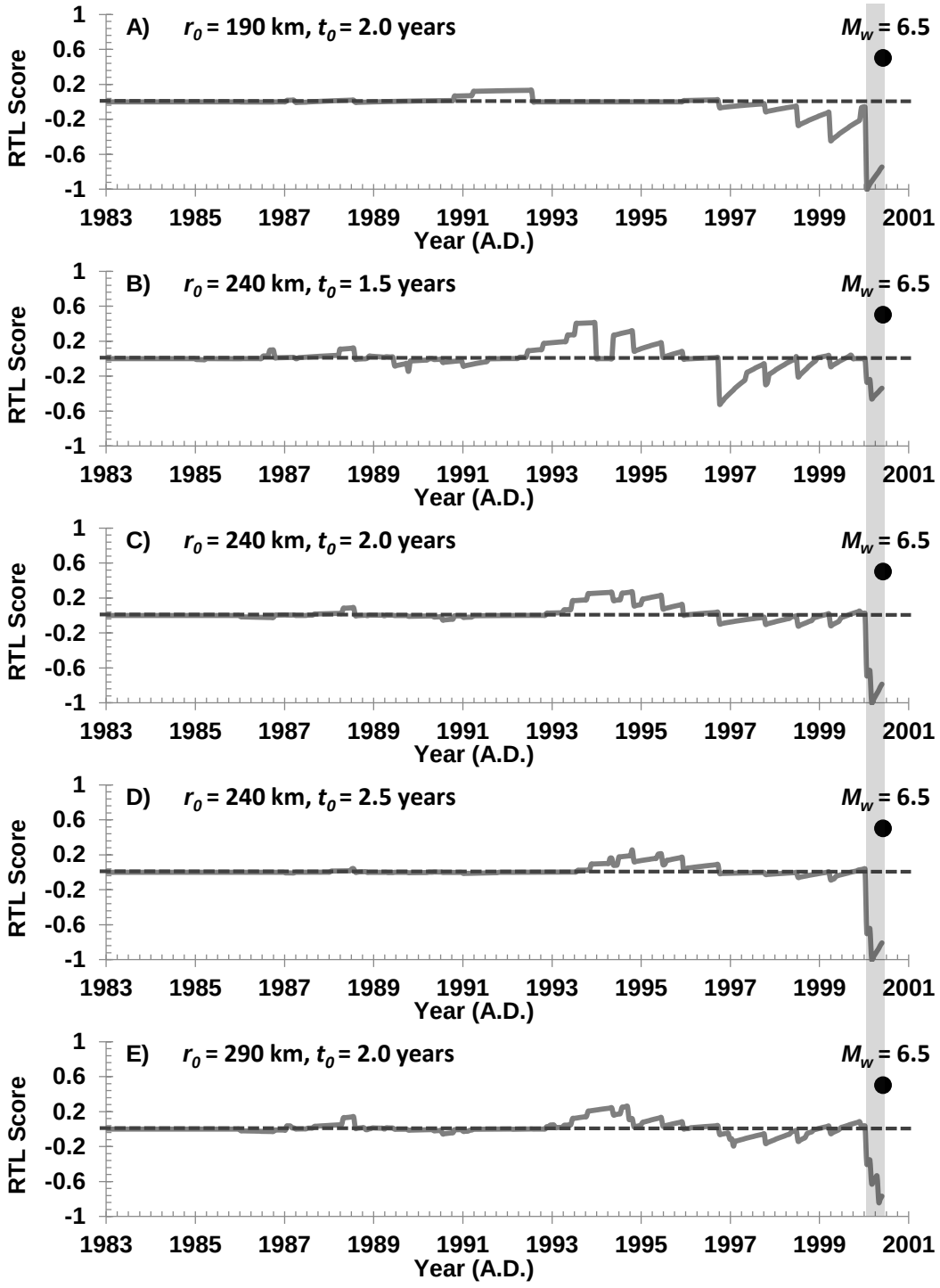

Figure 6.13. Temporal variation of *RTL* scores (grey lines) evaluate from different characteristic parameter. Black circles denote the occurrence time of the M_w-6.5 earthquake on June 7, 2000. Grey shade indicated the duration of quiescence which is used to generate spatial distribution in Figure 5.3.

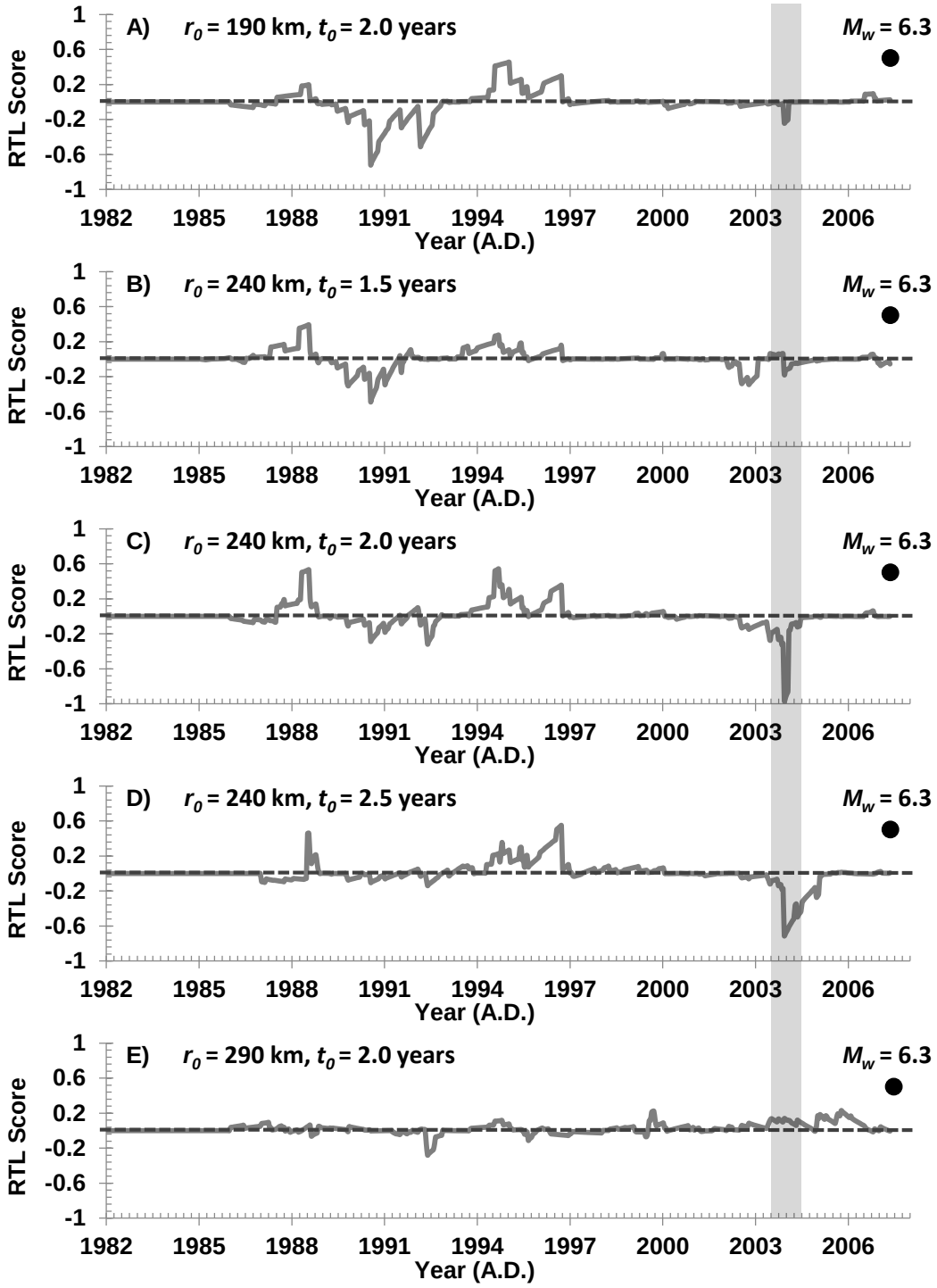

Figure 6.14. Temporal variation of *RTL* scores (grey lines) evaluate from different characteristic parameter. Black circles denote the occurrence time of the M_w-6.3 earthquake on May 16, 2007. Grey shade indicated the duration of quiescence which is used to generate spatial distribution in Figure 5.4.

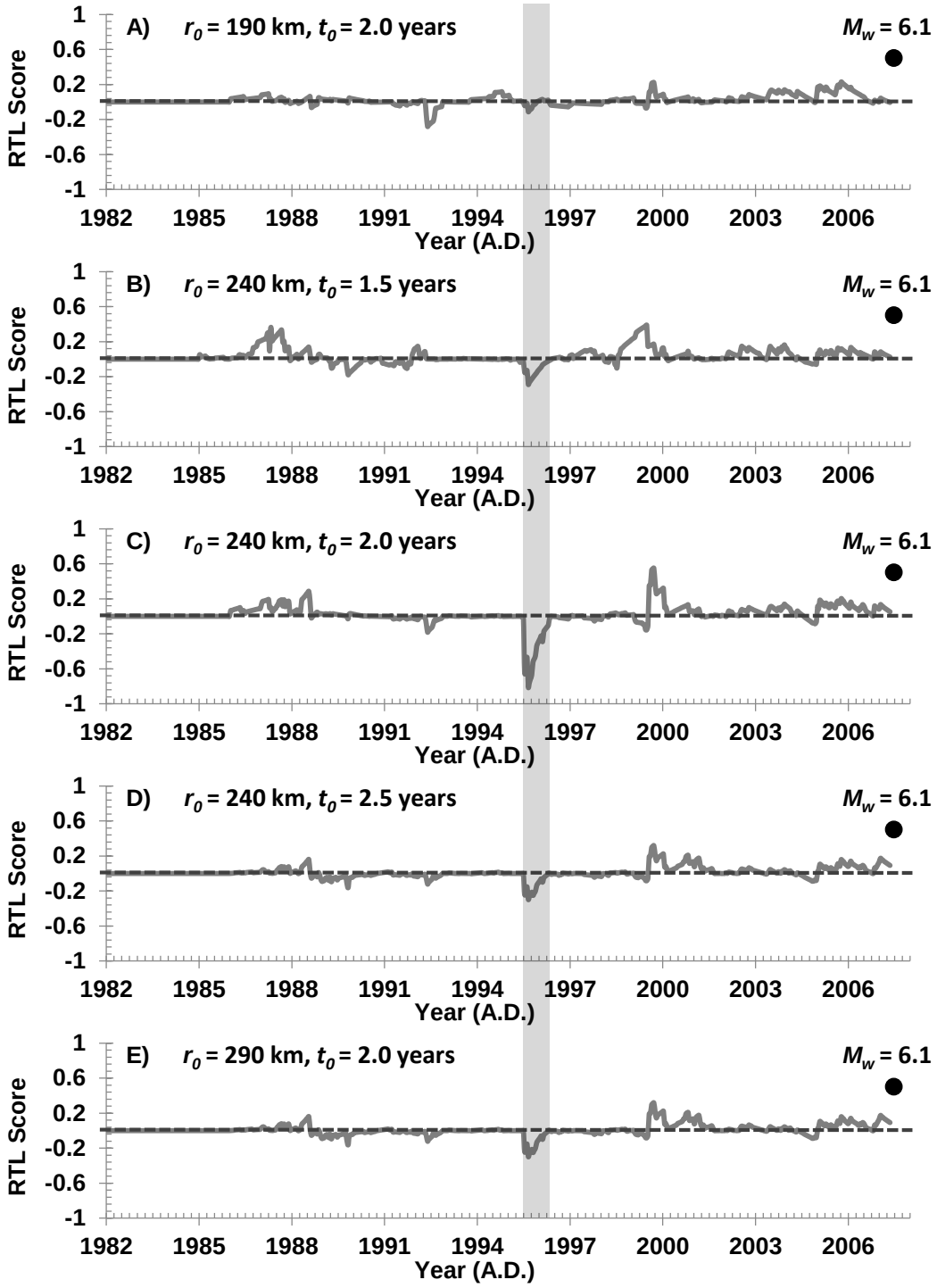

Figure 6.15. Temporal variation of *RTL* scores (grey lines) evaluate from different characteristic parameter. Black circles denote the occurrence time of the M_w-6.1 earthquake on June 23, 2007. Grey shade indicated the duration of quiescence which is used to generate spatial distribution in Figure 5.5.

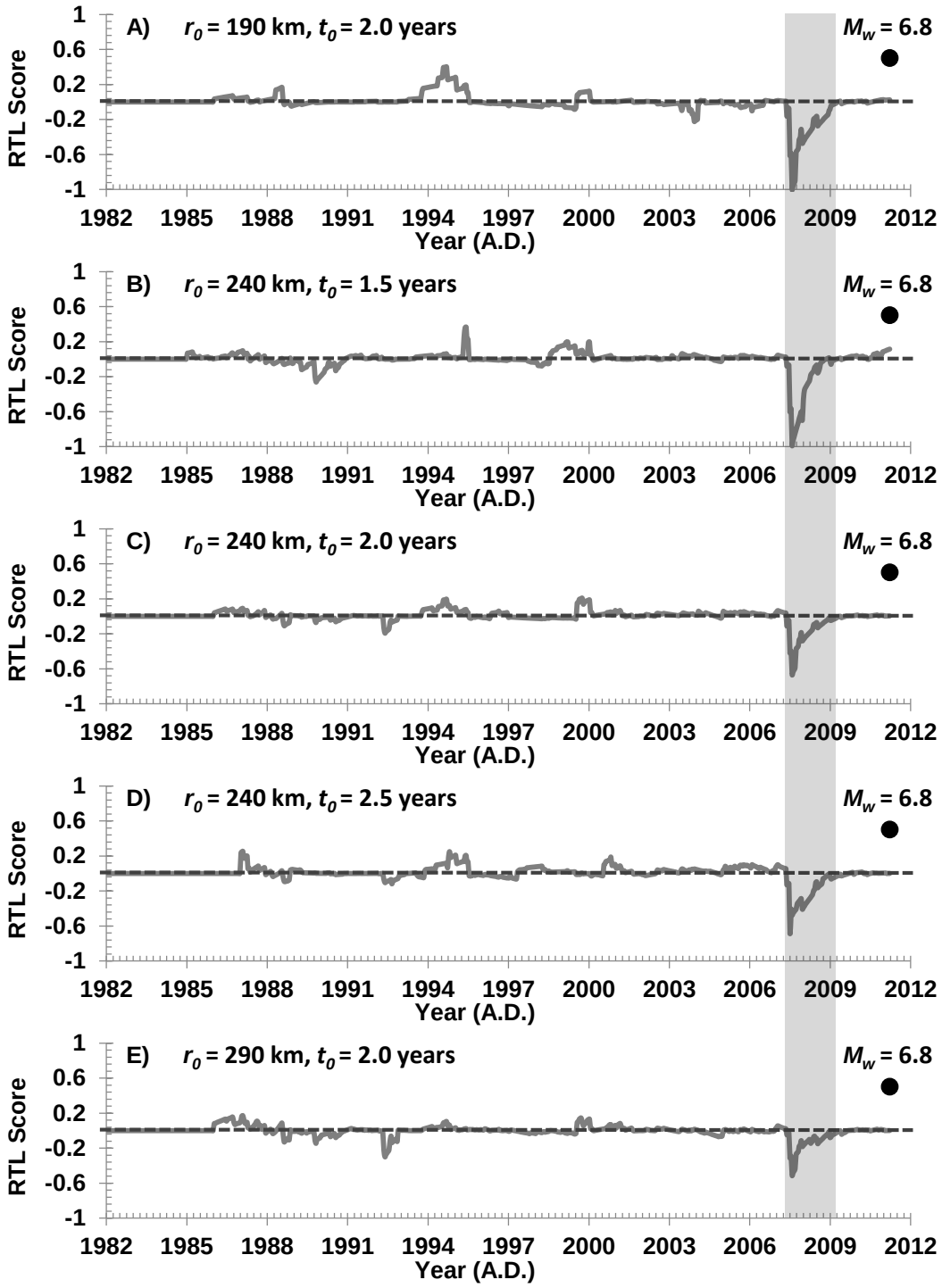

Figure 6.16. Temporal variation of *RTL* scores (grey lines) evaluate from different characteristic parameter. Black circles denote the occurrence time of the M_w-6.8 earthquake on March 24, 2011. Grey shade indicated the duration of quiescence which is used to generate spatial distribution in Figure 5.6.

CHAPTER VII

CONCLUSIONS AND RECOMMENDATIONS

This work attempt to investigate the precursory seismicity rate changes before the occurrence of strong earthquakes in Thailand-Laos-Myanmar borders by using simultaneously both *Z* value and *RTL* algorithm. The obtained results lead to the conclusions and recommendations as follows;

7.1 Conclusions

According to all results of the completeness of seismicity data, *Z* and *RTL* value investigation in Thailand-Laos-Myanmar borders, it can be conclude that:

i) The completeness of seismicity data can provide the homogenous catalogues which directly relate to the tectonic activities.

ii) By using the characteristic parameters of *Z*, i.e., the number of earthquake (n) = 50 events, time window (T_w) = 1.2 years, including the fixed radius = 250 km of earthquake considering, the results of *Z* value investigation found 5 seismicity precursors from 8 strong earthquakes, 4 of 5 calculable anomalous areas can forecast the occurrence location of strong earthquakes.

iii) Moreover, by applying the characteristic *RTL* parameter with characteristic distance r_0 = 120 km, characteristic time-span t_0 = 2 and fixed the minimum number of collecting earthquake events (n) = 30, the results of *RTL* value investigation can detect 5 seismicity precursors from 8 strong earthquakes, all of those anomalies areas can forecast the occurrence location of strong earthquakes.

iv) The cumulative number curves of *Z* value investigation indicate the duration time between the detection quiescence stage and the occurrence time of strong earthquake varies in the range of intermediate-term forecasting.

v) The *RTL* curves investigation also indicate the duration time between the detection quiescence stage and the occurrence time of strong earthquake varies in the

range of intermediate-term forecasting except the event of M_w-6.1 earthquake on June 23, 2007.

vi) In this work, *Z* value at the epicenter of earthquake varies in the acceptable range when compared to previous works. Almost results from this work can generated high *Z* value.

vii) In this work, although the normalized *RTL* values at the location of main shock are not comparable with previous studies, the temporal variation of *RTL* curve cleary indicate seismic quiescence similar to previous researches.

viii) The comparison between *Z* value and normalized *RTL* can indicate that the more positive Z corresponding to the more negative RTL significantly.

ix) Results of both methods in this work indicate that the main shocks occurred after the quiescence stage with a moment of time delay. That means, the main shocks not need to occur in the duration of quiescence stage. They can occur after the end of quiescence stage with variation of time delay. Even though the existence stage of time delay which mentioned above makes it hard to estimate and determine the occurrence time accurately in short-term earthquake forecasting, the investigation of seismicity pattern changes both techniques may provide useful information for forecasting future earthquake.

x) The comparison of *Z*, *b*, and *RTL* parameter distribution reveal that the regions indicate comparatively low *RTL* and high *Z* (this study) quite conform to the area with comparatively low *b* value at the same duration. Moreover, the latest spatial map (during 2008 and 2010) of these methods indicates the overlap anomalous areas around Kengtung and Chiang Rai city followed by the M_w-6.8 earthquake on March 24, 2011 and M_w-6.8 earthquake on March 5, 2014, respectively. Then, the overlap area without subsequent by strong earthquake may be at risk to impending earthquake.

xi) Although both *Z* and *RTL* methods can investigate seismic precursor prior to main shock in Thailand-Laos-Myanmar borders, the stochastic test of *RTL* algorithm indicate a more reliable probability than *Z* investigation.

xii) The correlation coefficient analysis of *RTL* algorithm (this work) indicates that almost all of the quiescence anomalies correlate at a significance of 0.05. Hence, the quiescence anomalies in Thailand-Laos-Myanmar borders, which are detected before the occurrence of strong earthquakes by using *RTL* algorithm, are not artificial anomalous and are meaningful for earthquake forecasting.

7.2 Recommendations

According to the usable seismicity data in Thailand-Laos-Myanmar borders started in 1982 and ended in 2012, the result obtained in this study was therefore scoped in specific short time period. Hence, for supporting the accuracy and reliability of further researches, the seismic recording networks in Thailand-Laos-Myanmar borders should be developed and improved. Furthermore, even though the *Z* and *RTL* value investigation can analyze seismic precursor in Thailand-Laos-Myanmar borders, the location and the occurrence time of main shock still cannot determine specifically. Then, in order to solve these unclear problems, the further study about *Z*, *RTL* or others algorithm in Thailand-Laos-Myanmar borders may strengthen the understanding of the activity of strong and major earthquakes in this area and provide more useful information for estimating the future hazard areas.

REFERENCES

Agnew, D.C., 2002. History of Seismology. International Handbook of Earthquake and Engineering Seismology, 81(A): 3-11.

Alves, E.I., 2006. Earthquake Forecasting Using Neural Networks: Results and Future Work. Nonlinear Dynamics 44: 341-349.

Bachmann, D., 2001. Precursory Seismic Quiescence: Two Methods of Quantifying Seismicity Rate Changes and an Application to Two Northern Californian Mainshocks, Swiss Federal Institute of Technology, Zurich.

Ben-Zion, Y. and Lyakhovsky, V., 2002. Accelerated seismic release and related aspects of seismicity patterns on earthquake faults. Pure and applied geophysics 159(10): 2385-2412.

Bendat, J.S. and Piersol, A.G., 2000. Random Data: Analysis and Measurement Procedures. John Wiley and Sons, New York.

Bertrand, G. and Rangin, C., 2003. Tectonics of the western margin of the Shan Plateau (central Myanmar): implications for the India-Indochina oblique convergence since the Oligocene. Journal of Asian Earth Sciences 21: 1139-1157.

Bodri, B., 2001. A neural-network model for earthquake occurrence. Journal of Geodynamics 32: 289-310.

Bufe, C.G., 2006. Coulomb Stress Transfer and Tectonic Loading Preceding the 2002 Denali Fault Earthquake. Bulletin of the Seismological Society of America 95(5): 1662–1674.

Cao, L., Fang, H., Li, Q. and Chen, J., 1996. Forecasting b-values for seismic events. Bulletin of the Seismological Society of America, 96(5): 1662–1674.

Cattin, R., Chamot-Rooke, N., P., M., , Rabaute, A., Delescluse, M., Vigny, C., Fleitout, L. and Dubernet, P., 2009. Stress change and effective friction coefficient along the Sumatra-Andaman-Sagaing fault system after the 26 December 2004 (Mw = 9.2) and the 28 March 2005 (Mw = 8.7) earthquakes. Geochemistry, Geophysics, Geosystems, 10(3): 1-21.

Charusiri, P., Daorerk, V., Wongvanich, T., Nakapadungrat, S. and Imsamut, S., 1999. Geology of the Quadrangle Economic Zone (emphasis on China and Thailand), Technical report, National Research Council of Thailand, Bangkok, Thailand.

Charusiri, P., Rhodes, B.P., Saithong, P., Kosuwan, S., Pailopli, S., Wiwegwin, W., Doarerk, V., Hinthong, C. and Klaipongpan, S., 2007. Regional tectonic setting and seismicity of Thailand with reference to reservoir construction, GEOTHAI'07 International Conference on Geology of Thailand: Towards Sustainable Development and Self Sufficient Economy, pp. 274-287.

Chen, C.C. and Wu, Y.X., 2006. An improved region-time-length algorithm applied to the 1999 Chi-Chi, Taiwan earthquake. Geophysical Journal International, 166(3): 1144-1148.

Chiangrai Times, 2014. Two tremors felt in Phan and Mae Lao Chiang Rai. Chiangrai Times.

Chouliaras, G., 2009a. Seismicity anomalies prior to 8 June 2008, M_w=6.4 earthquake in Western Greece. Natural Hazards and Earth System Sciences, 9(2): 327-335.

Chouliaras, G., 2009b. Seismicity anomalies prior to the 13 December 2008, M_s=5.7 earthquake in Central Greece. Natural Hazards and Earth System Sciences, 9(2): 501-506.

Chouliaras, G., 2009c. Investigating the earthquake catalog of the National Observatory of Athens. Natural Hazards and Earth System Sciences, 9(3): 905-912.

Chouliaras, G. and Stavrakakis, G.N., 2001. Current seismic quiescence in Greece: Implications for seismic hazard. Journal of Seismology, 5(4): 595-608.

Cornell, C.A., 1968. Engineering seismic risk analysis. Bulletin of the Seismological Society of America 58: 1583-1606.

Das, S., Gupta, I.D. and Gupta, V.K., 2006. A Probabilistic Seismic Hazard Analysis of Northeast India. Earthquake Spectra 22(1): 1-27.

Du, W. and Sykes, L.R., 2001. Changes in Frequency of Moderate-Size Earthquakes and Coulomb Failure Stress before and after the Landers, California, Earthquake of 1992. Bulletin of the Seismological Society of America, 91(4): 725–738.

Ebel, J.E., Chambers, D.W., Kafka, A.L. and Baglivo, J.A., 2007. Non-Poissonian earthquake clustering and the hidden Markov model as bases for earthquake forecasting in California. Seismological Research Letters 78: 57–65.

Evison, F.F. and Rhoades, D.A., 1997. The precursory earthquake swarm in New Zealand: hypothesis tests II. New Zealand Journal of Geology and Geophysics 40: 537–547.

Federica, R. and Mikio, I., 2014. Learning from Megadisasters: Lessons from the Great East Japan Earthquake. World Bank.

Fenton, C.H., Charusiri, P. and Wood, S.H., 2003. Recent paleoseismic investigations in Northern and Western Thailand. Annals of Geophysics 46(5): 957– 981.

Fu, G. and Sun, W., 2006. Global co-seismic displacements caused by the 2004 Sumatra-Andaman earthquake (Mw 9.1). Earth Planets Space, 58: 149-152.

Gambino, S., Laudani, A. and Mangiagli, S., 2014. Seismicity pattern changes before the M = 4.8 Aeolian Archipelago (Italy) earthquake of August 16, 2010. ScientificWorldJournal, 2014: 531212.

Gardner, J.K. and Knopoff, L., 1974. s the sequence of earthquakes in Southern California, with aftershocks removed, Poissonian? Bulletin of the Seismological Society of America, 64(1): 363–367.

Gentili, S., 2010. Distribution of Seismicity Before the Larger Earthquakes in Italy in the Time Interval 1994–2004. Pure and Applied Geophysics, 167(8-9): 933-958.

Giovambattista, R.D. and Tyupkin, Y.S., 2000. Spatial and temporal distribution of seismicity before the Umbria-Marche September 26, 1997 earthquakes. Journal of Seismology, 4(4): 589-598.

Giovambattista, R.D. and Tyupkin, Y.S., 2009. The fine structure of dynamics seismicity before M $\geq$ 4.5 earthquakes the area of Reggio Emilia (Northern Italy). Annali di Geofisica, 42(5): 897-909.

Gutenberg, B., 1945. Amplitudes of surface waves and magnitude of shallow earthquake. Bulletin of the Seismological Society of America, 35: 3-12.

Gutenberg, B. and Richter, C.F., 1944. Frequency of earthquake in California. Bulletin of the Seismological Society of America, 34: 185-188.

Gutenberg, B. and Ritchter, C.F., 1956. Earthquake Magnitude, Intensity, Energy, and Acceleration (Second Paper). Bulletin of the Seismological Society of America, 46(2): 105-145.

Habermann, R.E., 1982. Consistency of teleseismic reporting since 1963. Bulletin ofthe Seismological Society of America, 72: 93–112.

Habermann, R.E., 1983. Teleseismic detection in the Aleutian Island Arc. Journal of Geophysical Research, 88: 5056–5064.

Habermann, R.E., 1987. Man-made changes of Seismicity rates. Bulletin of the Seismological Society of America, 77: 141-159.

Habermann, R.E. and Wyss, M., 1984. Background seismicity rates and precursory seismic quiescence: Imperial Valley, California. Bulletin of the Seismological Society of America, 74: 1743–1755.

Hanks, T.C. and Kanamori, H., 1979. A moment-magnitude scale. Journal of Geophysical Research, 84: 2348–2350.

Holliday, J.R., Nanjo, K.Z., Tiampo, K.F., Rundle, J.B. and Turcotte, D.L., 2005. Earthquake forecasting and its verification. Nonlinear Processes in Geophysics, 12: 965-977.

Holliday, J.R., Rundle, J.B., Tiampo, K.F., Klein, W. and Donnellan, A., 2006. Systematic procedural and sensitivity analysis of the Pattern Informatics method for forecasting large (M > 5) earthquake events in southern California. Pure and Applied Geophysics, 163(11-12): 2433-2454.

Howell, B.F., 1981. On the saturation of earthquake magnitudes. Bulletin of the Seismological Society of America, 71(5): 1401–1422.

Huang, Q., 2004. Seismicity pattern changes prior to large earthquakes - an approach of the RTL algorithm. Terrestrial, Atmospheric and Oceanic Sciences (TAO), 15(3): 469-491.

Huang, Q., 2005. A method of evaluating reliability of earthquake precursors. Chinese Journal of Geophysic, 48(3): 701-707.

Huang, Q. and Sobolev, G.A., 2002. Precursory seismicity changes associated with the Nemuro Peninsula earthquake, January 28,2000. Journal of Asian Earth Sciences, 21(2): 135-146.

Huang, Q., Sobolev, G.A. and Nagao, T., 2001. Characteristics of the seismic quiescence and activation patterns before the *M*=7.2 Kobe earthquake, January 17, 1995. Tectonophysics, 337(1-2): 99-116.

Imoto, M., Hurukawa, N. and Ogata, Y., 1990. Three-dimensional spatial variations of bvalue in the Kanto area, Japan. Zishin, 43: 321-326.

Ishimoto, M. and Iida, K., 1939. Observations sur les seismes enregistres parle microsismographe construit dernierement. Bulletin of the Earthquake Research Institute, University of Tokyo, 17: 443-478.

Jarl, G.L., 2005. GIS Disaster Management. LUMA-GIS, GIS Center, University of Lund Sweden.

Jiang, H.K., Hou, H.F., Zhou, H.P. and Zhou, C.Y., 2004. Region-time-length algorithm and its application to the study of intermediate-short term earthquake precursor in North China. ACTA SEISMOLOGICA SINICA, 17(2): 164-176.

Kanamori, H., 1977. The energy release in great earthquake. Journal of Geophysical Research, 82: 2981-2987.

Katsumata, K., 2011a. Precursory seismic quiescence before theMw= 8.3 Tokachi-oki, Japan, earthquake on 26 September 2003 revealed by a re-examined earthquake catalog. Journal of Geophysical Research, 116(B10).

Katsumata, K., 2011b. A long-term seismic quiescence started 23 years before the 2011 off the Pacific coast of Tohoku Earthquake (M= 9.0). Earth, Planets and Space, 63(7): 709-712.

Katsumata, K. and Sakai, S., 2013. Seismic quiescence and activation anomalies from 2005 to 2008 beneath the Kanto district, central Honshu, Japan. Earth, Planets and Space, 65(12): 1463-1475.

Keilis-Borok, V.I. and Kossobokov, V.G., 1990. Times of increased probability of strong earthquakes (M ≥ 7.5) diagnosed by Algorithm M8 in Japan and adjacent territories. Journal of Geophysical Research: Solid Earth, 95(B8): 12413-12422.

Kirschvink, J.L., 2000. Earthquake Prediction by Animals: Evolution and Sensory Perception. Bulletin of the Seismological Society of America 90(2): 312–323.

Kramer, S.L., 1996. Geotechnical Earthquake Engineering, Prentice Hall, Inc., Upper Saddle River, New Jersey, 563 pp.

Lacassin, R., Replumaz A. and Leloup, P.H., 1998. Hairpin river loops and strike-slip sense inversion of Southeast Asian strike-slip faults. Geology, 26: 703–706.

Lepvrier, C., Maluski, H., Tich, V.V. and Leyreloup, A., 2004. The Early Triassic Indosinian orogeny in Vietnam (Truong Son Belt and Kontum Massif); implications for the geodynamic evolution of Indochina. Tectonophysics, 393(1-4): 87–118.

Maeda, K. and Wiemer, S., 1999. Significance test for seismicity rate changes before the 1987 Chiba-toho-oki earthquake (M 6.7) Japan. Annali di Geofisica, 42(5): 833-850.

Martin, S., 2005. Intensity distribution from the 2004 M 9.0 Sumatra-Andaman earthquake. Seismological Research Letters 76: 321–330.

Maryanto, S. and Mulyana, I., 2008. Temporal Change of Fractal Dimension of Explosion Earthquakes and Harmonic Tremors at Semeru Volcano, East Java, Indonesia, using Critical Exponent Method. World Academy of Science, Engineering and Technology, 42: 537-541.

McCalpin, J.P., 1996. Paleoseismology. Academic Press, New York, 588 pp.

McCue, K., 2004. Australia: Historical earthquake studies. Annals of Geophysics, 47(2/3): 387-397.

Menshikov, V.A., Perminov, A.N. and M., U.Y., 2012. Global Aerospace Monitoring and Disaster Management. Springer, Wien New York.

Mignan, A. and Giovambattista, R.D., 2008. Relationship between accelerating seismicity and quiescence, two precursors to large earthquakes. Geophysical Research Letters, 35(15).

Mignan, A. and Woessner, J., 2012. Estimating the magnitude of completeness in earthquake catalogs. Community Online Resource for Statistical Seismicity Analysis.

Morley, C.K., 2007. Variations in Late Cenozoic-Recent strike-slip and obliqueextensional geometries, within Indochina: The influence of pre-existing fabrics. Journal of Structural Geology, 29: 36–58.

Murru, M., Console, R. and Montuori, C., 1999. Seismic quiescence precursor to the 1983 Nihonkai-Chubu (M7.7) earthquake, Japan. Annali di Geofisica 42(5): 871-882.

Nagao, T., Takeuchi, A. and Nakamura, K., 2011. A new algorithm for the detection of seismic quiescence: introduction of the RTM algorithm, a modified RTL algorithm. Earth, Planets and Space, 63(3): 315-324.

Nuannin, P., Kulhanek, O. and Persson, L., 2005. Spatial and temporal b value anomalies preceding the devastating off coast of NW Sumatra earthquake of December 26, 2004. Geophysical Research Letters, 32(11): L11307.

Ogata, Y., 1988. Statistical models for earthquake occurrence and residual analysis for point process. Journal of the American Statistical Association 83: 9-27.

Oki, Y. and Hiraga, S., 1988. Groundwater Monitoring for Earthquake Prediction by an Amateur Network in Japan. Pure and Applied Geophysics 126(2-4): 211-240.

Ottemoller, L. and Havskov, J., 2003. Moment magnitude determination for local and regional earthquakes based on source spectra. Bulletin of the Seismological Society of America, 93(1): 203–214.

Öztürk, S., 2013. A statistical assessment of current seismic quiescence along the north anatolian fault zone: Earthquake precursors. Austrian jurnal of earth sciences, 106(2): 4-17.

Öztürk, S. and Bayrak, Y., 2009. Precursory seismic quiescence before 1 may 2003 bingÖl (turkey) earthquake: A statistical evaluation. Journal Of Applied Functional Analysis, 4(4): 600-610.

Öztürk, S. and Bayrak, Y., 2012. Spatial variations of precursory seismic quiescence observed in recent years in the eastern part of Turkey. Acta Geophysica, 60(1).

Pailoplee, S., 2009c. Seismic hazard assessment in Thailand using probabilistic and deterministic methods, Chulalongkorn University, Bangkok, 163 pp.

Pailoplee, S., Channarong, P. and Chutakositkanon, V., 2013. Earthquake Activities in the Thailand-Laos-Myanmar Border Region: A Statistical Approach. Terrestrial Atmospheric And Oceanic Sciences, 24(4): 721-730.

Pailoplee, S. and Choowong, M., 2014. Earthquake frequency-magnitude distribution and fractal dimension in mainland Southeast Asia. Earth, Planets and Space, 66(1): 1-10.

Pailoplee, S., Sugiyama, Y. and Charusiri, P., 2009b. Deterministic and probabilistic seismic hazard analyses in Thailand and adjacent areas using active fault data. Earth, Planets and Space, 61(12): 1313-1325.

Pailoplee, S., Takashima, I., Kosuwan, S. and Charusiri, P., 2009a. Earthquake activities along the Lampang-Theon Fault Zone, Northen Thailand: Evidence from Paleoseismological and Seismicity Data. Journal of Applied Sciences Research, 5(2): 168-180.

Palasri, C., 2006. Probabilistic seismic hazard map of Thailand, Chulalongkorn University, Bangkok, Thailand.

Perawongmetha, A., 2014. Destruction in N. Thailand after 6.0 earthquake. Reuters.

Petersen, M., Dewey, J., Hartzell, S., Mueller, C., Harmsen, S., Frankel, A.D. and Rukstales, K., 2004. Probabilistic seismic hazard analysis for Sumatra, Indonesia and across the Southern Malaysian Peninsula. Tectonophysics, 390: 141-158.

Polachan, S., Pradidtan, S., Tongtaow, C., Janmaha, S., Intarawijitr, K. and Sangsuwan, C., 1991. Development of Cenozoic basins in Thailand. Marine and Petroleum Geology, 8: 84-97.

Richter, C.F., 1935. An instrumental earthquake magnitude scale* Bulletin of the Seismological Society of America 25(1): 1-32.

Rong, D.L. and Li, Y.R., 2007. Estimation of characteristic parameters in region-time-length algorithm and its application. Acta Seismologica Sinica, 20(3): 265-272.

Rudolf-Navarro, A.H., Munoz-Diosdado, A. and Angulo-Brown, F., 2010. Seismic quiescence patterns as possible precursors of great earthquakes in Mexico. International Journal of the Physical Sciences, 5(6): 651-670.

Santi Pailoplee, Pantarak Channarong and Vichai Chutakositkanon, 2013. Earthquake Activities in the Thailand-Laos-Myanmar Border Region: A Statistical Approach. Terrestrial Atmospheric And Oceanic Sciences, 24(4): 721-730.

Schwartz, D.P., Coppersmith, K.J., Swan, F.H.I., Somerville, P. and Savage, W.U., 1981. Characteristic earthquakes on intraplate normal faults. Earthquake Notes 52: 71.

Shebalin, P., Keilis-Borok, V., Gabrielov, A., Zaliapin, I. and Turcotte, D., 2006. Short-term earthquake prediction by reverse analysis of lithosphere dynamics. Tectonophysics, 413(1–2): 63-75.

Sobolev, G.A., 1995. Fundamental of Earthquake Prediction. Electromagnetic Research Center, Moscow.

Sobolev, G.A. and Tyupkin, Y.S., 1997. Low-seismicity precursors of large earthquakes in Kamchatka. Volcanology and Seismology, 18: 433-446.

Sobolev, G.A. and Tyupkin, Y.S., 1999. Precursory phases, seismicity precursors, and earthquake prediction in Kamchatka. Volcanology and Seismology 20: 615-627.

Socquet, A. and Pubellier, M., 2005. Cenozoic deformation in western Yunnan (China–Myanmar border). Journal of Asian Earth Sciences 24(4): 495-515.

Stiphout, V.T., Zhuang, J. and Marsan, D., 2012. Seismicity declustering. Community Online Resource for Statistical Seismicity Analysis, Zurich.

Stirling, M. and Petersen, M., 2006. Comparison of the Historical Record of Earthquake Hazard with Seismic- Hazard Models for New Zealand and the Continental United States. Bulletin of the Seismological Society of America 96(6): 1978-1994.

Suckale, J. and Grünthal, G., 2009. A probabilistic seismic hazard model for Vanuatu. Bulletin of the Seismological Society of America, 99(4): 2108-2126.

Sykes, L.R., 1996. Intermediate- and long-term earthquake prediction. 93(Proceedings of the National Academy of Sciences of the United States of America): 3732-3739.

Tiampo, K.F. and Shcherbakov, R., 2012. Seismicity-based earthquake forecasting techniques: Ten years of progress. Tectonophysics, 522-523: 89-121.

USGS, 2014. Earthquake Fact. USGS.

Ward, S.N., 2007. Methods for evaluating earthquake potential and likelihood in and around California. Seismological Research Letters 78: 121–133.

Wells, D.L. and Coppersmith, K.J., 1994. Updated empirical relationships among magnitude, rupture length, rupture area, and surface displacement. Bulletin of the Seismological Society of America, 84: 974–1002.

Werner, M.J., Helmstetter, A., Jackson, D.D., Kagan, Y.Y. and Wiermer, S., 2010. Adaptively smoothed seismicity earthquake forecasts for Italy. Annals of Geophysics, 53(3): 107-116.

Wiemer, S. and Wyss, M., 1994. Seismic Quiescence before the Landers (M = 7.5) and Big Bear (M = 6.5) 1992 Earthquakes. Bulletin of the Seismological Society of America, 84(3): 900-916.

Woessner, J., Hardebeck, J.L. and Haukkson, E., 2010. What is an instrumental seismicity catalog. Community Online Resource for Statistical Seismicity Analysis, 10.

Wu, Y.-M., Chen, C.-C., Zhao, L. and Chang, C.-H., 2008. Seismicity characteristics before the 2003 Chengkung, Taiwan, earthquake. Tectonophysics, 457(3-4): 177-182.

Wu, Y.M. and Chiao, L.Y., 2006. Seismic Quiescence before the 1999 Chi-Chi, Taiwan, Mw 7.6 Earthquake. Bulletin of the Seismological Society of America, 96(1): 321-327.

Wyss, M., 1991. Reporting history of the central Aleutians seismograph network and the quiescence preceding the 1986 Andreanof Island earthquake. Bulletin of the Seismological Society of America, 81: 1231–1254.

Wyss, M. and Burford, R.O., 1985. Current episodes of seismic quiescence along the San Andreas fault between San Juan Bautista and Stone Canyon, California: Possible Precursors to local moderate mainshocks? The United States Geological Survey, 85–745: 367–426.

Wyss, M. and Habermann, R.E., 1988. Precursory seismicquiescence. Pure and Applied Geophysics, 126: 319-332.

Wyss, M., Hasegawa, A., Wiemer, S. and Umino, N., 1999. Quantitative mapping of precursory seismic quiescence before the 1989 M7.1 off-Sanriku earthquake, Japan. Annali di Geofisica 42(5): 851-869.

Yagi, Y., Kikuchi, M. and Sagiya, T., 2001. Co-seismic slip, post-seismic slip, and aftershocks associated with two large earthquakes in 1996 in Hyuga-nada, Japan. Earth Planets Space, 53: 793-803.

Yin, X.C., Chen, X.Z., Song, Z.P. and Yin, C., 1995. A new approach to earthquake prediction – the Load-Unload Response Ratio (LURR) theory. Pure and applied geophysics, 145(3/4): 701–715.

Zechar, J.D. and Jordan, T.H., 2010. Simple smoothed seismicity earthquake forecasts for Italy. Annals of Geophysics 53(3): 99-105.

Zmazek, B., Vaupoti, J., Ziv-ci, M., Premru, U. and Kobal, I., 2000. Radon Monitoring for Earthquale Prediction in Slovenis. Fizika B (Zagreb), 9(3): 111-118.

Zuchiewicz, W., Cuong, N.Q., Bluszcz, A. and Michalik, M., 2004. Quaternary sediments in the Dien Bien Phu fault zone, NW Vietnam: a record of young tectonic processes in the light of OSL-SAR dating results. Geomorphology, 60: 269–302.

Zuniga, F.R., 1989. A study of the homogeneity of the NOAA earthquake data file in the Mid-America region by the magnitude signaturetechnique. Geofisica Internacional 28: 103–119.

Zuniga, F.R., Reyes, M.A. and C., V., 2000. A general overview of the catalog of recent seismicity compiled by the Mexican Seismological Survey. Geofísica Internacional, 39(2): 161-170.

Zuniga, F.R., Reyners, M. and Villamor, P., 2005. Temporal variation of the earthquake data in the catalogue of seismicity of new Zealand. Bulletin of the New Zealand Society for Earthquake Engineering, 38(2): 87-105.

Zuniga, F.R. and Wyss, M., 1995. Inadvertent changes in magnitude reported in earthquake catalogs: Influence on b-value estimates. Bulletin of the Seismological Society of America, 85: 1858–1866.

APPENDICES

APPENDIX A

VARIATION OF CHARACTERISTIC Z PARAMETERS

Table A.1. The example list of calculated strong earthquake ($M_w \geq 6.0$) that it detected seismic quiescence anomaly after investigating *Z* value in Thailand-Laos-Myanmar borders (16.76° – 22.30°N and 97.48° – 103.16°E) by using different characteristic *Z* parameters. The yellow highlighted indicate the condition, which used in this study. The parameters *N*, Q_s, *Z* and *Q*-time indicate the number of investigating events, starting time of seismic quiescence, maximum of *Z* values at the epicenter of strong earthquakes and the duration between the starting time of seismic quiescence and the occurrence time of main shock, respectively.

N	T_w (Year)	Lon (Deg)	Lat (Deg)	Year	Mag (M_w)	Radius (km)	Q_s (Year)	Z_{max}	*Q*-time (Year)
25	1	99.3	22	1984.31	6.3	360.53	1982.15	0.4	2.2
25	1	98.91	20.43	1989.74	6.2	192.89	1984.33	4.5	5.4
25	1	99.16	21.93	1995.53	6.8	132.31	1992.35	4.7	3.2
25	1	101.895	18.773	2000.43	6.5	216.16	1991.01	3.8	9.4
25	1	100.96	20.57	2007.37	6.3	128.13	2003.93	4.6	3.4
25	1	99.95	21.44	2007.48	6.1	112.63	2005.66	4.9	1.8
25	1	99.822	20.687	2011.23	6.8	118.89	2007.96	4.9	3.3
25	1.5	99.3	22	1984.31	6.3	360.53	1982.64	-0.4	1.7
25	1.5	98.91	20.43	1989.74	6.2	192.89	1984.33	2.9	5.4
25	1.5	99.16	21.93	1995.53	6.8	132.31	1992.35	4.7	3.2
25	1.5	101.895	18.773	2000.43	6.5	216.16	1991.01	3.8	9.4
25	1.5	100.96	20.57	2007.37	6.3	128.13	2003.93	4.6	3.4
25	1.5	99.95	21.44	2007.48	6.1	112.63	1995.61	4.9	11.9
25	1.5	99.822	20.687	2011.23	6.8	118.89	2007.96	4.9	3.3
25	2	99.3	22	1984.31	6.3	360.53	1981.99	-0.3	2.3
25	2	98.91	20.43	1989.74	6.2	192.89	1984.33	2.6	5.4
25	2	99.16	21.93	1995.53	6.8	132.31	1992.35	4.7	3.2
25	2	101.895	18.773	2000.43	6.5	216.16	1991.01	3.8	9.4
25	2	100.96	20.57	2007.37	6.3	128.13	2003.93	4.6	3.4
25	2	99.95	21.44	2007.48	6.1	112.63	1995.61	4.9	11.9
25	2	99.822	20.687	2011.23	6.8	118.89	1997.07	4.9	14.2
25	2.5	99.3	22	1984.31	6.3	360.53	1981.99	-0.3	2.3
25	2.5	98.91	20.43	1989.74	6.2	192.89	1984.33	2.4	5.4

25	2.5	99.16	21.93	1995.53	6.8	132.31	1989.16	4.7	6.4
25	2.5	101.895	18.773	2000.43	6.5	216.16	1991.01	3.8	9.4
25	2.5	100.96	20.57	2007.37	6.3	128.13	2003.93	4.6	3.4
25	2.5	99.95	21.44	2007.48	6.1	112.63	1995.61	4.9	11.9
25	2.5	99.822	20.687	2011.23	6.8	118.89	1992.08	4.9	19.1
25	3	99.3	22	1984.31	6.3	360.53	1981.99	-0.3	2.3
25	3	98.91	20.43	1989.74	6.2	192.89	1983.6	2.3	6.1
25	3	99.16	21.93	1995.53	6.8	132.31	1992.35	2.2	3.2
25	3	101.895	18.773	2000.43	6.5	216.16	1991.01	3.8	9.4
25	3	100.96	20.57	2007.37	6.3	128.13	2003.93	4.6	3.4
25	3	99.95	21.44	2007.48	6.1	112.63	1987.94	4.9	19.5
25	3.5	99.3	22	1984.31	6.3	360.53	1981.99	-0.3	2.3
25	3.5	98.91	20.43	1989.74	6.2	192.89	1983.64	2	6.1
25	3.5	99.16	21.93	1995.53	6.8	132.31	1988.21	1.8	7.3
25	3.5	101.895	18.773	2000.43	6.5	216.16	1991.01	3.8	9.4
25	3.5	100.96	20.57	2007.37	6.3	128.13	2003.74	2.1	3.6
25	3.5	99.95	21.44	2007.48	6.1	112.63	1987.94	4.9	19.5
25	4	99.3	22	1984.31	6.3	360.53	1981.99	-0.3	2.3
25	4	98.91	20.43	1989.74	6.2	192.89	1982.49	2.1	7.3
25	4	99.16	21.93	1995.53	6.8	132.31	1988.21	1	7.3
25	4	101.895	18.773	2000.43	6.5	216.16	1991.01	3.8	9.4
25	4	100.96	20.57	2007.37	6.3	128.13	1990.55	2.4	16.8
25	4	99.95	21.44	2007.48	6.1	112.63	1987.94	4.9	19.5
25	4.5	99.3	22	1984.31	6.3	360.53	1981.99	-0.3	2.3
25	4.5	98.91	20.43	1989.74	6.2	192.89	1982.49	2.2	7.3
25	4.5	99.16	21.93	1995.53	6.8	132.31	1989.16	1.3	6.4
25	4.5	101.895	18.773	2000.43	6.5	216.16	1991.01	3.8	9.4
25	4.5	99.95	21.44	2007.48	6.1	112.63	1985.83	2.8	21.6
25	5	99.3	22	1984.31	6.3	360.53	1981.99	-0.3	2.3
25	5	98.91	20.43	1989.74	6.2	192.89	1981.99	2.3	7.8
25	5	99.16	21.93	1995.53	6.8	132.31	1989.16	1.7	6.4
25	5	101.895	18.773	2000.43	6.5	216.16	1991.01	3	9.4
25	5	100.96	20.57	2007.37	6.3	128.13	1983.49	2.9	23.9
25	5	99.95	21.44	2007.48	6.1	112.63	1985.83	3.1	21.6
25	5	99.822	20.687	2011.23	6.8	118.89	1981.99	4.9	29.2
25	5.5	99.3	22	1984.31	6.3	360.53	1981.99	-0.3	2.3
25	5.5	98.91	20.43	1989.74	6.2	192.89	1981.99	1.6	7.8
25	5.5	99.16	21.93	1995.53	6.8	132.31	1989.16	2	6.4
25	5.5	101.895	18.773	2000.43	6.5	216.16	1991.01	3.1	9.4

25	5.5	100.96	20.57	2007.37	6.3	128.13	1981.99	2.1	25.4
25	5.5	99.95	21.44	2007.48	6.1	112.63	1985.83	3.3	21.6
25	5.5	99.822	20.687	2011.23	6.8	118.89	1981.99	4.9	29.2
25	6	99.3	22	1984.31	6.3	360.53	1981.99	-0.3	2.3
25	6	98.91	20.43	1989.74	6.2	192.89	1982.49	1.1	7.3
25	6	99.16	21.93	1995.53	6.8	132.31	1988.63	1.5	6.9
25	6	101.895	18.773	2000.43	6.5	216.16	1989.78	3.2	10.7
25	6	100.96	20.57	2007.37	6.3	128.13	1981.99	2.3	25.4
25	6	99.95	21.44	2007.48	6.1	112.63	1985.83	3.5	21.6
25	6	99.822	20.687	2011.23	6.8	118.89	1981.99	4.9	29.2
25	6.5	99.3	22	1984.31	6.3	360.53	1981.99	-0.3	2.3
25	6.5	98.91	20.43	1989.74	6.2	192.89	1981.99	1.3	7.8
25	6.5	99.16	21.93	1995.53	6.8	132.31	1988.86	1.4	6.7
25	6.5	101.895	18.773	2000.43	6.5	216.16	1989.78	2.8	10.7
25	6.5	100.96	20.57	2007.37	6.3	128.13	1981.99	2.5	25.4
25	6.5	99.95	21.44	2007.48	6.1	112.63	1987.94	2.7	19.5
25	7	99.3	22	1984.31	6.3	360.53	1981.99	-0.3	2.3
25	7	98.91	20.43	1989.74	6.2	192.89	1981.99	-0.4	7.8
25	7	99.16	21.93	1995.53	6.8	132.31	1988.21	0.9	7.3
25	7	101.895	18.773	2000.43	6.5	216.16	1989.47	2.5	11
25	7	100.96	20.57	2007.37	6.3	128.13	1991.54	0.8	15.8
25	7	99.95	21.44	2007.48	6.1	112.63	1987.94	2.9	19.5
25	7	99.822	20.687	2011.23	6.8	118.89	1981.99	3.5	29.2
50	0.5	98.91	20.43	1989.74	6.2	278.45	1982.49	6.6	7.3
50	0.5	99.16	21.93	1995.53	6.8	221.26	1992.39	6.4	3.1
50	0.5	101.895	18.773	2000.43	6.5	319.98	1999.25	6	1.2
50	0.5	100.96	20.57	2007.37	6.3	188.41	2005.66	6.8	1.7
50	0.5	99.95	21.44	2007.48	6.1	148.53	2006.08	6.9	1.4
50	0.5	99.822	20.687	2011.23	6.8	147.98	2010.22	6.8	1
50	1	99.16	21.93	1995.53	6.8	221.26	1990.55	2.5	5
50	1	101.895	18.773	2000.43	6.5	319.98	1993.08	6	7.4
50	1	100.96	20.57	2007.37	6.3	188.41	2005.66	6.9	1.7
50	1	99.95	21.44	2007.48	6.1	148.53	1999.52	6.9	8
50	1	99.822	20.687	2011.23	6.8	147.98	2008.53	6.8	2.7
50	1.2	99.16	21.93	1995.53	6.8	379.62	1985.83	3	9.7
50	1.2	101.895	18.773	2000.43	6.5	319.98	1993.08	6	7.4
50	1.2	100.96	20.57	2007.37	6.3	188.41	2003.93	6.9	3.4
50	1.2	99.95	21.44	2007.48	6.1	148.53	1999.52	7.0	8
50	1.2	99.822	20.687	2011.23	6.8	147.98	2008.53	6.8	2.7

50	1.5	99.16	21.93	1995.53	6.8	221.26	1985.33	2.3	10.2
50	1.5	101.895	18.773	2000.43	6.5	319.98	1993.08	2.7	7.4
50	1.5	100.96	20.57	2007.37	6.3	188.41	2003.93	6.9	3.4
50	1.5	99.95	21.44	2007.48	6.1	148.53	1992.35	6.9	15.1
50	1.5	99.822	20.687	2011.23	6.8	147.98	1992.08	6.8	19.1
50	2	99.16	21.93	1995.53	6.8	221.26	1989.16	2.4	6.4
50	2	101.895	18.773	2000.43	6.5	319.98	1992.08	3.5	8.4
50	2	100.96	20.57	2007.37	6.3	188.41	2003.93	2.7	3.4
50	2	99.95	21.44	2007.48	6.1	148.53	1992.35	6.9	15.1
50	2	99.822	20.687	2011.23	6.8	147.98	1992.08	6.8	19.1
50	2.5	99.16	21.93	1995.53	6.8	221.26	1984.6	3.1	10.9
50	2.5	101.895	18.773	2000.43	6.5	319.98	1992.08	2.9	8.4
50	2.5	100.96	20.57	2007.37	6.3	188.41	2003.93	3.4	3.4
50	2.5	99.95	21.44	2007.48	6.1	148.53	1992.35	7	15.1
50	2.5	99.822	20.687	2011.23	6.8	147.98	1992.08	6.8	19.1
50	3	99.16	21.93	1995.53	6.8	221.26	1984.14	2.5	11.4
50	3	101.895	18.773	2000.43	6.5	319.98	1991.54	2.7	8.9
50	3	100.96	20.57	2007.37	6.3	188.41	2003.74	2.6	3.6
50	3	99.95	21.44	2007.48	6.1	148.53	1992.35	4	15.1
50	3	99.822	20.687	2011.23	6.8	147.98	1984.33	6.8	26.9
50	3.5	99.16	21.93	1995.53	6.8	221.26	1983.72	2.2	11.8
50	3.5	101.895	18.773	2000.43	6.5	319.98	1991.01	2.5	9.4
50	3.5	100.96	20.57	2007.37	6.3	188.41	1993.08	2.1	14.3
50	3.5	99.95	21.44	2007.48	6.1	148.53	1983.72	3.1	23.8
50	3.5	99.822	20.687	2011.23	6.8	147.98	1984.33	6.8	26.9
50	4	99.16	21.93	1995.53	6.8	221.26	1983.07	1.5	12.5
50	4	101.895	18.773	2000.43	6.5	319.98	1990.55	2.4	9.9
50	4	100.96	20.57	2007.37	6.3	188.41	2002.51	1.9	4.9
50	4	99.95	21.44	2007.48	6.1	148.53	1990.55	2.7	16.9
50	4	99.822	20.687	2011.23	6.8	147.98	1984.33	6.8	26.9
50	4.5	99.16	21.93	1995.53	6.8	221.26	1981.99	1.4	13.5
50	4.5	101.895	18.773	2000.43	6.5	319.98	1989.78	2.3	10.7
50	4.5	100.96	20.57	2007.37	6.3	188.41	1992.16	2.3	15.2
50	4.5	99.95	21.44	2007.48	6.1	148.53	1990.58	2.4	16.9
50	4.5	99.822	20.687	2011.23	6.8	147.98	1983.3	4.8	27.9
50	5	99.16	21.93	1995.53	6.8	221.26	1981.99	1.9	13.5
50	5	101.895	18.773	2000.43	6.5	319.98	1983.49	2.3	16.9
50	5	100.96	20.57	2007.37	6.3	188.41	1983.49	2.1	23.9
50	5	99.95	21.44	2007.48	6.1	148.53	1995.61	2.2	11.9

50	5	99.822	20.687	2011.23	6.8	147.98	1983.3	5	27.9
50	5.5	99.16	21.93	1995.53	6.8	221.26	1981.99	1.4	13.5
50	5.5	101.895	18.773	2000.43	6.5	319.98	1991.01	1.9	9.4
50	5.5	100.96	20.57	2007.37	6.3	188.41	1983.03	1.9	24.3
50	5.5	99.95	21.44	2007.48	6.1	148.53	1989.28	2.5	18.2
50	5.5	99.822	20.687	2011.23	6.8	147.98	1983.3	4.2	27.9
50	6	99.16	21.93	1995.53	6.8	221.26	1981.99	1	13.5
50	6	101.895	18.773	2000.43	6.5	319.98	1990.55	1.9	9.9
50	6	100.96	20.57	2007.37	6.3	188.41	1990.55	1.8	16.8
50	6	99.95	21.44	2007.48	6.1	148.53	1989.28	2.4	18.2
50	6	99.822	20.687	2011.23	6.8	147.98	1981.99	4.4	29.2
50	6.5	99.16	21.93	1995.53	6.8	221.26	1981.99	1.2	13.5
50	6.5	101.895	18.773	2000.43	6.5	319.98	1989.78	1.6	10.7
50	6.5	100.96	20.57	2007.37	6.3	188.41	1981.99	2.2	25.4
50	6.5	99.95	21.44	2007.48	6.1	148.53	1988.21	2.7	19.3
50	6.5	99.822	20.687	2011.23	6.8	147.98	1981.99	4.7	29.2
50	7	99.16	21.93	1995.53	6.8	221.26	1984.6	1.1	10.9
50	7	101.895	18.773	2000.43	6.5	319.98	1989.47	1.7	11
50	7	100.96	20.57	2007.37	6.3	188.41	1992.16	1.2	15.2
50	7	99.95	21.44	2007.48	6.1	148.53	1988.21	2.6	19.3
50	7	99.822	20.687	2011.23	6.8	147.98	1981.99	2.9	29.2
75	0.5	98.91	20.43	1989.74	6.2	371.57	1985.87	3.6	3.9
75	0.5	99.16	21.93	1995.53	6.8	254.44	1990.55	8.3	5
75	0.5	101.895	18.773	2000.43	6.5	378.87	1998.52	7.4	1.9
75	0.5	100.96	20.57	2007.37	6.3	217.61	2005.77	7.9	1.6
75	0.5	99.95	21.44	2007.48	6.1	177.64	2006.08	8.5	1.4
75	0.5	99.822	20.687	2011.23	6.8	177.41	2010.38	7.9	0.9
75	1	98.91	20.43	1989.74	6.2	371.57	1985.98	2.9	3.8
75	1	99.16	21.93	1995.53	6.8	254.44	1990.55	2.4	5
75	1	101.895	18.773	2000.43	6.5	378.87	1997.07	2.8	3.4
75	1	100.96	20.57	2007.37	6.3	217.61	2005.77	7.9	1.6
75	1	99.95	21.44	2007.48	6.1	177.64	1999.75	8.5	7.7
75	1	99.822	20.687	2011.23	6.8	177.41	1997.07	7.9	14.2
75	1.5	98.91	20.43	1989.74	6.2	371.57	1985.14	1.9	4.6
75	1.5	99.16	21.93	1995.53	6.8	254.44	1989.78	2.2	5.7
75	1.5	101.895	18.773	2000.43	6.5	378.87	1983.68	4.2	16.8
75	1.5	100.96	20.57	2007.37	6.3	217.61	1993.08	3.1	14.3
75	1.5	99.95	21.44	2007.48	6.1	177.64	1992.39	8.5	15.1
75	1.5	99.822	20.687	2011.23	6.8	177.41	1992.65	7.9	18.6

75	2	98.91	20.43	1989.74	6.2	371.57	1984.6	1.9	5.1
75	2	99.16	21.93	1995.53	6.8	254.44	1989.82	2.7	5.7
75	2	101.895	18.773	2000.43	6.5	378.87	1997.07	2.8	3.4
75	2	100.96	20.57	2007.37	6.3	217.61	1992.35	2.6	15
75	2	99.95	21.44	2007.48	6.1	177.64	1992.39	8.5	15.1
75	2	99.822	20.687	2011.23	6.8	177.41	1992.65	8	18.6
75	2.5	98.91	20.43	1989.74	6.2	371.57	1984.48	1.9	5.3
75	2.5	99.16	21.93	1995.53	6.8	254.44	1989.16	2.6	6.4
75	2.5	101.895	18.773	2000.43	6.5	378.87	1992.08	2.9	8.4
75	2.5	100.96	20.57	2007.37	6.3	217.61	1992.16	2.4	15.2
75	2.5	99.95	21.44	2007.48	6.1	177.64	1992.39	5.1	15.1
75	2.5	99.822	20.687	2011.23	6.8	177.41	1985.83	4.5	25.4
75	3	98.91	20.43	1989.74	6.2	371.57	1984.6	1.7	5.1
75	3	99.16	21.93	1995.53	6.8	254.44	1988.86	1.8	6.7
75	3	101.895	18.773	2000.43	6.5	378.87	1991.77	2.4	8.7
75	3	100.96	20.57	2007.37	6.3	217.61	1985.25	2.3	22.1
75	3	99.95	21.44	2007.48	6.1	177.64	1992.39	3.2	15.1
75	3	99.822	20.687	2011.23	6.8	177.41	1985.25	3.6	26
75	3.5	98.91	20.43	1989.74	6.2	371.57	1984.6	1.3	5.1
75	3.5	99.16	21.93	1995.53	6.8	254.44	1983.72	1.5	11.8
75	3.5	101.895	18.773	2000.43	6.5	378.87	1991.01	2.6	9.4
75	3.5	100.96	20.57	2007.37	6.3	217.61	1984.33	2.3	23
75	3.5	99.95	21.44	2007.48	6.1	177.64	1984.33	2.6	23.1
75	3.5	99.822	20.687	2011.23	6.8	177.41	1990.55	3.2	20.7
75	4	98.91	20.43	1989.74	6.2	371.57	1984.52	1.2	5.2
75	4	99.16	21.93	1995.53	6.8	254.44	1983.07	1.1	12.5
75	4	101.895	18.773	2000.43	6.5	378.87	1990.55	2.8	9.9
75	4	100.96	20.57	2007.37	6.3	217.61	1984.33	2.9	23
75	4	99.95	21.44	2007.48	6.1	177.64	1995.61	2.4	11.9
75	4	99.822	20.687	2011.23	6.8	177.41	1990.55	3.7	20.7
75	4.5	98.91	20.43	1989.74	6.2	371.57	1982.53	1.6	7.2
75	4.5	99.16	21.93	1995.53	6.8	254.44	1982.53	1.2	13
75	4.5	101.895	18.773	2000.43	6.5	378.87	1989.82	2.9	10.6
75	4.5	100.96	20.57	2007.37	6.3	217.61	1983.49	2.3	23.9
75	4.5	99.95	21.44	2007.48	6.1	177.64	1995.61	2.4	11.9
75	4.5	99.822	20.687	2011.23	6.8	177.41	1990.58	2.8	20.6
75	5	98.91	20.43	1989.74	6.2	371.57	1981.99	1.7	7.8
75	5	99.16	21.93	1995.53	6.8	254.44	1981.99	1.6	13.5
75	5	101.895	18.773	2000.43	6.5	378.87	1990.35	2.4	10.1

75	5	100.96	20.57	2007.37	6.3	217.61	1983.49	2.8	23.9
75	5	99.95	21.44	2007.48	6.1	177.64	1995.61	2.9	11.9
75	5	99.822	20.687	2011.23	6.8	177.41	1990.35	2.7	20.9
75	5.5	98.91	20.43	1989.74	6.2	371.57	1982.07	1.7	7.7
75	5.5	99.16	21.93	1995.53	6.8	254.44	1981.99	1.5	13.5
75	5.5	101.895	18.773	2000.43	6.5	378.87	1989.82	2.5	10.6
75	5.5	100.96	20.57	2007.37	6.3	217.61	1983.03	1.9	24.3
75	5.5	99.95	21.44	2007.48	6.1	177.64	1995.61	2.5	11.9
75	5.5	99.822	20.687	2011.23	6.8	177.41	1989.78	2.6	21.4
75	6	98.91	20.43	1989.74	6.2	371.57	1982.07	1.4	7.7
75	6	99.16	21.93	1995.53	6.8	254.44	1982.53	0.9	13
75	6	101.895	18.773	2000.43	6.5	378.87	1990.55	2.1	9.9
75	6	100.96	20.57	2007.37	6.3	217.61	1990.55	1.7	16.8
75	6	99.95	21.44	2007.48	6.1	177.64	1992.39	2	15.1
75	6	99.822	20.687	2011.23	6.8	177.41	1981.99	2.4	29.2
75	6.5	99.16	21.93	1995.53	6.8	254.44	1981.99	1.3	13.5
75	6.5	101.895	18.773	2000.43	6.5	378.87	1989.82	2.3	10.6
75	6.5	100.96	20.57	2007.37	6.3	217.61	1981.99	1.6	25.4
75	6.5	99.95	21.44	2007.48	6.1	177.64	1992.39	2.1	15.1
75	6.5	99.822	20.687	2011.23	6.8	177.41	1981.99	2.8	29.2
75	7	98.91	20.43	1989.74	6.2	371.57	1982.07	-0.2	7.7
75	7	99.16	21.93	1995.53	6.8	254.44	1984.6	1.4	10.9
75	7	101.895	18.773	2000.43	6.5	378.87	1989.51	1.7	10.9
75	7	100.96	20.57	2007.37	6.3	217.61	1989.47	0.9	17.9
75	7	99.95	21.44	2007.48	6.1	177.64	1992.39	2.5	15.1
75	7	99.822	20.687	2011.23	6.8	177.41	1992.65	2	18.6
100	0.5	98.91	20.43	1989.74	6.2	431.6	1985.9	3.2	3.8
100	0.5	99.16	21.93	1995.53	6.8	295.75	1990.55	8.4	5
100	0.5	101.895	18.773	2000.43	6.5	438.43	1998.52	9	1.9
100	0.5	100.96	20.57	2007.37	6.3	241.85	2006.08	9.4	1.3
100	0.5	99.95	21.44	2007.48	6.1	207.42	2006.08	9.5	1.4
100	0.5	99.822	20.687	2011.23	6.8	206.42	2010.38	9.1	0.9
100	1	98.91	20.43	1989.74	6.2	431.6	1985.98	3	3.8
100	1	99.16	21.93	1995.53	6.8	295.75	1989.82	3.5	5.7
100	1	101.895	18.773	2000.43	6.5	438.43	1984.33	4	16.1
100	1	100.96	20.57	2007.37	6.3	241.85	1995.61	9.5	11.8
100	1	99.95	21.44	2007.48	6.1	207.42	1995.61	9.5	11.9
100	1	99.822	20.687	2011.23	6.8	206.42	1997.07	9.1	14.2
100	1.5	98.91	20.43	1989.74	6.2	431.6	1985.14	1.9	4.6

100	1.5	99.16	21.93	1995.53	6.8	295.75	1989.78	3.3	5.7
100	1.5	101.895	18.773	2000.43	6.5	438.43	1983.68	4	16.8
100	1.5	100.96	20.57	2007.37	6.3	241.85	1993.08	4.4	14.3
100	1.5	99.95	21.44	2007.48	6.1	207.42	1992.62	4.4	14.9
100	1.5	99.822	20.687	2011.23	6.8	206.42	1992.69	3.8	18.5
100	2	98.91	20.43	1989.74	6.2	431.6	1984.33	2	5.4
100	2	99.16	21.93	1995.53	6.8	295.75	1989.82	3.3	5.7
100	2	101.895	18.773	2000.43	6.5	438.43	1983.68	3.3	16.8
100	2	100.96	20.57	2007.37	6.3	241.85	1992.39	3.8	15
100	2	99.95	21.44	2007.48	6.1	207.42	1992.62	5.6	14.9
100	2	99.822	20.687	2011.23	6.8	206.42	1992.65	4.9	18.6
100	2.5	98.91	20.43	1989.74	6.2	431.6	1984.48	2.3	5.3
100	2.5	99.16	21.93	1995.53	6.8	295.75	1989.16	2.8	6.4
100	2.5	101.895	18.773	2000.43	6.5	438.43	1992.16	1.6	8.3
100	2.5	100.96	20.57	2007.37	6.3	241.85	1985.83	3.7	21.5
100	2.5	99.95	21.44	2007.48	6.1	207.42	1984.33	2.9	23.1
100	2.5	99.822	20.687	2011.23	6.8	206.42	1997.07	3.1	14.2
100	3	98.91	20.43	1989.74	6.2	431.6	1983.91	1.8	5.8
100	3	99.16	21.93	1995.53	6.8	295.75	1988.86	2.4	6.7
100	3	101.895	18.773	2000.43	6.5	438.43	1989.82	2.1	10.6
100	3	100.96	20.57	2007.37	6.3	241.85	1985.25	3.7	22.1
100	3	99.95	21.44	2007.48	6.1	207.42	1992.39	2.1	15.1
100	3	99.822	20.687	2011.23	6.8	206.42	1995.8	3	15.4
100	3.5	98.91	20.43	1989.74	6.2	431.6	1983.49	1.9	6.3
100	3.5	99.16	21.93	1995.53	6.8	295.75	1984.33	0.8	11.2
100	3.5	101.895	18.773	2000.43	6.5	438.43	1990.55	1.8	9.9
100	3.5	100.96	20.57	2007.37	6.3	241.85	1984.33	3.7	23
100	3.5	99.95	21.44	2007.48	6.1	207.42	1995.61	1.9	11.9
100	3.5	99.822	20.687	2011.23	6.8	206.42	1995.8	3.7	15.4
100	4	98.91	20.43	1989.74	6.2	431.6	1984.52	1.7	5.2
100	4	99.16	21.93	1995.53	6.8	295.75	1984.33	0.9	11.2
100	4	101.895	18.773	2000.43	6.5	438.43	1990.55	1.9	9.9
100	4	100.96	20.57	2007.37	6.3	241.85	1984.33	4.3	23
100	4	99.95	21.44	2007.48	6.1	207.42	1995.61	2.1	11.9
100	4	99.822	20.687	2011.23	6.8	206.42	1995.61	3	15.6
100	4.5	98.91	20.43	1989.74	6.2	431.6	1982.53	1.9	7.2
100	4.5	99.16	21.93	1995.53	6.8	295.75	1983.91	0.6	11.6
100	4.5	101.895	18.773	2000.43	6.5	438.43	1989.82	2.2	10.6
100	4.5	100.96	20.57	2007.37	6.3	241.85	1983.72	3.1	23.7

100	4.5	99.95	21.44	2007.48	6.1	207.42	1992.39	2.2	15.1
100	4.5	99.822	20.687	2011.23	6.8	206.42	1990.58	2.2	20.6
100	5	99.16	21.93	1995.53	6.8	295.75	1981.99	0.9	13.5
100	5	101.895	18.773	2000.43	6.5	438.43	1990.35	2	10.1
100	5	100.96	20.57	2007.37	6.3	241.85	1983.49	2.9	23.9
100	5	99.95	21.44	2007.48	6.1	207.42	1992.62	2.1	14.9
100	5	99.822	20.687	2011.23	6.8	206.42	1990.35	2.3	20.9
100	5.5	98.91	20.43	1989.74	6.2	431.6	1982.07	1.4	7.7
100	5.5	99.16	21.93	1995.53	6.8	295.75	1989.28	0.9	6.2
100	5.5	101.895	18.773	2000.43	6.5	438.43	1989.82	2.3	10.6
100	5.5	100.96	20.57	2007.37	6.3	241.85	1989.82	2.5	17.6
100	5.5	99.95	21.44	2007.48	6.1	207.42	1992.39	2	15.1
100	5.5	99.822	20.687	2011.23	6.8	206.42	1992.65	2.6	18.6
100	6	98.91	20.43	1989.74	6.2	431.6	1982.49	1.6	7.3
100	6	99.16	21.93	1995.53	6.8	295.75	1985.83	0.8	9.7
100	6	101.895	18.773	2000.43	6.5	438.43	1989.78	1.9	10.7
100	6	100.96	20.57	2007.37	6.3	241.85	1990.55	2.2	16.8
100	6	99.95	21.44	2007.48	6.1	207.42	1993.42	1.8	14.1
100	6	99.822	20.687	2011.23	6.8	206.42	1992.65	2.4	18.6

APPENDIX B

VARIATION CONDITION OF RTL ALGORITHM

Table B.1. The example list of calculated strong earthquake ($M_w \geq 6.0$) that it detected seismic quiescence anomaly after investigating RTL score in Thailand-Laos-Myanmar borders (16.76° – 22.30°N and 97.48° – 103.16°E) by using different characteristic *RTL* parameters. The yellow highlighted indicate the condition, which used in this study. The parameters *N*, Q_s, *RTL*, and *Q*-time indicate a minimum number of investigating events, starting time of seismic quiescence, minimum of *RTL* scores at the epicenter of strong earthquakes and the duration between the starting time of seismic quiescence and the occurrence time of main shock, respectively.

R_{max} (km)	T_{max} (Year)	Lon (Deg)	Lat (Deg)	Year	Mag (M_w)	*N*	Q_s (Year)	*RTL*	*Q*-time (Year)
190	1	102.578	21.363	1983.48	6.3	3	1983.45	-0.713322598	0
190	1	99.3	22	1984.31	6.3	6	1983.91	-0.705186748	0.4
190	1	98.91	20.43	1989.74	6.2	23	1987.71	-0.207197939	2
190	1	99.16	21.93	1995.53	6.8	38	1992.39	-0.700715355	3.1
190	1	101.895	18.773	2000.43	6.5	14	1996.76	-1	3.7
190	1	100.96	20.57	2007.37	6.3	52	1989.47	-0.687712524	17.9
190	1	99.95	21.44	2007.48	6.1	89	1995.65	-0.538589298	11.8
190	1	99.822	20.687	2011.23	6.8	88	2007.58	-0.854924648	3.7
190	1.5	99.3	22	1984.31	6.3	6	1983.91	-0.168241638	0.4
190	1.5	98.91	20.43	1989.74	6.2	23	1988.17	-0.242460424	1.6
190	1.5	99.16	21.93	1995.53	6.8	38	1984.33	-0.457683114	11.2
190	1.5	101.895	18.773	2000.43	6.5	14	1996.76	-0.97553306	3.7
190	1.5	100.96	20.57	2007.37	6.3	52	1989.82	-0.958449648	17.6
190	1.5	99.95	21.44	2007.48	6.1	89	1995.65	-0.495506998	11.8
190	1.5	99.822	20.687	2011.23	6.8	88	2007.58	-0.561524475	3.7
190	2	99.3	22	1984.31	6.3	6	1984.02	0	0.3
190	2	98.91	20.43	1989.74	6.2	23	1988.63	-0.301273094	1.1
190	2	99.16	21.93	1995.53	6.8	38	1989.2	-0.804524402	6.3
190	2	101.895	18.773	2000.43	6.5	14	1996.76	-0.477107684	3.7
190	2	100.96	20.57	2007.37	6.3	52	1990.55	-0.731768743	16.8
190	2	99.95	21.44	2007.48	6.1	89	1988.93	-0.341762433	18.5
190	2	99.822	20.687	2011.23	6.8	88	2007.58	-1	3.7

190	2.5	98.91	20.43	1989.74	6.2	23	1989.2	-0.539670981	0.5
190	2.5	99.16	21.93	1995.53	6.8	38	1988.93	-0.468647041	6.6
190	2.5	101.895	18.773	2000.43	6.5	14	2000.06	-0.477829174	0.4
190	2.5	100.96	20.57	2007.37	6.3	52	1990.55	-0.788301733	16.8
190	2.5	99.95	21.44	2007.48	6.1	89	1988.93	-0.162891445	18.5
190	2.5	99.822	20.687	2011.23	6.8	88	2007.58	-0.783602131	3.7
190	3	98.91	20.43	1989.74	6.2	23	1989.28	-0.636719664	0.5
190	3	99.16	21.93	1995.53	6.8	38	1989.2	-0.290611473	6.3
190	3	101.895	18.773	2000.43	6.5	14	1998.52	-0.581584371	1.9
190	3	100.96	20.57	2007.37	6.3	52	1990.55	-0.695001608	16.8
190	3	99.95	21.44	2007.48	6.1	89	1989.82	-0.133015768	17.7
190	3	99.822	20.687	2011.23	6.8	88	2007.58	-0.906147587	3.7
190	3.5	98.91	20.43	1989.74	6.2	23	1989.28	-0.692139087	0.5
190	3.5	99.16	21.93	1995.53	6.8	38	1989.2	-0.125991674	6.3
190	3.5	101.895	18.773	2000.43	6.5	14	2000.06	-1	0.4
190	3.5	100.96	20.57	2007.37	6.3	52	1990.55	-0.786074681	16.8
190	3.5	99.95	21.44	2007.48	6.1	89	1992.35	-0.208699596	15.1
190	3.5	99.822	20.687	2011.23	6.8	88	2007.58	-0.810567511	3.7
190	5	98.91	20.43	1989.74	6.2	23	1989.28	-0.530276979	0.5
190	5	99.16	21.93	1995.53	6.8	38	1989.2	-0.538211786	6.3
190	5	101.895	18.773	2000.43	6.5	14	2000.06	-1	0.4
190	5	100.96	20.57	2007.37	6.3	52	1990.55	-0.466191053	16.8
190	5	99.95	21.44	2007.48	6.1	89	1992.39	-0.175946909	15.1
190	5	99.822	20.687	2011.23	6.8	88	2007.5	-0.84289893	3.7
210	1	102.578	21.363	1983.48	6.3	4	1983.45	-0.544738848	0
210	1	99.3	22	1984.31	6.3	8	1983.91	-0.708505867	0.4
210	1	98.91	20.43	1989.74	6.2	28	1987.71	-0.262083874	2
210	1	99.16	21.93	1995.53	6.8	45	1992.39	-0.7956643	3.1
210	1	101.895	18.773	2000.43	6.5	24	1996.76	-0.996529479	3.7
210	1	100.96	20.57	2007.37	6.3	64	1989.47	-0.675379107	17.9
210	1	99.95	21.44	2007.48	6.1	102	1995.65	-0.57336685	11.8
210	1	99.822	20.687	2011.23	6.8	102	2007.58	-0.861929383	3.7
210	1.5	99.3	22	1984.31	6.3	8	1983.91	-0.158901106	0.4
210	1.5	98.91	20.43	1989.74	6.2	28	1988.63	-0.284577709	1.1
210	1.5	99.16	21.93	1995.53	6.8	45	1992.39	-0.514389194	3.1
210	1.5	101.895	18.773	2000.43	6.5	24	1996.76	-0.977502291	3.7

210	1.5	100.96	20.57	2007.37	6.3	64	1989.82	-0.895193164	17.6
210	1.5	99.95	21.44	2007.48	6.1	102	1995.65	-0.552997969	11.8
210	1.5	99.822	20.687	2011.23	6.8	102	2007.58	-0.559272113	3.7
210	2	99.3	22	1984.31	6.3	8	1984.14	-0.36	0.2
210	2	98.91	20.43	1989.74	6.2	28	1988.63	-0.329737483	1.1
210	2	99.16	21.93	1995.53	6.8	45	1989.2	-0.747776999	6.3
210	2	101.895	18.773	2000.43	6.5	24	1996.76	-0.491410887	3.7
210	2	100.96	20.57	2007.37	6.3	64	1990.55	-0.682070524	16.8
210	2	99.95	21.44	2007.48	6.1	102	1988.93	-0.310095955	18.5
210	2	99.822	20.687	2011.23	6.8	102	2007.58	-1	3.7
210	2.5	98.91	20.43	1989.74	6.2	28	1989.2	-0.473010909	0.5
210	2.5	99.16	21.93	1995.53	6.8	45	1988.93	-0.462950101	6.6
210	2.5	101.895	18.773	2000.43	6.5	24	2000.06	-0.561106864	0.4
210	2.5	100.96	20.57	2007.37	6.3	64	1990.55	-0.713441434	16.8
210	2.5	99.95	21.44	2007.48	6.1	102	1989.82	-0.180798844	17.7
210	2.5	99.822	20.687	2011.23	6.8	102	2007.58	-0.817929695	3.7
210	3	98.91	20.43	1989.74	6.2	28	1989.28	-0.409782395	0.5
210	3	99.16	21.93	1995.53	6.8	45	1989.2	-0.291262642	6.3
210	3	101.895	18.773	2000.43	6.5	24	2000.06	-0.418889863	0.4
210	3	100.96	20.57	2007.37	6.3	64	1990.55	-0.703417108	16.8
210	3	99.95	21.44	2007.48	6.1	102	1989.82	-0.203984546	17.7
210	3	99.822	20.687	2011.23	6.8	102	2007.58	-0.860510305	3.7
210	3.5	98.91	20.43	1989.74	6.2	28	1988.86	-0.540679804	0.9
210	3.5	99.16	21.93	1995.53	6.8	45	1989.2	-0.117671014	6.3
210	3.5	101.895	18.773	2000.43	6.5	24	2000.06	-1	0.4
210	3.5	100.96	20.57	2007.37	6.3	64	1990.55	-0.784728686	16.8
210	3.5	99.95	21.44	2007.48	6.1	102	1992.35	-0.210263828	15.1
210	3.5	99.822	20.687	2011.23	6.8	102	2007.58	-0.77678516	3.7
210	5	98.91	20.43	1989.74	6.2	28	1989.28	-0.492825566	0.5
210	5	99.16	21.93	1995.53	6.8	45	1989.2	-0.432040658	6.3
210	5	101.895	18.773	2000.43	6.5	24	2000.06	-1	0.4
210	5	100.96	20.57	2007.37	6.3	64	1990.55	-0.422660161	16.8
210	5	99.95	21.44	2007.48	6.1	102	1992.65	-0.173279799	14.8
210	5	99.822	20.687	2011.23	6.8	102	2007.5	-0.831805411	3.7
230	1	102.578	21.363	1983.48	6.3	5	1983.07	-0.331899153	0.4
230	1	99.3	22	1984.31	6.3	10	1983.91	-0.329200709	0.4

230	1	98.91	20.43	1989.74	6.2	36	1989.28	-0.277340367	0.5
230	1	99.16	21.93	1995.53	6.8	54	1992.39	-0.807803352	3.1
230	1	101.895	18.773	2000.43	6.5	28	1996.76	-0.996504059	3.7
230	1	100.96	20.57	2007.37	6.3	82	1989.82	-0.887991898	17.6
230	1	99.95	21.44	2007.48	6.1	128	1995.65	-0.904192056	11.8
230	1	99.822	20.687	2011.23	6.8	122	2007.58	-0.961553615	3.7
230	1.5	99.3	22	1984.31	6.3	10	1984.29	-0.440105125	0
230	1.5	98.91	20.43	1989.74	6.2	36	1989.28	-0.298053174	0.5
230	1.5	99.16	21.93	1995.53	6.8	54	1992.39	-0.530411734	3.1
230	1.5	101.895	18.773	2000.43	6.5	28	1996.76	-0.978645779	3.7
230	1.5	100.96	20.57	2007.37	6.3	82	1989.82	-1	17.6
230	1.5	99.95	21.44	2007.48	6.1	128	1995.65	-0.875877769	11.8
230	1.5	99.822	20.687	2011.23	6.8	122	2007.58	-0.745060654	3.7
230	2	99.3	22	1984.31	6.3	10	1984.29	-1	0
230	2	98.91	20.43	1989.74	6.2	36	1989.01	-0.339846836	0.7
230	2	99.16	21.93	1995.53	6.8	54	1988.93	-0.739770828	6.6
230	2	101.895	18.773	2000.43	6.5	28	1996.76	-0.621658615	3.7
230	2	100.96	20.57	2007.37	6.3	82	1990.55	-0.597060145	16.8
230	2	99.95	21.44	2007.48	6.1	128	1995.65	-0.414574938	11.8
230	2	99.822	20.687	2011.23	6.8	122	2007.58	-1	3.7
230	2.5	98.91	20.43	1989.74	6.2	36	1989.2	-0.599870265	0.5
230	2.5	99.16	21.93	1995.53	6.8	54	1988.93	-0.51712885	6.6
230	2.5	101.895	18.773	2000.43	6.5	28	1996.76	-0.621329171	3.7
230	2.5	100.96	20.57	2007.37	6.3	82	1990.55	-0.528708735	16.8
230	2.5	99.95	21.44	2007.48	6.1	128	1995.65	-0.278877455	11.8
230	2.5	99.822	20.687	2011.23	6.8	122	2007.58	-0.953932718	3.7
230	3	98.91	20.43	1989.74	6.2	36	1989.28	-0.668514505	0.5
230	3	99.16	21.93	1995.53	6.8	54	1989.28	-0.42167016	6.2
230	3	101.895	18.773	2000.43	6.5	28	1996.76	-0.438862054	3.7
230	3	100.96	20.57	2007.37	6.3	82	1990.55	-0.529670129	16.8
230	3	99.95	21.44	2007.48	6.1	128	1995.65	-0.15257953	11.8
230	3	99.822	20.687	2011.23	6.8	122	2007.58	-0.983860394	3.7
230	3.5	98.91	20.43	1989.74	6.2	36	1988.9	-0.4522066	0.8
230	3.5	99.16	21.93	1995.53	6.8	54	1992.35	-0.307773488	3.2
230	3.5	101.895	18.773	2000.43	6.5	28	2000.06	-0.907596696	0.4
230	3.5	100.96	20.57	2007.37	6.3	82	1990.55	-0.568193691	16.8

230	3.5	99.95	21.44	2007.48	6.1	128	1995.53	-0.395469666	11.9
230	3.5	99.822	20.687	2011.23	6.8	122	2007.58	-0.900514628	3.7
230	5	98.91	20.43	1989.74	6.2	36	1989.28	-0.537399567	0.5
230	5	99.16	21.93	1995.53	6.8	54	1992.39	-0.527971621	3.1
230	5	101.895	18.773	2000.43	6.5	28	2000.06	-0.922755875	0.4
230	5	100.96	20.57	2007.37	6.3	82	2003.93	-0.478852577	3.4
230	5	99.95	21.44	2007.48	6.1	128	1995.65	-0.172053588	11.8
230	5	99.822	20.687	2011.23	6.8	122	2007.5	-0.864634575	3.7
240	1	102.578	21.363	1983.48	6.3	5	1983.07	-0.331899153	0.4
240	1	99.3	22	1984.31	6.3	11	1983.91	-0.328793379	0.4
240	1	98.91	20.43	1989.74	6.2	39	1988.9	-0.258790253	0.8
240	1	99.16	21.93	1995.53	6.8	61	1992.39	-0.752390023	3.1
240	1	101.895	18.773	2000.43	6.5	32	1996.76	-0.941146994	3.7
240	1	100.96	20.57	2007.37	6.3	94	1989.82	-0.602185745	17.6
240	1	99.95	21.44	2007.48	6.1	138	1995.65	-0.912117991	11.8
240	1	99.822	20.687	2011.23	6.8	133	2007.58	-0.824605348	3.7
240	1.5	99.3	22	1984.31	6.3	11	1984.29	-0.4483164	0
240	1.5	98.91	20.43	1989.74	6.2	39	1989.28	-0.274686224	0.5
240	1.5	99.16	21.93	1995.53	6.8	61	1984.33	-0.663776442	11.2
240	1.5	101.895	18.773	2000.43	6.5	32	1996.76	-1	3.7
240	1.5	100.96	20.57	2007.37	6.3	94	1989.82	-0.882045724	17.6
240	1.5	99.95	21.44	2007.48	6.1	138	1995.65	-0.910412957	11.8
240	1.5	99.822	20.687	2011.23	6.8	133	2007.58	-0.659261997	3.7
240	2	99.3	22	1984.31	6.3	11	1984.29	-1	0
240	2	98.91	20.43	1989.74	6.2	39	1989.01	-0.346132487	0.7
240	2	99.16	21.93	1995.53	6.8	61	1988.93	-0.735423799	6.6
240	2	101.895	18.773	2000.43	6.5	32	1996.76	-0.729541618	3.7
240	2	100.96	20.57	2007.37	6.3	94	1990.55	-0.522953374	16.8
240	2	99.95	21.44	2007.48	6.1	138	1995.65	-0.557551512	11.8
240	2	99.822	20.687	2011.23	6.8	133	2007.58	-0.909527709	3.7
240	2.5	98.91	20.43	1989.74	6.2	39	1989.2	-0.521212169	0.5
240	2.5	99.16	21.93	1995.53	6.8	61	1988.93	-0.465278649	6.6
240	2.5	101.895	18.773	2000.43	6.5	32	1996.76	-0.739855184	3.7
240	2.5	100.96	20.57	2007.37	6.3	94	1990.55	-0.474858054	16.8
240	2.5	99.95	21.44	2007.48	6.1	138	1995.53	-0.425009079	11.9
240	2.5	99.822	20.687	2011.23	6.8	133	2007.58	-0.904229882	3.7

240	3	98.91	20.43	1989.74	6.2	39	1989.28	-0.544249015	0.5
240	3	99.16	21.93	1995.53	6.8	61	1989.28	-0.355244106	6.2
240	3	101.895	18.773	2000.43	6.5	32	1996.76	-0.521493545	3.7
240	3	100.96	20.57	2007.37	6.3	94	1990.55	-0.48539586	16.8
240	3	99.95	21.44	2007.48	6.1	138	1995.65	-0.288219486	11.8
240	3	99.822	20.687	2011.23	6.8	133	2007.58	-0.98456805	3.7
240	3.5	98.91	20.43	1989.74	6.2	39	1988.9	-0.38972393	0.8
240	3.5	99.16	21.93	1995.53	6.8	61	1992.35	-0.242693678	3.2
240	3.5	101.895	18.773	2000.43	6.5	32	2000.17	-0.973284731	0.3
240	3.5	100.96	20.57	2007.37	6.3	94	1990.55	-0.506623912	16.8
240	3.5	99.95	21.44	2007.48	6.1	138	1995.53	-0.64296779	11.9
240	3.5	99.822	20.687	2011.23	6.8	133	2007.58	-0.564924593	3.7
240	3.6	98.91	20.43	1989.74	6.2	39	1988.9	-0.489677522	0.8
240	3.6	99.16	21.93	1995.53	6.8	61	1992.39	-0.419163129	3.1
240	3.6	101.895	18.773	2000.43	6.5	32	2000.17	-0.981737255	0.3
240	3.6	100.96	20.57	2007.37	6.3	94	1990.55	-0.410090627	16.8
240	3.6	99.95	21.44	2007.48	6.1	138	1995.65	-0.869105565	11.8
240	3.6	99.822	20.687	2011.23	6.8	133	2007.58	-0.525635199	3.7
240	3.7	98.91	20.43	1989.74	6.2	39	1989.01	-0.522333061	0.7
240	3.7	99.16	21.93	1995.53	6.8	61	1992.39	-0.311114565	3.1
240	3.7	101.895	18.773	2000.43	6.5	32	2000.17	-0.990361934	0.3
240	3.7	100.96	20.57	2007.37	6.3	94	2003.74	-0.447413911	3.6
240	3.7	99.95	21.44	2007.48	6.1	138	1995.65	-0.740674461	11.8
240	3.7	99.822	20.687	2011.23	6.8	133	2007.58	-0.591852884	3.7
240	3.8	98.91	20.43	1989.74	6.2	39	1989.28	-0.706090451	0.5
240	3.8	99.16	21.93	1995.53	6.8	61	1992.39	-0.529973468	3.1
240	3.8	101.895	18.773	2000.43	6.5	32	2000.17	-0.99918187	0.3
240	3.8	100.96	20.57	2007.37	6.3	94	1990.55	-0.395522528	16.8
240	3.8	99.95	21.44	2007.48	6.1	138	1995.65	-0.715920751	11.8
240	3.8	99.822	20.687	2011.23	6.8	133	2007.58	-0.57288052	3.7
240	3.9	98.91	20.43	1989.74	6.2	39	1989.28	-0.610238619	0.5
240	3.9	99.16	21.93	1995.53	6.8	61	1992.39	-0.577120035	3.1
240	3.9	101.895	18.773	2000.43	6.5	32	2000.17	-1	0.3
240	3.9	100.96	20.57	2007.37	6.3	94	2003.93	-0.968493875	3.4
240	3.9	99.95	21.44	2007.48	6.1	138	1995.65	-0.840496421	11.8
240	3.9	99.822	20.687	2011.23	6.8	133	2007.58	-0.676510883	3.7

240	4	98.91	20.43	1989.74	6.2	39	1989.28	-0.626913045	0.5
240	4	99.16	21.93	1995.53	6.8	61	1992.39	-0.542760704	3.1
240	4	101.895	18.773	2000.43	6.5	32	2000.17	-1	0.3
240	4	100.96	20.57	2007.37	6.3	94	2003.93	-0.967292984	3.4
240	4	99.95	21.44	2007.48	6.1	138	1995.65	-0.809721221	11.8
240	4	99.822	20.687	2011.23	6.8	133	2007.58	-0.667449714	3.7
240	4.1	98.91	20.43	1989.74	6.2	39	1989.28	-0.502833987	0.5
240	4.1	99.16	21.93	1995.53	6.8	61	1992.65	-0.471785138	2.9
240	4.1	101.895	18.773	2000.43	6.5	32	2000.17	-1	0.3
240	4.1	100.96	20.57	2007.37	6.3	94	2003.93	-0.928938801	3.4
240	4.1	99.95	21.44	2007.48	6.1	138	1995.65	-0.665289534	11.8
240	4.1	99.822	20.687	2011.23	6.8	133	2007.58	-0.614071934	3.7
240	4.2	98.91	20.43	1989.74	6.2	39	1989.28	-0.360343376	0.5
240	4.2	99.16	21.93	1995.53	6.8	61	1992.35	-0.361751427	3.2
240	4.2	101.895	18.773	2000.43	6.5	32	2000.06	-0.810117606	0.4
240	4.2	100.96	20.57	2007.37	6.3	94	2003.93	-0.902525214	3.4
240	4.2	99.95	21.44	2007.48	6.1	138	1995.65	-0.694235395	11.8
240	4.2	99.822	20.687	2011.23	6.8	133	2007.58	-0.699752932	3.7
240	4.3	98.91	20.43	1989.74	6.2	39	1989.28	-0.301006312	0.5
240	4.3	99.16	21.93	1995.53	6.8	61	1992.39	-0.496348686	3.1
240	4.3	101.895	18.773	2000.43	6.5	32	2000.17	-1	0.3
240	4.3	100.96	20.57	2007.37	6.3	94	2003.93	-0.909749039	3.4
240	4.3	99.95	21.44	2007.48	6.1	138	1995.65	-0.626315081	11.8
240	4.3	99.822	20.687	2011.23	6.8	133	2007.58	-0.704288367	3.7
240	4.4	98.91	20.43	1989.74	6.2	39	1988.63	-0.232243548	1.1
240	4.4	99.16	21.93	1995.53	6.8	61	1992.39	-0.33254414	3.1
240	4.4	101.895	18.773	2000.43	6.5	32	2000.17	-1	0.3
240	4.4	100.96	20.57	2007.37	6.3	94	2003.93	-0.814241691	3.4
240	4.4	99.95	21.44	2007.48	6.1	138	1995.65	-0.675444576	11.8
240	4.4	99.822	20.687	2011.23	6.8	133	2007.58	-0.695609176	3.7
240	4.5	98.91	20.43	1989.74	6.2	39	1988.63	-0.138894959	1.1
240	4.5	99.16	21.93	1995.53	6.8	61	1992.39	-0.710510103	3.1
240	4.5	101.895	18.773	2000.43	6.5	32	2000.17	-1	0.3
240	4.5	100.96	20.57	2007.37	6.3	94	2003.93	-0.939933847	3.4
240	4.5	99.95	21.44	2007.48	6.1	138	1995.65	-0.619501358	11.8
240	4.5	99.822	20.687	2011.23	6.8	133	2007.58	-0.655999829	3.7

240	5	98.91	20.43	1989.74	6.2	39	1989.28	-0.485041876	0.5
240	5	99.16	21.93	1995.53	6.8	61	1992.65	-0.457961571	2.9
240	5	101.895	18.773	2000.43	6.5	32	2000.17	-1	0.3
240	5	100.96	20.57	2007.37	6.3	94	2003.93	-0.713952738	3.4
240	5	99.95	21.44	2007.48	6.1	138	1995.65	-0.252137973	11.8
240	5	99.822	20.687	2011.23	6.8	133	2007.5	-0.680027247	3.7
250	1	102.578	21.363	1983.48	6.3	6	1983.07	-0.331899153	0.4
250	1	99.3	22	1984.31	6.3	11	1983.91	-0.328924573	0.4
250	1	98.91	20.43	1989.74	6.2	40	1988.9	-0.252444975	0.8
250	1	99.16	21.93	1995.53	6.8	72	1992.39	-0.74078075	3.1
250	1	101.895	18.773	2000.43	6.5	32	1996.76	-0.941146994	3.7
250	1	100.96	20.57	2007.37	6.3	107	1989.82	-0.512552598	17.6
250	1	99.95	21.44	2007.48	6.1	146	1995.65	-0.740701021	11.8
250	1	99.822	20.687	2011.23	6.8	142	2007.58	-0.823456543	3.7
250	1.5	99.3	22	1984.31	6.3	11	1984.29	-0.456205913	0
250	1.5	98.91	20.43	1989.74	6.2	40	1989.28	-0.256926666	0.5
250	1.5	99.16	21.93	1995.53	6.8	72	1992.65	-0.623398815	2.9
250	1.5	101.895	18.773	2000.43	6.5	32	1996.76	-1	3.7
250	1.5	100.96	20.57	2007.37	6.3	107	1989.82	-0.731308478	17.6
250	1.5	99.95	21.44	2007.48	6.1	146	1995.65	-0.706833334	11.8
250	1.5	99.822	20.687	2011.23	6.8	142	2007.58	-0.594426765	3.7
250	2	99.3	22	1984.31	6.3	11	1984.29	-1	0
250	2	98.91	20.43	1989.74	6.2	40	1989.01	-0.311845947	0.7
250	2	99.16	21.93	1995.53	6.8	72	1988.93	-0.525705913	6.6
250	2	101.895	18.773	2000.43	6.5	32	1996.76	-0.739044344	3.7
250	2	100.96	20.57	2007.37	6.3	107	1989.82	-0.390604401	17.6
250	2	99.95	21.44	2007.48	6.1	146	1995.65	-0.389233162	11.8
250	2	99.822	20.687	2011.23	6.8	142	2007.58	-0.868481408	3.7
250	2.5	98.91	20.43	1989.74	6.2	40	1989.2	-0.465734439	0.5
250	2.5	99.16	21.93	1995.53	6.8	72	1988.93	-0.306649253	6.6
250	2.5	101.895	18.773	2000.43	6.5	32	1996.76	-0.754603381	3.7
250	2.5	100.96	20.57	2007.37	6.3	107	2002.55	-0.451785697	4.8
250	2.5	99.95	21.44	2007.48	6.1	146	1995.53	-0.301160283	11.9
250	2.5	99.822	20.687	2011.23	6.8	142	2007.58	-0.837290694	3.7
250	3	98.91	20.43	1989.74	6.2	40	1989.28	-0.496712017	0.5
250	3	99.16	21.93	1995.53	6.8	72	1989.28	-0.201847325	6.2

250	3	101.895	18.773	2000.43	6.5	32	1996.76	-0.530185598	3.7
250	3	100.96	20.57	2007.37	6.3	107	1990.55	-0.458959239	16.8
250	3	99.95	21.44	2007.48	6.1	146	1995.65	-0.233241792	11.8
250	3	99.822	20.687	2011.23	6.8	142	2007.58	-0.985294784	3.7
250	3.5	98.91	20.43	1989.74	6.2	40	1988.9	-0.345945718	0.8
250	3.5	99.16	21.93	1995.53	6.8	72	1992.35	-0.1610395	3.2
250	3.5	101.895	18.773	2000.43	6.5	32	2000.17	-0.973284731	0.3
250	3.5	100.96	20.57	2007.37	6.3	107	2003.47	-0.38963457	3.9
250	3.5	99.95	21.44	2007.48	6.1	146	1995.53	-0.593059988	11.9
250	3.5	99.822	20.687	2011.23	6.8	142	2007.58	-0.594484389	3.7
250	4.5	98.91	20.43	1989.74	6.2	40	1988.63	-0.156803453	1.1
250	4.5	99.16	21.93	1995.53	6.8	72	1992.39	-0.542287748	3.1
250	4.5	101.895	18.773	2000.43	6.5	32	2000.17	-1	0.3
250	4.5	100.96	20.57	2007.37	6.3	107	2003.93	-0.692117076	3.4
250	4.5	99.95	21.44	2007.48	6.1	146	1995.65	-0.560651684	11.8
250	4.5	99.822	20.687	2011.23	6.8	142	2007.58	-0.667280727	3.7
250	5	98.91	20.43	1989.74	6.2	40	1989.28	-0.496623579	0.5
250	5	99.16	21.93	1995.53	6.8	72	1992.65	-0.49141813	2.9
250	5	101.895	18.773	2000.43	6.5	32	2000.17	-1	0.3
250	5	100.96	20.57	2007.37	6.3	107	2003.93	-0.56426778	3.4
250	5	99.95	21.44	2007.48	6.1	146	1995.65	-0.23815596	11.8
250	5	99.822	20.687	2011.23	6.8	142	2007.5	-0.677379468	3.7
260	5	101.895	18.773	2000.43	6.5	36	2000.17	-0.921093304	0.3
260	5	100.96	20.57	2007.37	6.3	121	2003.93	-0.532565177	3.4
260	5	99.95	21.44	2007.48	6.1	159	1995.65	-0.214785284	11.8
260	5	99.822	20.687	2011.23	6.8	151	2007.5	-0.667501869	3.7
290	1	102.578	21.363	1983.48	6.3	6	1983.07	-0.331899153	0.4
290	1	99.3	22	1984.31	6.3	15	1983.91	-0.147902164	0.4
290	1	98.91	20.43	1989.74	6.2	52	1988.9	-0.945473792	0.8
290	1	99.16	21.93	1995.53	6.8	97	1992.39	-0.741613603	3.1
290	1	101.895	18.773	2000.43	6.5	42	1996.76	-0.916746674	3.7
290	1	100.96	20.57	2007.37	6.3	155	1988.97	-0.49810458	18.4
290	1	99.95	21.44	2007.48	6.1	182	1988.9	-0.516941632	18.6
290	1	99.822	20.687	2011.23	6.8	181	2007.58	-0.788746845	3.7
290	1.5	99.3	22	1984.31	6.3	15	1983.53	-0.345594566	0.8
290	1.5	98.91	20.43	1989.74	6.2	52	1989.01	-0.830649792	0.7

290	1.5	99.16	21.93	1995.53	6.8	97	1992.39	-0.514414811	3.1
290	1.5	101.895	18.773	2000.43	6.5	42	1997.07	-0.987281398	3.4
290	1.5	100.96	20.57	2007.37	6.3	155	1989.82	-0.44959475	17.6
290	1.5	99.95	21.44	2007.48	6.1	182	1988.97	-0.58952491	18.5
290	1.5	99.822	20.687	2011.23	6.8	181	2007.58	-0.522392456	3.7
290	2	99.3	22	1984.31	6.3	15	1984.29	-0.958542296	0
290	2	98.91	20.43	1989.74	6.2	52	1989.01	-0.911171094	0.7
290	2	99.16	21.93	1995.53	6.8	97	1988.93	-0.785027504	6.6
290	2	101.895	18.773	2000.43	6.5	42	1997.07	-0.743542836	3.4
290	2	100.96	20.57	2007.37	6.3	155	1989.82	-0.36847784	17.6
290	2	99.95	21.44	2007.48	6.1	182	1988.97	-0.606333058	18.5
290	2	99.822	20.687	2011.23	6.8	181	2007.58	-0.729554091	3.7
290	2.5	98.91	20.43	1989.74	6.2	52	1988.9	-0.916779917	0.8
290	2.5	99.16	21.93	1995.53	6.8	97	1988.93	-0.454237182	6.6
290	2.5	101.895	18.773	2000.43	6.5	42	1997.07	-0.965912156	3.4
290	2.5	100.96	20.57	2007.37	6.3	155	1989.82	-0.366037787	17.6
290	2.5	99.95	21.44	2007.48	6.1	182	1988.97	-0.370424848	18.5
290	2.5	99.822	20.687	2011.23	6.8	181	2007.58	-0.674963113	3.7
290	3	98.91	20.43	1989.74	6.2	52	1989.32	-1	0.4
290	3	99.16	21.93	1995.53	6.8	97	1989.28	-0.246025065	6.2
290	3	101.895	18.773	2000.43	6.5	42	1997.07	-0.823256688	3.4
290	3	100.96	20.57	2007.37	6.3	155	1989.82	-0.398539704	17.6
290	3	99.95	21.44	2007.48	6.1	182	1989.82	-0.393027908	17.7
290	3	99.822	20.687	2011.23	6.8	181	2007.58	-0.822675898	3.7
290	3.5	98.91	20.43	1989.74	6.2	52	1989.32	-0.979824842	0.4
290	3.5	99.16	21.93	1995.53	6.8	97	1992.35	-0.240507306	3.2
290	3.5	101.895	18.773	2000.43	6.5	42	2000.17	-0.710202941	0.3
290	3.5	100.96	20.57	2007.37	6.3	155	1989.82	-0.33648314	17.6
290	3.5	99.95	21.44	2007.48	6.1	182	1995.53	-0.271225185	11.9
290	3.5	99.822	20.687	2011.23	6.8	181	2007.58	-0.45071251	3.7
290	4.5	98.91	20.43	1989.74	6.2	52	1989.32	-0.793583172	0.4
290	4.5	99.16	21.93	1995.53	6.8	97	1992.39	-0.634653325	3.1
290	4.5	101.895	18.773	2000.43	6.5	42	2000.33	-0.898638225	0.1
290	4.5	100.96	20.57	2007.37	6.3	155	1993.08	-0.25386173	14.3
290	4.5	99.95	21.44	2007.48	6.1	182	1995.65	-0.194086911	11.8
290	4.5	99.822	20.687	2011.23	6.8	181	2007.58	-0.522726849	3.7

290	5	98.91	20.43	1989.74	6.2	52	1989.28	-0.534259841	0.5
290	5	99.16	21.93	1995.53	6.8	97	1988.93	-0.620229295	6.6
290	5	101.895	18.773	2000.43	6.5	42	2000.33	-0.934462153	0.1
290	5	100.96	20.57	2007.37	6.3	155	1993.08	-0.287008214	14.3
290	5	99.95	21.44	2007.48	6.1	182	1992.65	-0.092643685	14.8
290	5	99.822	20.687	2011.23	6.8	181	2007.5	-0.505634228	3.7

VITA

Prayot Puangjaktha was born on August 24, 1987 in Chiang Mai, Thailand. He studied in Montfort College, Chiang Mai for 12 years during 1994 to 2006. Then, he came to Bangkok and decided to study at Chulalongkorn University. He started his bachelor degree at the Department of Physics, Faculty of Sciences. During his studies, he works in the field of Solid State Physics and he received his Bachelor of Science degree (B.SC.) in 2011.

In 2012, he began his master degree in Earth Sciences Program, at the Department of Geology, Faculty of Sciences, Chulalongkorn University. During his studies, he focused in the field of Natural Disasters (i.e., Climate Change, Coastline Change, Seismology and so on). He graduated with a Master degree in 2015 and still interests in hazard analyses, especially involves in the field of Earthquake Forecasting.